SPURENELEMENTE IN SEDIMENTEN DES SÜDATLANTIK. PRIMÄRER EINTRAG UND FRÜHDIAGENETISCHE ÜBERPRÄGUNG.

Dissertation
zur Erlangung des Doktorgrades der Naturwissenschaften
am Fachbereich Geowissenschaften der Universität Bremen

vorgelegt von

Verena Heuer
(Dipl.-Geoökologin)

Bremen, September 2002

Tag des Kolloquiums:
22. November 2002

Gutachter:
Prof. Dr. H.D. Schulz
Prof. Dr. B.B. Jørgensen

Prüfer:
Prof. Dr. C.W. Devey
Prof. Dr. G. Bohrmann

Vorwort

Die vorliegende Arbeit entstand im Rahmen des Sonderforschungsbereichs 261 "Der Südatlantik im Spätquartär: Rekonstruktion von Stoffhaushalt und Stromsystemen" an der Universität Bremen, wo sie im Fachbereich Geowissenschaften als Dissertation eingereicht wurde. Fragestellung und Untersuchungsprogramm waren im Teilprojekt A2 "Umwandlungsprozesse und Stoff-Flüsse in Sediment/Porenwasser-Systemen" angesiedelt und wurden von Professor Dr. Horst D. Schulz betreut. Für die Finanzierung dieser Arbeit möchte ich der Deutschen Forschungsgemeinschaft ausdrücklich danken.

Im SFB 261 wurden von Mitte 1989 bis Ende 2001 Sedimentationsprozesse in der Wassersäule und am Meeresboden des Südatlantik untersucht. Dabei galt es unter anderem weiter aufzuklären, wie marine Sedimente den Stoffhaushalt des Meeres widerspiegeln, der über den CO_2 Verbrauch planktischer Algen in einer unmittelbaren Wechselbeziehung mit dem CO_2 Gehalt der Atmosphäre steht. Marine Sedimente speichern Informationen über lange Zeiträume hinweg und erlauben so auch Rückschlüsse auf vergangene Produktions- und Strömungssysteme. Auf diese Weise ermöglichen sie ein besseres Verständnis der langfristigen Klimaprozesse.

Allerdings ist der ozeanische Stoffhaushalt mit der Sedimentablagerung am Meeresboden nicht beendet. Vielmehr führt dort der weitere Abbau von organischer Substanz zu frühdiagenetischen Reaktionen, die erheblichen Einfluß auf die chemische Zusammensetzung des Sedimentes und seines Porenwassers haben und darüber hinaus Stoffflüsse aus dem Sediment in das überstehende Meerwasser antreiben. Dabei können einerseits die aus der Wassersäule stammenden Umweltsignale (Proxies) verändert werden, andererseits aber auch neue Signale im Sediment gebildet werden, die selbst Aussagen über den marinen Stoffhaushalt erlauben.

Mit den biogeochemischen Prozessen und Stoffflüssen in Sediment/Porenwasser-Systemen befaßte sich das Teilprojekt A2 des SFB 261. In den ersten drei Bearbeitungsabschnitten lag dabei der Schwerpunkt auf der Erkundung und Quantifizierung der verschiedenen im Südatlantik vorkommenden geochemischen Milieus der Frühdiagenese. Durch Untersuchungen des Porenwassers wurden zum einen die charakteristischen Prozesse gekennzeichnet und zum anderen das Ausmaß diffusiver Nährstoffflüsse durch die Sediment/Bodenwasser Grenzschicht ermittelt. Daneben zeigten Untersuchungen in tieferen Sedimentbereichen, dass frühdiagenetische Prozesse zu typischen Elementanreicherungen in der Festphase des Sedimentes führen können, und zwar insbesondere dann, wenn starke Veränderung des Klimas und der marinen Produktivität auch einen deutlichen Wechsel im geochemischen Milieu des Sedimentes auslösen.

Im vierten Bearbeitungsabschnitt, in dem diese Studie entstand, konzentrierten sich die geochemisch-analytischen Arbeiten des Teilprojekts A2 auf die Festphase langer Sedimentkerne. Dabei galt es aufzuklären, wie die verschiedenen geochemischen Milieus durch

unterschiedlich mobile Spurenmetalle in der Festphase des Sedimentes dokumentiert werden, denn nur so werden die über das Porenwasser bereits gut verstandenen frühdiagenetischen Prozesse auch auf fossile Situationen übertragbar. Für die Untersuchungen stand ein den Südatlantik weitgehend abdeckendes Netz von Sedimentproben zur Verfügung, das im Rahmen des SFB 261 durch zahlreiche METEOR-Expeditionen gewonnen worden war. Aufgrund der bereits vorliegenden Porenwasserdaten konnten aus dem Untersuchungsgebiet gezielt 10 - 20 m lange Sedimentkerne ausgewählt werden, die eine große Bandbreite geochemischer Milieus abdecken. Daneben ermöglichten schon bestehende Altersmodelle außerdem eine zeitliche Einordnung der Sedimente. Somit kann die Verteilung von Spurenelemente in der Festphase dieser Sedimente auch vor dem Hintergrund betrachtet werden, dass sich geochemische Ablagerungsmilieus durch einschneidende Klimaänderungen im Laufe der Zeit verändert haben können.

Im folgenden werden nach einer Einführung in das geochemische Verhalten von Spurenelementen in marinen Sedimenten (Kapitel 1) Ergebnisse des Teilprojekts A2 anhand von drei Beispielen aus dem östlichen Südatlantik dargestellt. Im ersten Beispiel wird die Verteilung von Spurenelementen zunächst in dem durchweg sulfidischen Schwerelotkern GeoB 1711 beschrieben, der aus dem hochproduktiven Auftriebsgebiet vor Namibia stammt und mit einer Länge von 10,7 m einen Sedimentationszeitraum von 125.000 Jahren umfaßt (Kapitel 2). Das zweite Beispiel stammt aus dem Tiefseefächer des Niger und zeigt, wie sich verschiedene Redoxzonen auf die Verteilung von Spurenelementen in der Festphase auswirken (Kapitel 3): im Schwerelotkern GeoB 4901 erstrecken sich die oxische und post-oxische Redoxzone zusammen über die oberen 12,5 m des Sedimentes, während in dem weiter durchteuften Sedimentbereich von 12,5 bis 20,3 m sulfidische Bedingungen vorherrschen. Durch die weite Aufdehnung der Redoxzonen können sich in diesem Sediment Verteilungsmuster von Spurenelementen besonders deutlich herausbilden. Daneben erlaubt der erfaßte Sedimentationszeitraum von 245.000 Jahren auch eine Betrachtung vor dem Hintergrund des vorletzten Glazial/Interglazial Wechsels (Termination II). Das dritte hier dargestellte Beispiel (Kapitel 4) stammt wiederum aus dem Auftriebsgebiet vor Namibia. Wie im ersten Beispiel ist auch der Schwerelotkern GeoB 3718 durchweg sulfidisch. Da mit ihm jedoch auch der methanhaltige Bereich des Sedimentes erreicht wurde, kann außerdem betrachtet werden, wie sich die tiefe Sulfatreduktion im Bereich der Sulfat/Methan Übergangszone auf die Festphasenchemie auswirkt.

Der Vorstellung dieser drei Beispiele folgt eine gesonderte Betrachtung des Einflusses von nicht stationären Bedingungen auf die Porenwasser- und Festphasenchemie mariner Sedimente (Kapitel 5) und eine abschließende Zusammenfassung der Ergebnisse (Kapitel 6). Eine Übersicht über die untersuchten Elemente gibt die Darstellung auf Seite 116 - 117. Alle Daten, die im Rahmen dieser Arbeit gewonnen wurden, können auch über die Umweltdatenbank Pangaea (http://www.pangaea.de) abgerufen werden.

Die Kapitel 2 - 4 beruhen vollständig auf meinen eigenen Arbeiten. Sie wurden von mir als drei eigenständige Manuskripte für die Publikation in internationalen Fachzeitschriften vorbereitet und erscheinen daher in englischer Sprache. Als Co-Autoren wurden die Kolleginnen und Kollegen aufgenommen, die das zugrunde liegende Forschungsprojekt beantragt und fachlich begleitet haben. Kapitel 5 beruht auf einem englischsprachigen Manuskript, an dem ich neben Dr. Sabine Kasten, Dr. Matthias Zabel und Dr. Christian Hensen als Co-Autorin beteiligt bin, da ich wesentliche Teile des Kapitels 5.5 (Redistribution of elements and formation of element enrichments within the zone of deep sulphate reduction) verfaßt habe und daneben die Analyse von Spurenelementen in den Kernen GeoB 2908-7 und GeoB 4216-1 (Kapitel 5.4) fachlich begleitet habe. Dieses Manuskript wurde einerseits wegen meines inhaltlichen Anteils und andererseits wegen seiner engen thematischen Verbindung zu den anderen Einzelarbeiten vollständig in die Dissertation aufgenommen. Um der vorliegenden Arbeit trotz der kumulativen Form ein einheitliches Erscheinungsbild zu geben, wurden auch die einleitenden und abschließenden Kapitel 1 und 6 in Englisch verfaßt und sämtliche Literaturangaben am Ende der Arbeit gebündelt. Eine deutsche Zusammenfassung und eine Übersicht über die Untersuchungsergebnisse folgt im Anschluß an Kapitel 6 (S. 112 ff.).

Contents

Chapter 1: Introduction

Marine sediments represent the major sink for material that leaves the sea water reservoir. They provide information about the productivity and chemistry of the oceans as well as about the nature and controls of terrigenous sedimentation in the deep sea. They are sensitive recorders of changes in the sedimentary environment, and they preserve evidence of fluctuations in biological productivity and climatic change (Kennett, 1982; Chester, 1999).

Geochemical investigations allow to characterise the material that is deposited in sediments as well as early diagenetic modifications that occur subsequent to the arrival of a particle at the sediment/water interface. Based on the relative abundance of single trace elements in the solid phase of sediments, Goldberg (1954) distinguished five potential sediment components of different origin, i.e. (a) lithogenous components - which arise from land erosion, from submarine volcanoes or from underwater weathering, (b) biogenous components - which are produced in the biosphere and include both organic matter and inorganic shell material, (c) hydrogenous components - which result from the formation of solid material in the sea by inorganic reactions, and additionally (d) atmogenous and (e) cosmogenous components with an atmospheric and extraterrestrial origin, respectively.

Similarly, different continental sources of lithogenous components may be distinguished due to their specific geochemical composition. Thus, in sediments the input of terrigenous material from various continental sources can be identified on the basis of interelement ratios. In this manner, a geochemical multi-element analysis can be useful for the reconstruction of sedimentation patterns in an ocean basin and in particular for the identification of changes in aeolian and fluvial input that result from variations in the intensity of the atmospheric circulation and hydrographic conditions (e.g., Leinen, 1987; Kyte et al., 1993; Fagel et al., 1997; Banakar et al., 1998; Sirocko et al., 2000).

As opposed to lithogenous components, biogenous material is easily decomposed after its deposition in sediments. This is particularly true for non-skeletal organic matter but carbonaceous shell material is subject to considerable dissolution as well (e.g., de Lange et al., 1994; Rullkötter, 2000, Pfeifer et al., in press). Nevertheless, a geochemical multi-element analysis can provide useful information about the input and degradation of biogenous components.

On the one hand, a reconstruction of marine productivity that is only based on the organic carbon (C_{org}) content of sediments comprises large uncertainties due to the heterogeneous preservation of the primary signal. Consequently, additional proxies are required for more reliable estimations of paleoproductivity (e.g., Rühlemann et al., 1999; Wefer et al., 1999) and these proxies might be derived from the chemistry of the inorganic sediment fraction (e.g., Kyte et al., 1993). For example, Ba has received considerable attention as a potential proxy for the primary productivity in marine surface waters (e.g., Dehairs et al., 1980;

Bishop, 1988; Dymond et al., 1992; Francois et al., 1995; Gingele et al., 1999). Although its biogeochemical relation to productivity is not completely understood Ba offers one major advantage over other productivity related parameters like C_{org} and $CaCO_3$. It forms discrete barite ($BaSO_4$) crystals that are well preserved in the sediment due to their highly refractive nature (Dehairs et al., 1980; Gingele and Dahmke, 1994). In principle, there is only one important diagenetic process that alters the sedimentary Ba record and limits its use as a proxy for paleoproductivity: the dissolution of barite in sulphate-depleted sediments (e.g., Brumsack, 1986; von Breymann et al., 1992; Torres et al., 1996; Dickens, 2001).

On the other hand, degradation of organic matter does not only obscure any relation between the productivity in surface waters and the preservation of organic carbon (C_{org}) in sediments (e.g., de Lange et al., 1994; Rullkötter, 2000). The remineralization process fuels also a variety of redox reactions which can alter the composition of the solid phase (e.g., Froelich et al., 1979; Berner, 1980; 1981). In particular, Mn and Fe are dissolved and mobilised by the reduction of Mn(IV) and Fe(III) oxides in post-oxic environments whereas the precipitation of sulphides binds metals to the solid phase in sulphidic sediment sections. Ultimately, these early diagenetic processes affect the distribution of all trace elements that are related to the biogeochemical cycles of organic carbon (C_{org}), manganese, iron, and sulphur, as well (e.g., Shaw et al., 1990).

The early diagenetic redistribution of trace elements has been shown to produce distinct new signals in the solid phase of sediments. These signals are potential indicators for variations in the primary input and early diagenetic degradation of organic matter. For example, metal enrichments have been shown to document periods of non-steady state diagenesis that are initiated by the formation of C_{org} rich sapropels (e.g., Pruysers et al., 1993; Thomson et al., 1995; Passier et al., 1996; 1998; van Santvoort et al., 1996; 1997), by glacial/interglacial transitions (e.g., Thomson et al., 1984b; 1996; Wallace et al., 1988; Kasten et al., 1998) or by the deposition of turbidites (e.g., Colley et al., 1984; Wilson et al., 1985; 1986b; Thomson et al., 1993; 1998a; 1998b).

Objectives of this study

In this study, a geochemical multi-element investigation was applied to further elucidate whether the distribution of trace elements in the solid phase of sediments documents (a) primary production and input of C_{org}, and/or (b) early diagenetic processes and redox conditions of the sediment. So far, comparable studies have usually focussed on the sediment-water interface or on sediment sequences that were deposited under non-steady state conditions. In the former case, a shallow sampling depth and a small vertical extension of redox zones may not allow to identify a relation of trace elements to productivity or early diagenesis. In the latter case, distinct secondary enrichments dominate the distribution of

trace elements in the solid phase of the sediment. In contrast, this investigation comprises pore water and solid phase and analyses over the whole length of three 10 - 20 m long gravity cores that were taken from the equatorial and Southeast Atlantic. The investigated sediments cover a variety of redox conditions in pore water and the vertical series of diagenetic zones shows a particularly large thickness of single zones. These characteristics support the identification of a correspondence between redox conditions in pore water and trace element patterns in the solid phase of the sediments.

A relation of trace elements to primary production and/or early diagenesis was expected, since many trace elements are related to the biogeochemical cycles of organic carbon (C_{org}), manganese, iron, and sulphur. Trace elements are drawn into the food chain by marine primary production until the decomposition of organic matter releases them again (Martin and Knauer, 1973; Brewer, 1975; Bruland, 1983; Collier and Edmond, 1984). They are adsorbed to particulate Mn and Fe oxides (Goldberg, 1954; Glasby, 2000) until the reduction of Mn and Fe mobilises them in post-oxic environments (Graybeal and Heath, 1984; Glasby, 2000). Finally, under sulphidic conditions they are fixed by the precipitation of insoluble sulphides (Elderfield et al., 1981; Kasten and Jørgensen, 2000). These processes are also summarised in Fig. 1.1 and will be described in more detail below.

Biogeochemical Processes in the Water Column

In sea water the involvement of trace elements in biogeochemical processes is reflected in their vertical distribution in the water column (Bruland, 1983). The vertical concentration profile of the dissolved element fraction corresponds either to a nutrient-type (internally-produced biotic particles) or to a scavenging-type (externally produced non-biotic particles) mechanism or to a combination of both. As opposed, trace elements that are not involved in biogeochemical processes show a conservative type of distribution. They have a constant concentration relative to salinity.

The characteristic features of a *nutrient-type distribution* are a depletion in surface waters and an enrichment at some depth within the water column. A nutrient-type distribution is displayed by those trace elements which are involved in the major oceanic biological cycles, for example As, Cd, Cu, Ni and Zn (Bruland, 1983). The depletion of elements in surface waters arises from the growth of phytoplankton that goes along with an extraction of nutrients and trace elements from the water. As the organisms die and sink down the water column they undergo oxidative decay during which there is a regeneration of the nutrients, and the associated trace elements, back into solution. In the open ocean, only about 1% of the primarily produced organic matter reaches the sediment surface and is ultimately buried in the sediment (e.g., Suess, 1980; Emerson and Hedges, 1988; Wakeham and Lee, 1989; Berger et al., 1989; Rullkötter, 2000).

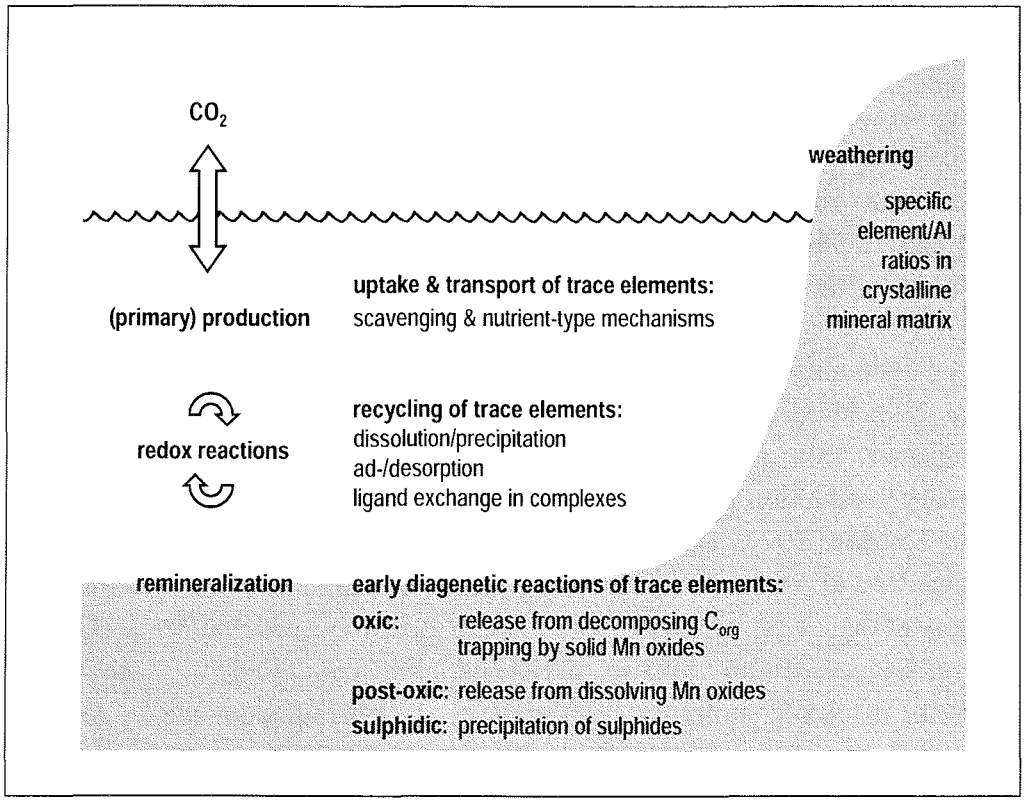

Fig. 1.1: *Biogeochemical processes of trace elements in marine environments.*

Elements can become associated with the biogenic carriers either because they are specific to biological requirements or because they are taken up by analogy with essential elements; i.e. they get involved in biochemical processes related to metabolism. Moreover, they can be scavenged by biogenic particles in association with terrigenous material, hydrous metal oxide precipitates or organics (Collier and Edmond, 1983). Collier et al. (1983) reported that the majority of trace elements are directly coupled to the non-skeletal organic phases of the plankton. Based on the general ease of metal release from decaying organic matter to sea water three types of host association were distinguished. These are a very labile association (which included the nutrient P and major fractions of the total amounts of Cd, Mn, Ni and Cu), a moderately refractory association (which included significant fractions of the total amounts of Cu, Ni, Cd, Ba, Mn and Zn), and a strongly refractory association (which included large fractions of the total amounts of Si, Al, Fe and Zn). In contrast, calcium carbonate and opal were not found to be significant carriers for any of the elements studied.

As opposed to a nutrient-type distribution, a *scavenging-type distribution* of trace elements is characterised by a surface enrichment and a depletion at depth. For example, Pb and ^{210}Pb show this type of distribution (Bruland, 1983). The term scavenging refers to the adsorption of trace metals to inorganic particles like aluminosilicates, manganese and iron oxides that sink down the water column (Goldberg, 1954). The dissolved down-column

concentration curves of scavenged elements are concave in deep water when plotted against a conservative tracer. This type of distribution indicates the loss of elements from the water column. The scavenging of trace elements from sea water is a complex process. The scavenging removal itself is dominated by the fine-particle population, but is then complicated by an association of the fine particles with the large-particle flux by reversible physical mechanisms (e.g. 'piggy-backing') and by reversible chemical adsorption that may tend towards an equilibrium state (Chester, 1999).

Aside from vertical concentration profiles that are related to a conservative, nutrient-type or scavenging-type behaviour of dissolved trace elements, further distribution patterns can occur in the water column as well. These include for example (a) a mid-depth minimum type that is caused by a surface and a deep water source; (b) a mid-depth maximum type that is associated with a mid-depth sources (e.g. hydrothermal input of Mn), and (c) maxima or minima associated with anoxic waters (Bruland, 1983).

The processes involved in the removal of trace elements from sea water can be summarised as (a) precipitation due to saturation, (b) adsorption onto particulate matter and (c) interactions with the biosphere (e.g. complexation with organic ligands). With respect to these processes the speciation of trace elements is an important factor. Speciation refers to the individual physicochemical forms of an element, i.e. its distributions between ions, ion pairs, complexes (both inorganic and organic), colloids and particles. Major processes that affect chemical speciation in sea water are solid-aqueous phase exchange, electron exchange (redox chemistry), proton exchange (acid-base chemistry) and ligand exchange (complex chemistry). The speciation of a trace element has a strong influence on both its particle reactivity and its bioavailability, and so exerts an important control on the processes that are involved in its removal from sea water (Chester, 1999; Stumm and Morgan, 1996).

Early Diagenetic Processes in Marine Sediments

On approaching the sea bed sinking particles enter the benthic boundary layer. This layer is an oceanic region of considerable reactivity where further recycling can occur before particulate matter is finally deposited as sediment (Zabel et al., 2000). Sediments, in turn can be subjected to a series of chemical, physical and biological reactions following their deposition. These reactions take place mainly via the medium of pore waters. They have been grouped together under the term early diagenesis, which has been defined by Berner (1980) as 'the sum total of processes that bring about changes in a sediment or sedimentary rock subsequent to its deposition in water' and 'during burial to a few hundred meters where elevated temperatures are not encountered and [...] pore spaces of the sediment are continually filled with water'.

Many early diagenetic reactions are redox-mediated, i.e. they depend on the redox environment in the sediment - interstitial water - sea water system. This redox environment, in turn, is largely controlled by the decomposition of organic matter. Of the total biomass that is formed in the photic zone of the ocean, only a very small portion reaches the underlying sea floor where most of the biogenic detritus is oxidised close to the sediment/water interface (e.g., Bender and Heggie, 1984). In the benthic boundary layer the consumption of organic matter is increased due to the activity of epibenthic organisms. This intensified consumption continues in the upper sediment layer where burrowing organisms depend on the supply from the water column. The further decay of C_{org} occurs largely via catabolic microbial reactions that are involved in the breakdown of organic molecules to simple molecules or inorganic species (e.g., Jørgensen, 2000). Organic matter degradation can eventually extent deeply into the sediment as became evident from the detection of a so-called deep biosphere at several hundred meters below the sea floor (Parkes et al., 1994).

As sedimentary organic matter is metabolised it donates electrons to several oxidised components in the pore water - solid phase complex, and when oxygen is present it is the preferred electron acceptor. However, as oxygen is exhausted, microbial organisms switch to alternative terminal electron acceptors. The general succession of alternatively used oxidants is $O_2 \rightarrow NO_3^- \rightarrow Mn(IV) \rightarrow Fe(III) \rightarrow SO_4^{2-} \rightarrow CO_2$. This sequence corresponds to a gradual decrease in redox potential of the oxidants and thus to a decreasing energy production per mole of oxidised organic carbon (e.g., Froelich et al., 1979). In sediments, the successive use of the different oxidants sets up a vertical series of redox zones. The thickness of these zones is largely controlled by the organic matter flux to the site of deposition (which is dependent of the degree of primary production in the overlying waters) and by the accumulation rate of the sediment.

Environments that contain measurable dissolved oxygen in pore water are termed oxic. In contrast, anoxic environments are those in which the sediment interstitial waters contain no measurable dissolved oxygen. Anoxic environments can be subdivided into a number of types. In post-oxic or sub-oxic environments diagenesis has proceeded beyond the oxic stage using nitrate, manganese oxides and iron oxides as oxidants, but the sequence does not reach the stage at which sulphate is utilised for this purpose. The formation of sulphide due to bacterial reduction of dissolved sulphate characterises sulphidic environments. In sediments with relatively large amounts of metabolisable organic matter early diagenesis can pass through the stages at which oxygen, nitrate, manganese oxides, iron oxides and sulphate are sequentially utilised. A continued decomposition of organic matter by fermentation results in the formation of methane.

During early diagenesis (trace) elements are released into solution as their carrier phases are decomposed or dissolved (e.g., Klinkhammer, 1980). Some (trace) elements are mobilised in the oxic zone close to the sediment/water interface where organic matter is effectively decomposed by oxygen. Others are released at a depth where secondary

oxidants, such as Mn oxides, are utilised for the remineralization of organic matter. In pore water diffusive fluxes will transport the dissolved elements in either upward or downward directions to the effect that they are either released into sea water or reincorporated into the solid phase of the sediment (e.g., Schulz et al., 1994; 2000).

Once liberated into pore water, the mobility of a particular element depends on its speciation, the prevailing redox conditions, the chemical composition of the pore water and the nature of the particulate phases present in the sediment. For elements whose valency varies as a function of redox potential (e.g. Fe, Mn, V, Cr, As, Mo, U) the prevailing redox conditions determine the species distribution and as a consequence their partitioning between the solid phase and pore water. For example, Fe and Mn form highly insoluble oxides under oxic conditions but are mobilised by microbial reduction in post-oxic environments. In contrast, V, Cr, Mo and U occur as highly soluble anionic species in oxic waters and are reduced to particle reactive or easily precipitating species of lower valency under post-oxic conditions.

A redox-cycling of these elements can result in marked element enrichments in the solid phase of a sediment. In particular the formation of Mn-rich bands is a well studied process. Mn(IV) oxides are deposited in a particulate form at the sediment surface. In the course of sediment burial these solid Mn(IV) oxides cross the Mn(IV)/Mn(II) redox boundary. Below of this redox boundary the reduction of Mn(IV) can produce dissolved Mn^{2+}. Molecular diffusion moves the latter across the Mn(IV)/Mn(II) redox boundary into the overlying sediment, where the oxidation of dissolved Mn^{2+} results in the precipitation of Mn(IV) oxides. As sedimentation proceeds, these oxides are again carried down into the reducing zone and the cycle starts again. The overall result of this recycling process is the trapping of solid-phase Mn in a narrow zone at the Mn(IV)/Mn(II) redox boundary (e.g., Lynn and Bonatti, 1965; Froelich et al., 1979).

If trace elements cannot undergo redox reactions themselves, changing redox conditions will still affect them via both the dissolution or precipitation of carrier phases like Mn oxides and the authigenic formation of mineral phases, in particular sulphides (e.g., Bonatti et al., 1971; Calvert and Price, 1972; McGeary and Damuth, 1973; Elderfield et al., 1981; Graybeal and Heath, 1984; Brumsack, 1986; Shaw et al., 1990; Calvert and Pedersen, 1993). For example, Ni, Co, and Cu are released in the manganese reduction zone (Shaw et al., 1990). Ni, Cu, and Zn are also known to form sulphides and their precipitation and enrichment in sulphidic environments has been reported in numerous studies (e.g., Francois, 1988; Huerta-Diaz and Morse, 1990; 1992; Calvert and Pedersen, 1993; Morse and Arakaki, 1993; Morse, 1994; Sternbeck et al., 2000).

On the whole, there is a complex coupling between trace elements and the various biogeochemical cycles in sediments. Due to this fact, scavenging of metals by the solid phase of sediments is still a poorly understood process. The remineralization of organic matter seems to be a key process for the distribution of trace elements since it acts in two

ways. On the one hand it goes along with the release of trace elements in a nutrient-type fashion. On the other hand it fuels a variety of redox reactions that control the valency state of trace metals, the availability of adsorption sites on Mn and Fe oxides and the formation of sulphides. However, it is not the only possible reaction in the sedimentary part of the organic carbon cycle. Sulphurization, i.e. the reaction of organic matter with reduced inorganic sulphur species (H_2S and/or polysulphides), is another important mechanism during the early stages of diagenesis (Sinninghe Damsté and de Leeuw, 1990; Kohnen et al., 1991; Schouten et al., 1994b; Lückge et al., 1999). It works as an antagonist to remineralization since the intra- and intermolecular incorporation of sulphur supports the preservation of organic compounds (Sinninghe Damsté et al., 1989; 1998; Werne et al., 2000). While in the last decade numerous studies have investigated possible mechanisms for sulphurization and provided hypotheses for various reduced sulphur species and classes of organic compounds little attention has been paid to its consequences for the fate of trace elements during early diagenesis.

Chapter 2: Does sulphurization create an early diagenetic link between trace elements and organic matter? – Evidence from the upwelling region off Namibia, Southeast Atlantic

Verena Heuer, Sabine Kasten, Horst D. Schulz
Fachbereich Geowissenschaften, Universität Bremen, Postfach 330 440, D-28334 Bremen

Abstract

In this study we present data from the highly productive upwelling region off Namibia that indicate a close relation between the sulphurization of organic matter and the distribution of trace elements in the solid phase of sulphidic sediments. Total solid phase contents of 26 elements were analysed over the whole length of a 10.7 m long gravity core. Subsequently, total measured element contents were split up into lithogenic and an excess fractions by a normative calculation. Based on this approach two groups of elements could be distinguished. Ce, Co, Cr, Fe, Ga, K, La, Mg, Mn, Nd, Pb, Pr, Sc, Sm, Ti, V, Yb, and Zr (group A) are closely correlated to Al and their total solid phase contents are controlled by the lithogenic contribution, i.e. by terrigenous aluminosilicates. In contrast, Cu, Mo, Ni, and Zn (group B) have large excess fractions that match both the solid phase contents of organic carbon (C_{org}) and total sulphur contents (S_{tot}). At the same time a close correlation between C_{org} and S_{tot} is observed throughout the investigated core. However, neither group B elements nor C_{org} match the distribution pattern of the paleoproductivity proxy Ba_{xs}.

We suggest that the correspondence of Ni, Cu, Zn, and Mo to C_{org} and S_{tot} does not result from the primary input of trace metals with organic matter but from an early diagenetic redistribution: solid phase contents of these trace elements might be controlled by a complexation with either sulphur containing functional groups or polysulphide bridges that result from the intra- and intermolecular incorporation of sulphur into organic matter.

2.1. Introduction

In the marine environment trace elements are closely linked to the production and remineralization of organic matter. Their uptake and enrichment by marine organisms can have both nutritional and toxic effects and has therefore been studied in detail (Martin and Knauer, 1973; Brewer, 1975; Collier and Edmond, 1984). The overall effect of these interactions is reflected in the nutrient type distribution of several trace elements in the water column (Bruland, 1983).

Of all the biogenic material that is produced in the water column only a minor part settles down to the seafloor where it is further degraded (e.g., Bender and Heggie, 1984; Reimers and Smith, 1986; Berelson et al., 1987). Numerous sediment studies have indicated that the degradation of organic matter induces the release of trace elements into pore water (e.g., Klinkhammer, 1980; Klinkhammer et al., 1982; Trefry and Presley, 1982; Sawlan and Murray, 1983; Heggie et al., 1986; Gobeil et al., 1987; Gerringa, 1990) and flux studies like those of Westerlund et al. (1986) and Zhang et al. (1995) support these observations.

Moreover, the remineralization of organic matter also fuels a variety of early diagenetic redox processes in the sediment (Froelich et al., 1979; Berner, 1981). Trace elements are influenced by these processes either directly or indirectly. If they can change their valency state in the redox field of sediments like V, Mo, and Cr they will be able to act as electron donors or acceptors in the course of redox cycling. If they cannot undergo redox reactions themselves, changing redox conditions will still affect them via both the dissolution or precipitation of carrier phases like Mn oxides and the authigenic formation of mineral phases, in particular sulphides (e.g., Bonatti et al., 1971; Calvert and Price, 1972; McGeary and Damuth, 1973; Elderfield et al., 1981; Graybeal and Heath, 1984; Brumsack, 1986; Shaw et al., 1990; Calvert and Pedersen, 1993). In addition, the mobility of many trace elements is influenced by complexation processes that in turn are sensitive to geochemical changes in the course of organic matter degradation (Brewer, 1975).

The impact of early diagenetic redox reactions on the redistribution of trace elements has been well documented for turbidites (e.g., Colley et al., 1984; Wilson et al., 1985; 1986b; Thomson et al., 1993; 1998a; 1998b), sapropels (e.g., Pruysers et al., 1993; Thomson et al., 1995; Passier et al., 1996; 1998; van Santvoort et al., 1996; 1997) and glacial/interglacial transitions (e.g., Thomson et al., 1984b; 1996; Wallace et al., 1988; Kasten et al., 1998; 2001). In these sediments the supply of organic matter from the water column is not constant over time and other environmental factors like the oxygen content of the seawater and the bulk sedimentation rate vary as well. The resulting change in the burial rate of organic matter forces early diagenesis into a non-steady state. Under these circumstances redox zones remain at a particular sediment depth for a prolonged period of time and distinct enrichments and depletions of trace elements can evolve in the solid phase of the sediment. These secondary signals, in turn, allow to infer past changes in biological

productivity and/or bottom water oxygen content from the sedimentary record (Calvert and Pedersen, 1993).

The remineralization of organic matter is a key process in early diagenesis and its effects on the distribution of trace elements have been shown in many studies. However, it is not the only possible reaction in the sedimentary organic carbon cycle. Sulphurization, i.e. the reaction of organic matter with reduced inorganic sulphur species (H_2S and/or polysulphides), is another important mechanism during the early stages of diagenesis (Sinninghe Damsté and de Leeuw, 1990; Kohnen et al., 1991; Schouten et al., 1994b; Lückge et al., 1999). It works as an antagonist to remineralization since the intra- and intermolecular incorporation of sulphur supports the preservation of organic compounds (Sinninghe Damsté et al., 1989; 1998; Werne et al., 2000). While in the last decade numerous studies have investigated possible mechanisms for sulphurization and provided hypotheses for various reduced sulphur species and classes of organic compounds little attention has been paid to its consequences for the fate of trace elements during early diagenesis.

In this study we present data from the highly productive upwelling region off Namibia that indicate a close relation between the sulphurization of organic matter and the burial of several trace elements in the upper tens of meters of diagenetically active sediments. This observation is based on a high resolution geochemical survey of 26 elements in the solid phase of a 10.7 m long gravity core that records the last 135 ka. The influence of productivity-related primary input and the potential effects of early diagenesis are checked with Ba as a proxy for paleoproductivity and pore water analysis, respectively.

2.2. Sampling Sites and Core Descriptions

Site GeoB 1711 is located in the upwelling region off Namibia (23°18.9'S, 12°22.6'E) and was sampled in January 1992 during RV Meteor cruise M 20/2 to the eastern South Atlantic (Fig. 2.1). The 10.66 m long gravity core GeoB 1711-4 was recovered from the continental slope at a water depth of 1967 m. A parallel core (GeoB 1711-3) of similar length was taken for pore water analysis. According to the age model that Little et al. (1997) have established from planktonic foraminifera the sedimentary record of GeoB 1711-4 covers the last 135,000 years and terminates in isotope stage 6.2. The corresponding sedimentation rates vary between 5 and 10 cm/ka.

At present Southeast-Northwest trade winds cause the upwelling of nutrient-rich water masses in this area (Wefer and Fischer, 1993) and thus enhance the primary productivity within the surface waters and the organic matter export to the sediment (Embley and Morley, 1980; Gingele, 1992). Mineralization patterns indicate that the input flux of organic

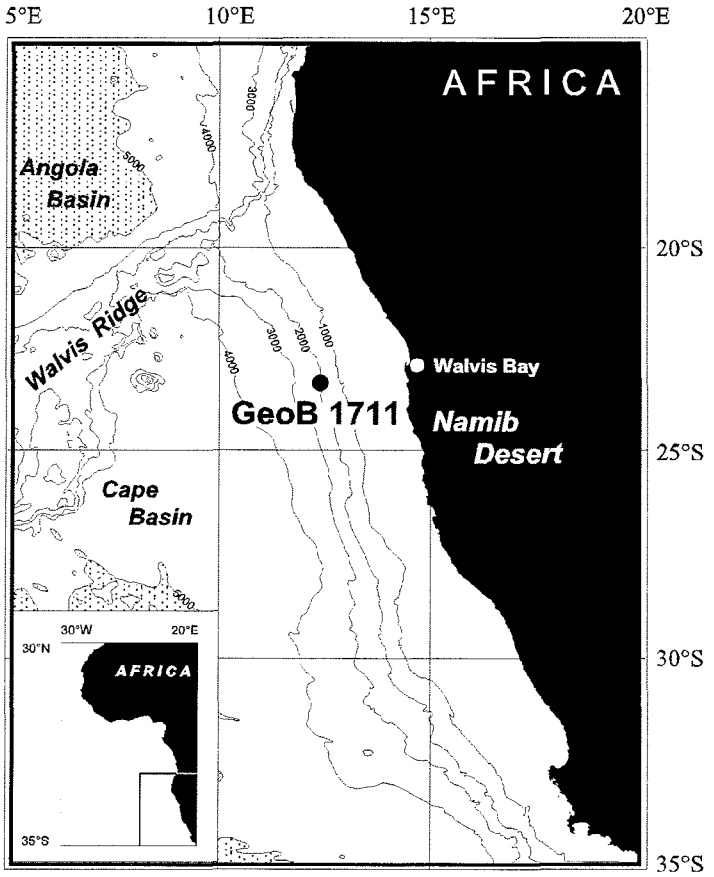

Fig. 2.1: *Map showing the location of site GeoB 1711 at the continental slope off Namibia (23°18.9'S, 12°22.6'E; water depth: 1967 m)*

matter is controlled by "vertical" transport through the water column (Hensen et al., 2000). At site GeoB 1711 the organic carbon content varies between 1 and 7 wt% (Kirst et al., 1999) and suggests intense early diagenetic degradation processes with strong effects on the pore water chemistry.

Due to the trade winds and the lack of large rivers terrigenous material reaches the continental slope off Namibia mainly via the aeolian pathway (Lisitzin, 1996). The contribution of the terrigenous sediment fraction to the bulk sediment is of minor importance at site GeoB 1711 while the biogenic sediment components dominate. Sedimentology and further core characteristics are given in the cruise report (Schulz et al., 1992).

2.3. Methods

2.3.1. Geochemical Analysis

Directly after recovery gravity core GeoB 1711-3 was cut into 1 m segments and taken to a refrigerated on-board laboratory (4°C) where pore water was extracted in the inert atmosphere of an argon filled glove-box. Sulphide was measured in the extracted pore water using an autoanalyzer and photometric standard procedures as described earlier (Schulz et al., 1994; Schulz, 2000). Subsamples of the pore water were preserved for the analysis of sulphate that was determined on land by ion chromatography.

Solid phase analysis was carried out on archived core material that is kept at the Department of Geosciences, University of Bremen, Germany. The whole length of gravity core GeoB 1711-4 was sampled every 5 cm. Samples (ca. 10 cm^3) were freeze-dried and ground in an agate mortar prior to further processing.

For bulk solid phase analysis 50 mg of dry sediment were digested in a microwave system (MLS – MEGA II and MLS – ETHOS 1600) with a mixture of concentrated nitric (3 ml), hydrofluoric (2 ml) and hydrochloric (2 ml) acids of supra-pure quality at a temperature of ~200°C and a pressure of 30 kbar. The digestion solutions were evaporated to dryness, redissolved in 0.5 ml concentrated nitric acid and 4.5 ml deionized water (MilliQ), homogenised and finally made up to a volume of 50 ml.

Major, minor and trace elements were analysed by inductively coupled plasma atomic emission spectrometry (ICP-AES) using a Perkin Elmer Optima 3300RL. For the measurement of trace elements an ultrasonic nebulizer was employed in order to improve the detection limit. The precision of the ICP-AES determination (three consecutive measurements on the same solution) was better than 1% for major and minor elements and in the range of 1-3% for all trace elements except for Pb (6%) and Pr (7%). The accuracy of the analytical procedure was checked using standard reference material USGS MAG-1 (Gladney and Roelandts, 1988). For all elements the difference between the measured element contents and the certified concentration ranges was less than 4% and standard deviations of 25 replicates were less than 3%.

A detailed description of the used methods is also available at our homepage (http://www.geochemie.uni-bremen.de).

2.3.2. Normative Calculation of Element Fractions

In order to distinguish between different potential carrier phases of trace elements we employed a normative calculation of element fractions. This calculation is based on the assumption that the total measured element concentration TE_{tot} consists of a lithogenic fraction TE_{lith} and an additional excess fraction TE_{xs} (Eq. 1). The lithogenic fraction, i.e. the detrital part present in aluminosilicates, can be calculated from a constant element-aluminium ratio k(TE/Al) and the measured total aluminium content Al_{tot} (Eq. 2). Consequently, the excess fraction results from the difference between the total measured element concentration and the calculated lithogenic fraction (Eq. 3).

(1) $TE_{tot} = TE_{lith} + TE_{xs}$

(2) $TE_{lith} = k(TE/Al) \cdot Al_{tot}$

(3) $TE_{xs} = TE_{tot} - k(TE/Al) \cdot Al_{tot}$

For the calculation of lithogenic element fractions we applied the constant element-aluminium ratios k(TE/Al) that result from the average composition of the continental crust as given by Wedepohl (1995) (Table 2.1).

2.4. Results and Discussion

The geochemical results for gravity core GeoB 1711-4 are summarised in Table 2.1. In addition, the full data set is available via the geological and environmental data network Pangaea (http://www.pangaea.de).

2.4.1. Overall Sediment Characteristics

In the solid phase of gravity core GeoB 1711-4 (Fig. 2.2) calcium carbonate dominates with 50 to 80 wt% while the terrigenous sediment fraction is of minor importance and contributes an aluminium-oxide content of only 2 to 7 wt%. The high organic carbon content (C_{org}) makes up 1 to 7 wt% (Kirst et al., 1999). On total, the mass balance leaves a rest of about 25 wt% for silicate phases that were not accessible with the employed methods.

The pore water analysis of gravity core GeoB 1711-3 confirms that the intense degradation of organic matter has caused reducing conditions in the sediment (Fig. 2.2). In particular,

				TE/Al				TE_{xs}
	mean	SD	r(Al)[a]	mean	SD	k(TE/Al)[b]	enrichment[c]	mean[d]
	[g/kg]	[%]		[g/g]	[%]	[g/g]		[%]
Al	22.0	26						
Ba	1.13	19	0.13	0.055	33	0.004[e]	13.8	92
Ca	262	12	-0.82					
C_{org}	34.6	47	0.59					
S	6.87	33	0.56					

	TE_{tot}			TE/Al				TE_{xs}
group A:	mean	SD	r(Al)[a]	mean	SD	k(TE/Al)[b]	enrichment[c]	mean[d]
	[g/kg]	[%]		[g/g]	[%]	[g/g]		[%]
Fe	13.2	26	0.98	0.600	5	0.543	1.1	10
K	7.39	24	0.99	0.339	5	0.269	1.3	21
Mg	7.13	18	0.93	0.334	13	0.276	1.2	16
Ti	1.17	26	0.99	0.053	3	0.050	1.1	5
	[mg/kg]	[%]		[mg/g]	[%]	[mg/g]		
Ce	21.7	17	0.94	1.02	13	0.75	1.4	25
Co	3.09	22	0.92	0.14	11	0.30	0.5	-57
Cr	68.3	29	0.93	3.09	12	1.58	2.0	48
Ga	6.29	24	0.98	0.29	5	0.19	1.5	35
La	11.7	18	0.93	0.55	11	0.38	1.4	30
Mn	82.0	21	0.88	3.82	15	8.99	0.4	-52
Nd	12.0	19	0.93	0.56	11	0.34	1.6	39
Pb	4.33	21	0.84	0.20	14	0.19	1.1	6
Pr	4.24	23	0.93	0.20	9	0.084	2.4	56
Sc	6.27	24	0.96	0.29	8	0.20	1.4	30
Sm	2.52	20	0.93	0.12	10	0.067	1.8	42
V	35.7	21	0.95	1.65	10	1.23	1.3	25
Yb	1.49	16	0.88	0.070	14	0.025	2.8	64
Zr	45.1	25	0.96	2.06	7	2.55	0.8	-19

	TE_{tot}			TE/Al				TE_{xs}
group B:	mean	SD	r(Al)[a]	mean	SD	k(TE/Al)[b]	enrichment[c]	mean[d]
	[mg/kg]	[%]		[mg/g]	[%]	[mg/g]		[%]
Cu	49.1	26	0.71	2.29	21	0.314	7.3	86
Mo	15.2	49	0.53	0.69	48	0.014	49.8	97
Ni	46.2	34	0.71	2.12	26	0.704	3.0	65
Zn	52.0	29	0.76	2.40	22	0.817	2.9	65

(a) Spearman correlation coefficient
(b) average continental crust value according to Wedepohl (1995)
(c) ratio between the TE/Al ratio in gravity core GeoB 1711 and the continental crust value k(TE/Al)
(d) relative contribution of the excess fraction to the total solid phase content
(e) Ba/Al ratio in aluminosilicates according to Gingele and Dahmke (1994)

Table 2.1: *Average composition of gravity core GeoB 1711-4: total solid phase contents of major, minor and trace elements (TE_{tot}) in group A and B; correlation coefficients r(Al) for the correlation between total solid phase contents of trace elements and Al; mean trace element - Al ratios (TE/Al) in the solid phase of gravity core GeoB 1711-4 and their enrichment with respect to the average continental crust values k(TE/Al); relative contribution of the excess fractions (TE_{xs}) to the total solid phase contents*

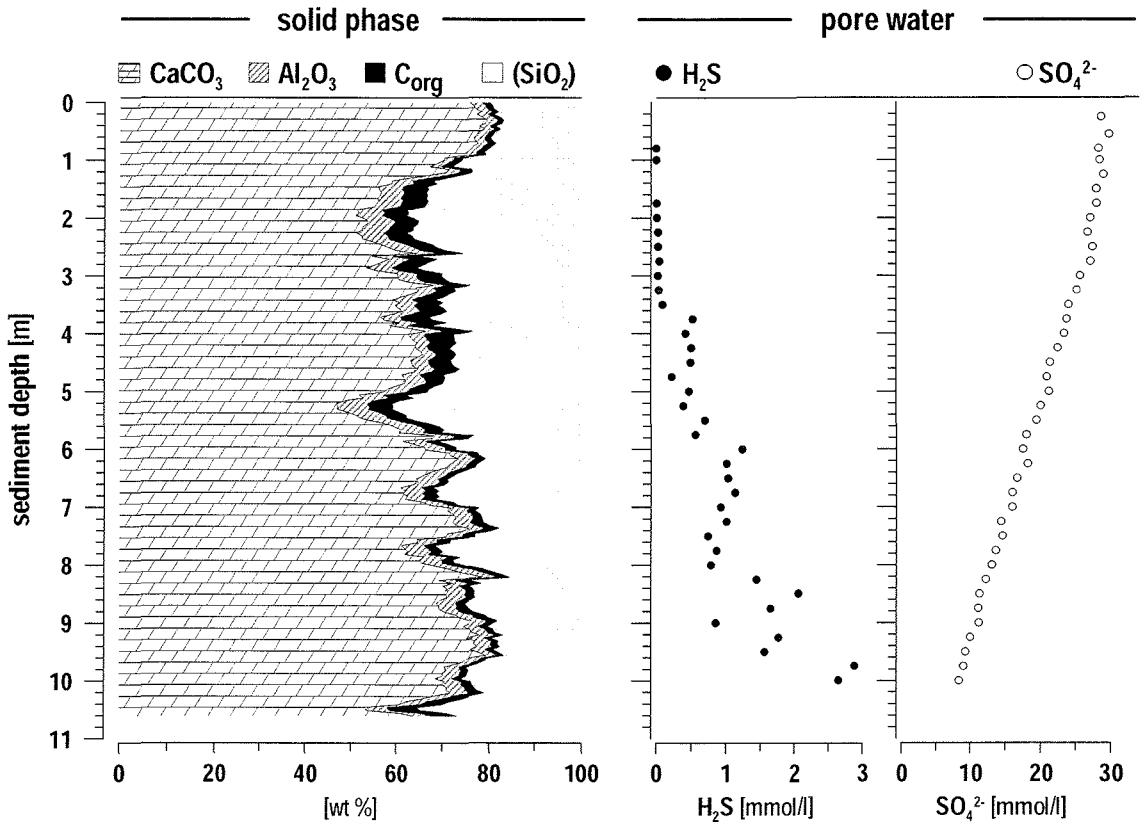

Fig. 2.2: Overall sediment characteristics of site GeoB 1711: bulk solid phase and pore water chemistry. C_{org} data taken from Kirst et al. (1999).

we find hydrogen sulphide in all depths greater than 0.8 meters. Sulphate concentrations decrease with depth and point to a deep sulphate reduction zone. However, this zone was not penetrated by the gravity core.

Figure 2.3 shows the fluctuations of total Al, C_{org}, S and excess Ba (Ba_{xs}) over time. The comparison with Fig. 2.2 reveals that the variations in the Al profile are basically due to the relative dilution by calcium carbonate. Both figures show low C_{org} contents during inter-glacial stages 1 and 5 but higher concentrations in sediments deposited during glacial stages 2, 3 and 6. Similar concentration profiles of C_{org} have been observed before and were attributed to changes in paleo-productivity (Müller and Suess, 1979; Müller et al., 1983; Pedersen and Calvert, 1990). However, if we consider Ba_{xs} as a proxy for paleoproductivity (e.g., Gingele et al., 1999) it is obvious that the effects of preservation have to be considered as well. While the relatively high Ba_{xs} values during stage 2 and 3 still point to enhanced productivity during glacial times the discrepancy between high Ba_{xs} and low C_{org} in stage 1 and 5 indicates intense degradation of organic matter in the sediment. On the whole the preserved C_{org} content is decoupled from its primary input that is still reflected in the Ba_{xs} signal. To the contrary, it is closely related to the total sulphur content (S_{tot}) (Fig. 2.3).

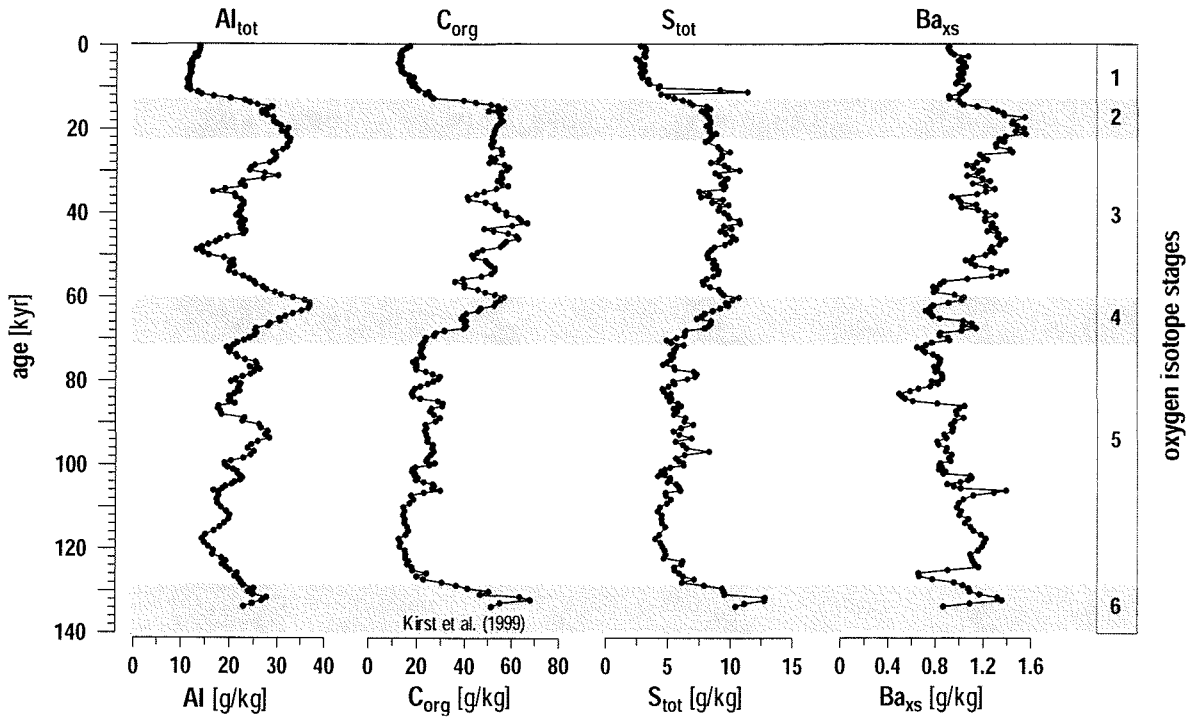

Fig. 2.3: *Distribution of total aluminium (Al_{tot}), total organic carbon (C_{org}), total sulphur (S_{tot}), and biogenic barium (Ba_{xs}) in the solid phase of gravity core GeoB 1711-4. C_{org} data taken from Kirst et al. (1999). Age model of the 10.66 m long core as established by Little et al. (1997).*

We suggest that the good correlation between C_{org} and S_{tot} (r = 0.92) is caused by the sulphurization of organic matter. The relevance of productivity related input and early diagenetic alteration is discussed in more detail below.

2.4.2. Element Associations

The overall characteristics of gravity core GeoB 1711 obviously control the distribution of minor and trace elements in the solid phase of the sediment. We can clearly distinguish two groups of minor and trace elements. Group A (Ce, Co, Cr, Fe, Ga, K, La, Mg, Mn, Nd, Pb, Sc, Sm, Ti, V, Yb, Zr) is governed by the lithogenic sediment fraction that is represented by Al (Fig. 2.4). Group B (Cu, Ni, Mo, Zn) shows a separate distribution pattern (Fig. 2.5) and is closely related to the organic carbon content (Fig. 2.6). However, the origin for this relation is not apparent at first sight. It could be due to productivity driven input as well as to early diagenesis and both possibilities require careful discussion.

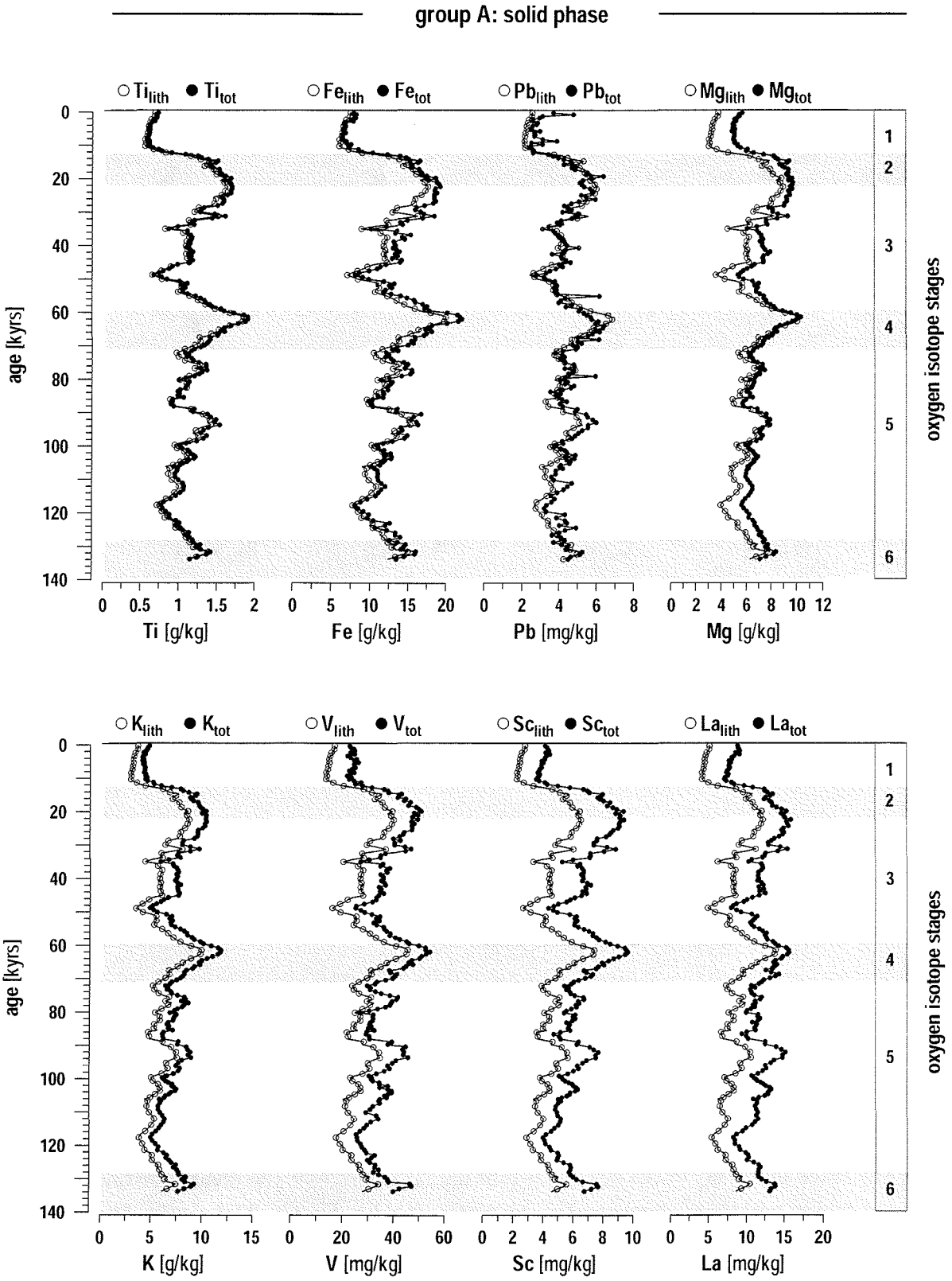

Fig. 2.4: *Distribution of group A elements in the solid phase of gravity core GeoB 1711-4. Calculated lithogenic element fractions of Ti, Fe, Pb, Mg, K, V, Sc, La, Ce, Nd, Sm, Yb, and Cr (Ti_{lith}, ...) closely correspond to the analysed total solid phase contents (Ti_{tot}, ...).*

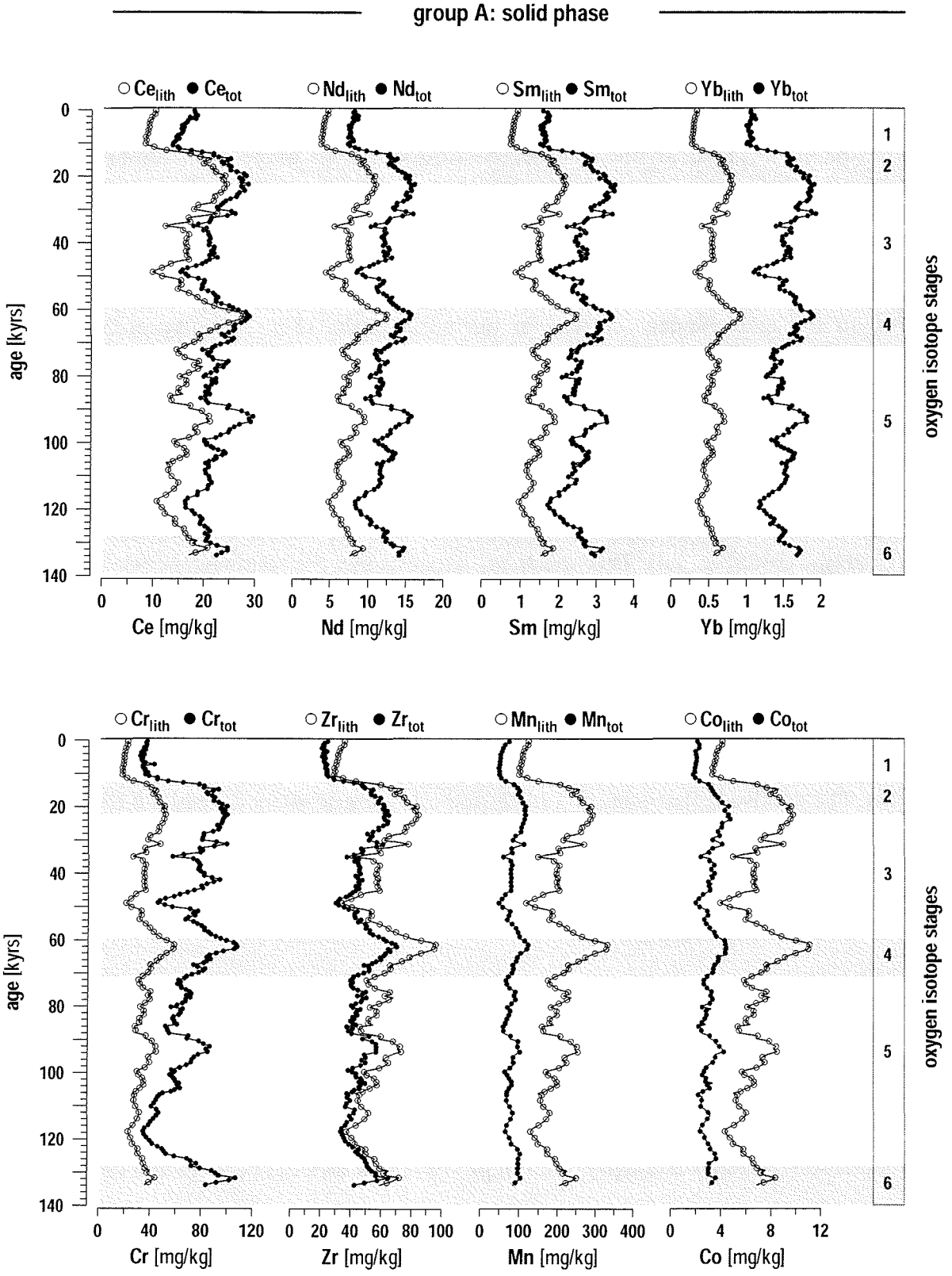

Fig. 2.4 (continued): *For Zr, Mn and Co total solid phase contents are lower than the estimated lithogenic fractions. Age model of the 10.66 m long core as established by Little et al. (1997).*

Group A: Ce, Co, Cr, Fe, Ga, K, La, Mg, Mn, Nd, Pb, Pr, Sc, Sm, Ti, V, Yb, Zr

Group A is characterised by a close correlation of the total element contents and the total Al content. According to the Spearman analysis correlation coefficients r range from 0.99 to 0.84 (Table 2.1). These highly significant correlations go along with almost constant element-aluminium ratios. Standard deviations of the element-aluminium ratios range from 3 to 15% and increase with decreasing correlation coefficients (Table 2.1).

A further feature of this element association is the dominating contribution of the lithogenic fraction to the total element content in the solid phase (Fig. 2.4). According to our normative estimation lithogenic fractions present 50 – 95 % of the total element contents (Table 2.1). For Ti, Fe and Pb the difference between the measured total element content and the calculated lithogenic fraction leaves a constant excess of 5 - 10%. These deviations are within the accuracy of the analytical procedure. For Mg, K, Ga, Sc, V, Cr, La, Ce, Pr, Nd, Sm and Yb the excess is larger and presents on average 16 - 64 % of the total element contents (Table 2.1). The relative contribution of the excess fractions remains constant throughout the core (Fig. 2.4). This constancy suggests that the continental crust values that were used for the normative calculation of the lithogenic element fractions (Table 2.1) systematically underestimate the content of the respective trace elements in the aluminosilicates of the source area. In other words, at site GeoB 1711 element-aluminium ratios of Mg, K, Ga, Sc, V, Cr, La, Ce, Pr, Nd, Sm and Yb are 1.2 to 2.8-fold enriched compared to the average continental crust values (Table 2.1). The opposite is true for Zr, Mn, and Co. These elements are depleted with respect to the estimated lithogenic element contents. The relative deficiencies of 19, 52, and 57 % are constant throughout the core and indicate that the used average continental crust values (Table 2.1) systematically overestimate the content of these elements in the terrigenous sediment fraction.

Group B: Cu, Mo, Ni, Zn

Group B shows a notably lower correspondence to the terrigenous sediment fraction than group A. The correlation coefficients r for the total element contents and Al range from 0.76 to 0.53 and decrease in the order Zn > Ni > Cu > Mo. Likewise standard deviations of the element-aluminium ratios are higher than in group A and vary between 21 and 48 % (Table 2.1).

Furthermore, the normative calculation of element fractions illustrates the minor contribution of the lithogenic element fractions to the total element contents (Fig. 2.5). As opposed to group A the excess fractions dominate in the solid phase of the sediment (Table 2.1). They make up 65 – 97 % of the total element contents and increase in the order Zn =Ni < Cu < Mo. The corresponding total element-aluminium ratios are up to 50-fold

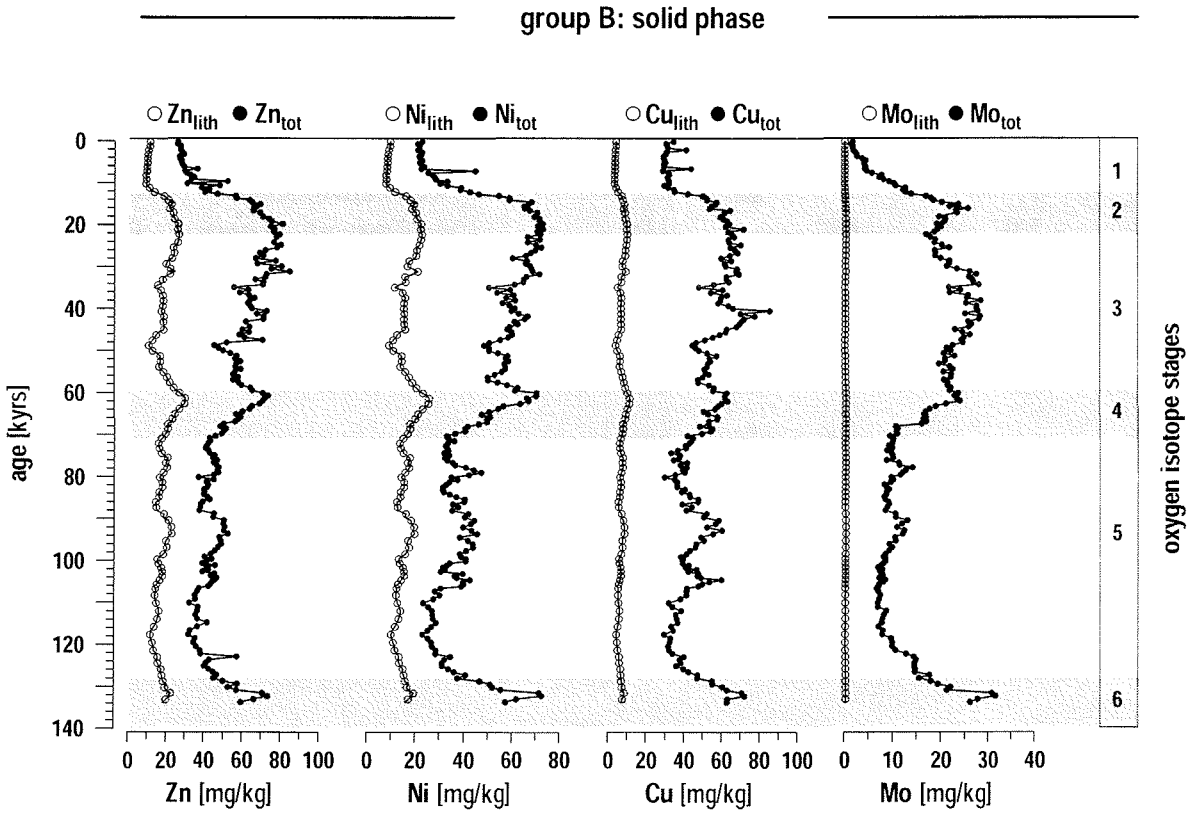

Fig. 2.5: *Distribution of group B elements in the solid phase of gravity core GeoB 1711-4. The lithogenic element fractions of Zn, Ni, Cu, and Mo (Zn_{lith}, ...) are of minor importance for the total solid phase contents (Zn_{tot}, ...) and the large deviations between total element contents and lithogenic element fractions are not constant but vary over depth. Age model of the 10.66 m long core as established by Little et al. (1997).*

enriched with respect to the average continental crust values (Table 2.1). At the same time, the deviation between the total element contents and the lithogenic element fractions is not constant but varies over depth (Fig. 2.5). Therefore, the excess does not result from a systematic underestimation of the trace element contents in the contributing aluminosilicates. Instead, it is associated with at least one further carrier aside from the terrigenous sediment fraction. Indeed Fig. 2.6 reveals its close relation to the organic carbon content. The corresponding correlation coefficients r of the excess fractions and C_{org} range from 0.88 to 0.95 and increase in the order Mo < Cu < Zn < Ni (Table 2.2). These findings point to organic matter as a potential host for the excess fractions of group B elements in the solid phase of the investigated sediment.

	mean	r:	C_{org}	S_{tot}	Ba_{xs}
	[g/kg]				
Ba_{xs}	1.04		0.49	0.42	
C_{org}	34.6			0.92	0.49
S_{tot}	6.87		0.92		0.42

group B:	mean	r:	C_{org}	S_{tot}	Ba_{xs}
	[mg/kg]				
Cu_{xs}	42.2		0.88	0.84	0.48
Mo_{xs}	14.9		0.88	0.90	0.45
Ni_{xs}	30.7		0.95	0.89	0.55
Zn_{xs}	34.0		0.90	0.88	0.54

Table 2.2: *Correlation of group B elements to C_{org}, S_{tot} and biogenic Ba (Ba_{xs}) in the solid phase of gravity core GeoB 1711-4. Excess fractions of group B elements show a close correlation to C_{org} and S_{tot} but a low correspondence to biogenic Ba (Ba_{xs})*

2.4.3. Productivity or Early Diagenesis?

While the close association between the organic carbon content and the excess fractions of Zn, Cu, Ni, and Mo is obvious, the origin of this relation is not as clear. For Zn, Cu, and Ni it might be related to the primary production in the surface water. The uptake and enrichment of these trace metals by marine organisms has been reported in numerous studies and is reflected in a nutrient-type distribution in the water column (Bruland, 1983). However, there is also a lot of evidence that the correlation between these trace elements and organic carbon is lost before or while the detritus is buried in the sediment.

By the exposure of sediment traps in the water column Kumar et al. (1996) have shown that as much as 70% of the particle fluxes of C_{org}, Cu and Ni are rapidly released into solution during the sampling period. They conclude that this extent of remineralization precludes the use of trace elements as proxies for paleoproductivity reconstructions. The overall decoupling between trace elements and organic matter has also been observed in the solid phase of sediments. Thomson et al. (1984a) have found authigenic metal fluxes that are independent of the accumulation rates of the sediment. They argue that the trace metal contents emanate from biogenic particles that are no longer present in the sediment because they have been decomposed after burial.

The actual release of trace metals from rapidly decomposing organic material has been demonstrated in pore water and flux studies at the sediment-water interface (Westerlund et al., 1986; Zhang et al., 1995). But although Cu, Ni, and Zn are clearly emitted during the

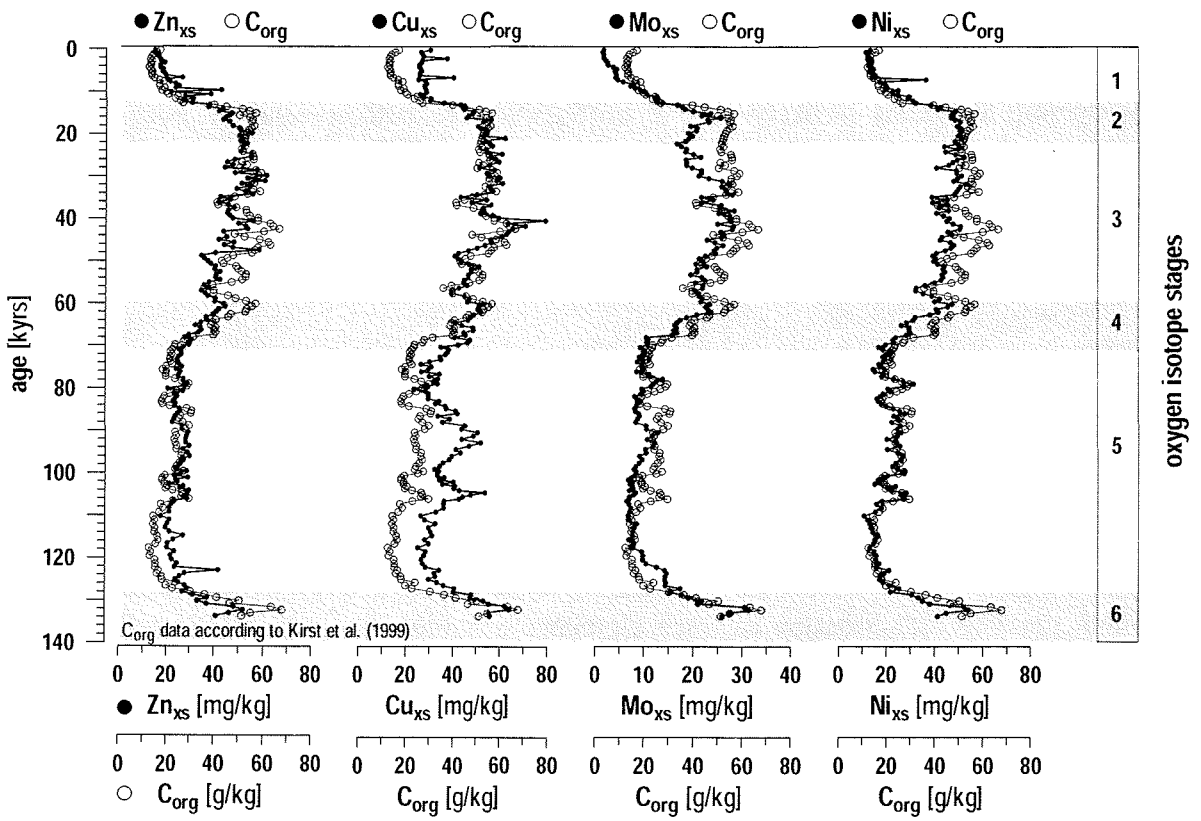

Fig. 2.6: *Calculated excess fractions of zinc, copper, molybdenum, and nickel (Zn_{xs}, Cu_{xs}, Mo_{xs}, Ni_{xs}) and their relation to the C_{org} content in the solid phase of gravity core GeoB 1711-4. C_{org} data taken from Kirst et al. (1999). Age model of the 10.66 m long core as established by Little et al. (1997).*

oxidative breakdown of organic matter there is no direct relationship between the metal fluxes and the degradation intensity. This lack of relationship is explained by the complexity of the sedimentary environment where numerous adsorption sites may prevent the quantitative release of the dissolved metals (Westerlund et al., 1986).

In this context the adsorption of trace metals to Mn oxides plays a prominent role (Goldberg, 1954; Glasby, 2000). However, it is not necessarily a permanent fixation in the solid phase. Mn is a redox-sensitive element that migrates under the influence of redox gradients. As a result, the adsorbed trace elements are subject to redistribution processes as well (Shaw et al., 1990). The intensity of redox-cycling is driven by the degradation of biogenic material. Consequently, the input of C_{org} controls not only the release of trace elements into the pore water but also their redistribution in the solid phase of the sediment (Shaw et al., 1990). This is in particular true under non-steady state conditions where trace elements form a clear succession of concentration peaks along the redox gradient of a progressive oxidation front (e.g., Thomson et al., 1993; 1995).

Considering that the release of trace elements is not proportional to the degradation of organic matter and that the latter fuels the redistribution of trace metals in the course of redox cycling it seems unlikely that a productivity related correlation between trace elements and C_{org} survives in the sediment. Investigations of organic carbon-rich sapropels support this point of view: many trace elements do not exhibit maximum contents within the C_{org}-rich zone of the remaining sapropels but show profile shapes similar to those of Mn or Fe (Thomson et al., 1995).

With all the evidence that early diagenesis decouples trace elements from their biogenic carrier phases it is surprising that we find a close correlation between a number of trace metals and C_{org} in the sediment underlying the upwelling region off Namibia (Fig. 2.6). From our data the question arises why this particular sediment supports a close relation between trace elements and C_{org}. There are three straightforward explanations: (1) The decay of organic matter and the accompanying release of trace elements have been inhibited. (2) The redistribution of trace elements is hampered by the availability of Mn oxides and other inorganic adsorption sites. Or (3) a further process creates a new link between C_{org} and trace metals during early diagenesis.

We can check the first option with Ba as a proxy for paleoproductivity. It is well established that the content of biogenic barite is related to C_{org} fluxes in the water column (Bishop, 1988; Francois et al., 1995; Dymond and Collier, 1996). In sediments Ba survives as barite ($BaSO_4$) as long as the pore water is saturated with respect to the barite solubility product (van Os et al., 1991; Dymond et al., 1992; Gingele and Dahmke, 1994). Therefore it is possible to use the sedimentary Ba record in order to estimate the primary production in surface waters (Pfeifer et al., 2001). Compared to C_{org} biogenic barite is a more reliable indicator for paleoproductivity because its low solubility supports a more effective preservation in the sediment (Thomson et al., 1995; Gingele et al., 1999; Kasten et al., 2001).

Figures 2.3 and 2.7 reveal that both C_{org} and the trace metals of group B do not correspond to the distribution of Ba_{xs} in the solid phase. As the sampled sediment sequence lies well above the deep sulphate reduction zone (Fig. 2.2), barite dissolution can be disregarded. Under these circumstances Ba_{xs} is a reliable proxy for paleoproductivity and the deviations between the concentration profiles of C_{org} and Ba_{xs} can be attributed to the remineralization of organic matter. Consequently, we can exclude the first option. The good correlation between C_{org} and the trace elements of group B does not reflect a complete preservation of marine organic matter and all the trace elements contained therein.

With this clear indication of organic matter degradation we proceed to the second possible explanation: the close relation between the trace elements of group B and C_{org} has been maintained because Mn oxides and other inorganic adsorption sites are not available and thus limit a redistribution of released trace metals within the solid phase of the sediment.

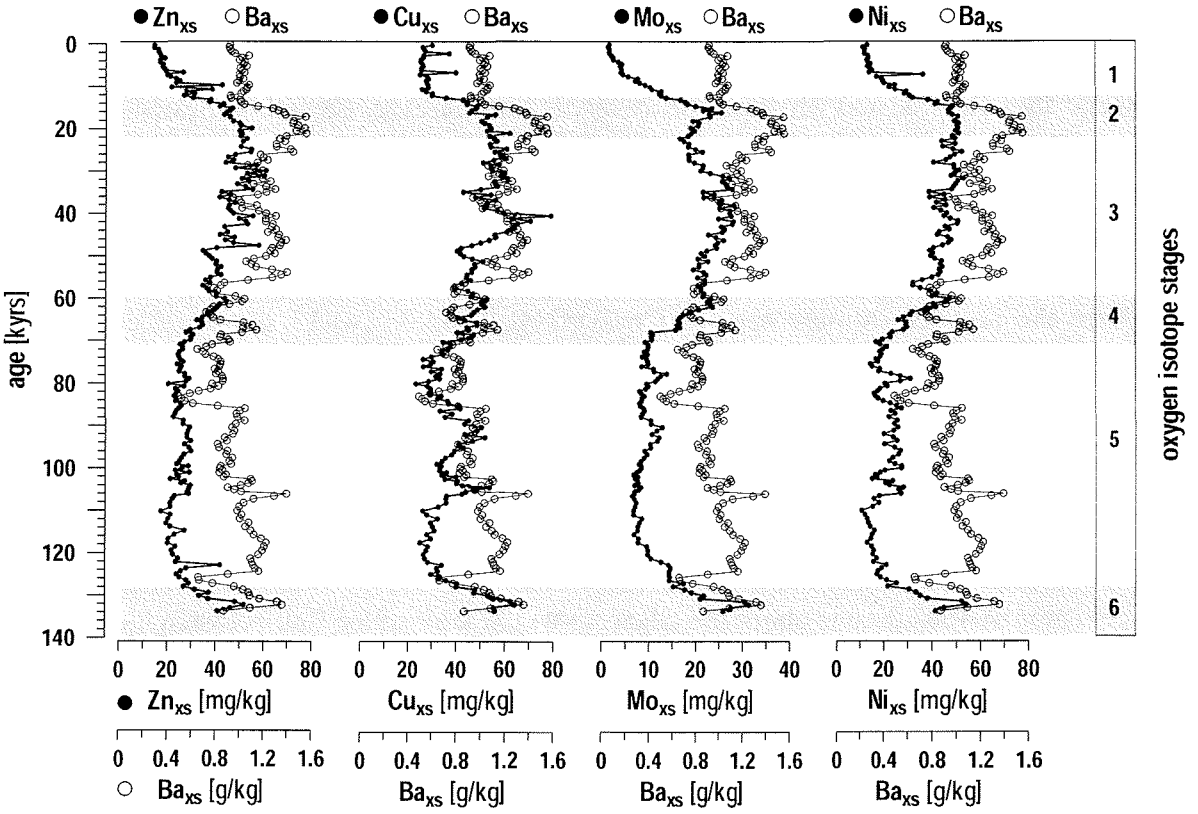

Fig. 2.7: *Calculated excess fractions of zinc, copper, molybdenum, and nickel (Zn_{xs}, Cu_{xs}, Mo_{xs}, Ni_{xs}) and their relation to the biogenic barium (Ba_{xs}) contents in the solid phase of gravity core GeoB 1711-4. Age model of the 10.66 m long core as established by Little et al. (1997).*

Indeed, the terrigenous sediment fraction is of minor importance at site GeoB 1711 while organic matter contributes a relatively large part to the bulk solid phase (Fig. 2.2). In particular, there is a lack of reactive Fe and Mn oxides. The total Fe content can be attributed to the detrital fraction present in aluminosilicates and Mn is even depleted with respect to the continental crust (Fig. 2.4). Further support for the second explanation comes from Co which is usually associated with Mn oxides (Goldberg, 1954; Daesslé et al., 2000). In the solid phase of gravity core GeoB 1711 the depletion of Co (Fig. 2.4) resembles the depletion of Mn. Thereby it corroborates the conclusion that the adsorption to Mn oxides and the associated redistribution by Mn-cycling can be neglected in this sediment. This leaves organic carbon as a predominant phase for the adsorption of trace elements.

However, if we explain the correlation between group B elements and C_{org} by adsorption some inconsistencies remain. Ni, Cu, and Zn are nutrient-type distributed elements. Thus it seems logical that they are released during the degradation of organic matter and subsequently adsorbed again to the remaining detritus if the latter is the dominating adsorbent

in the sedimentary system. But Cr and V are also mobilised during the oxidation of particulate C_{org} (Heggie et al., 1986; Shaw et al., 1990) and we would expect them to be distributed like Ni, Cu, and Zn. This, however, is not the case. Cr and V clearly belong to group A. They are only slightly enriched with respect to the continental crust and their excess corresponds primarily to the terrigenous sediment fraction whereas it is not related to the organic matter content (Fig. 2.4). The incompatible behaviour of Cr and V is even enhanced by the fact that both elements are reduced in the absence of oxygen. As a result they form the smaller cationic species $Cr(III)(OH)_2^+$ and $V(IV)O^{2+}$ that bind even more strongly to chelating surface groups (Bruland, 1983; Morford and Emerson, 1999). Due to this fact enrichments of Cr and V have been found in reducing sedimentary environments (Francois, 1988; Shaw et al., 1990; Calvert and Pedersen, 1993) and we would also expect them in gravity core GeoB 1711. However, we find large discrepancies between the excess fractions of V and Cr and those of group B elements (Fig. 2.5). This is true for both the quantity and the distribution of the enrichments. Thus, the inconsistent behaviour of Cr and V leaves some serious doubts about the adsorptive character of the link between the group B elements and C_{org}.

A further, even more important inconsistency arises from the distribution of Mo. Mo is a group B element. In the investigated sediment it is significantly enriched with respect to the continental crust (Fig. 2.5) and the distribution of its excess fraction corresponds to the organic matter content (Fig. 2.6). However, in the water-column the distribution of Mo is not nutrient-type but conservative (Bruland, 1983). Consequently, a new link between Mo and organic matter must have been formed in the sediment.

The conservative distribution distinguishes Mo from the remaining elements of group B which are all characterised by a nutrient-type distribution in the water column. Nevertheless Zn, Cu, Ni, and Mo have one common feature and that is the formation of sulphides. Considering the sulphidic character of the pore water and the close relation of both C_{org} and group B elements to the total S content (Fig. 2.2, Fig. 2.8, Table 2.2) we suggest that the link between these trace metals and C_{org} is mediated by sulphide. This explanation would also offer an answer for the missing enrichment of V and Cr. Since the latter elements are hard acids that form oxo- rather than sulphur-complexes they are not affected by a sulphide mediated binding to organic matter.

The incorporation of inorganic sulphur (H_2S, HS^-, HS_x^-) into organic matter is termed sulphurization and has received increasing attention during the last two decades. For the sulphurization process two primary classes of reactions have been distinguished. On the one hand intramolecular incorporation of S leads to low-molecular-weight compounds with specific sulphur-containing functional groups and carbon skeletons that are related to biochemical precursors. On the other hand intermolecular S incorporation or "natural vulcanisation" binds organic compounds into macromolecular material through (poly)sulphide linkages (e.g., Sinninghe Damsté et al., 1988; Sinninghe Damsté and de Leeuw, 1990; Kohnen et al., 1991; Adam et al., 1993; Schouten et al., 1994a). These reactions can already

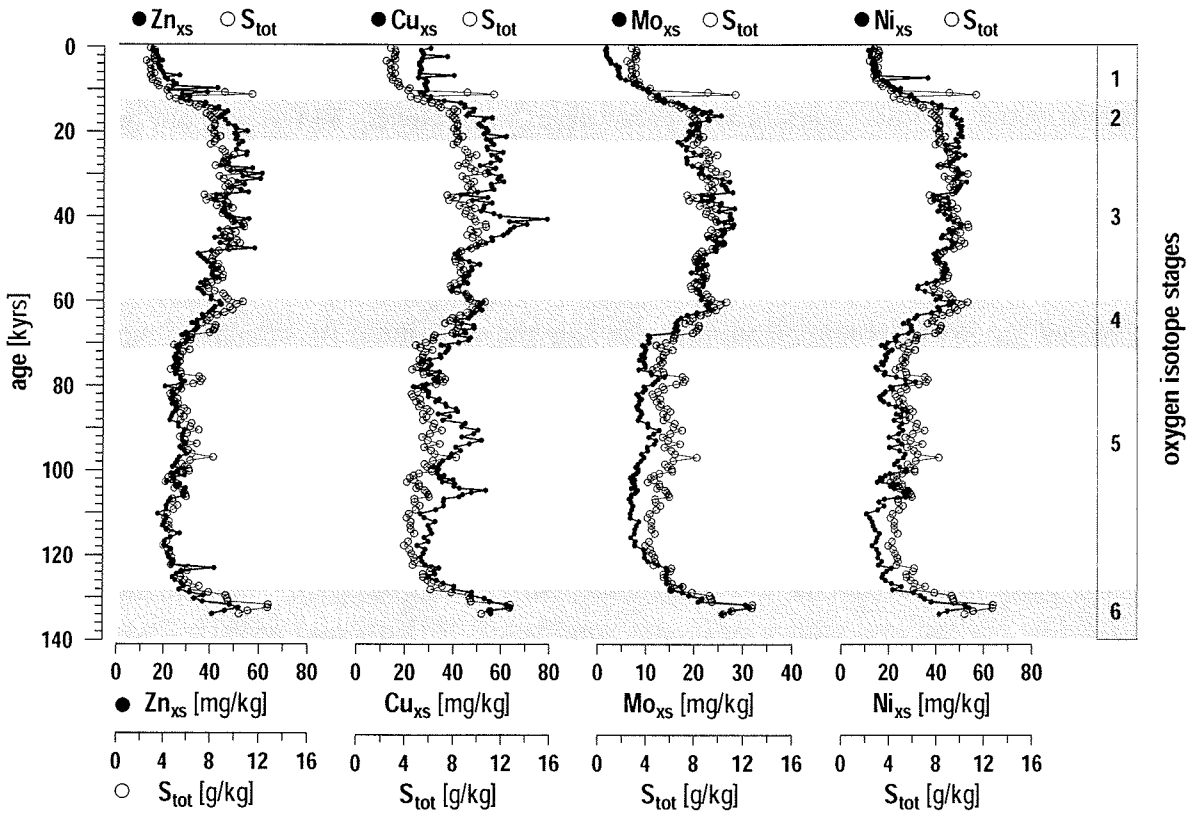

Fig. 2.8: *Calculated excess fractions of zinc, copper, molybdenum, and nickel (Zn_{xs}, Cu_{xs}, Mo_{xs}, Ni_{xs}) and their relation to the total sulphur (S_{tot}) content in the solid phase of gravity core GeoB 1711-4. Age model of the 10.66 m long core as established by Little et al. (1997).*

occur during the very early stages of diagenesis in the upper meters of sediment and even at the sediment-water interface (e.g., Mossmann et al., 1991; de Graaf et al., 1992; Eglinton et al., 1994; Wakeham et al., 1995; Adam et al., 2000). Recently, Werne et al. (2000) were the first to positively identify a precursor-product relationship for a sulphurization reaction in the upper 6 m of a sediment that met the required conditions as there are: an available supply of reactive organic matter, an available supply of inorganic sulphides, and a small enough supply of reactive Fe so that the sulphide is not trapped as Fe sulphides but remains available for sulphurization of organic matter.

Considering the high C_{org} content, the sulphidic pore water and the lack of reactive Fe at site GeoB 1711 it is highly probable that sulphur has been incorporated into organic matter via both intra- and intermolecular reactions. Support for this assumption comes from the results of Adams et al. (2000) who have revealed that the cross-linking by sulphur contributes significantly to the formation of macromolecular organic matter in a young sediment from Walvis Bay. In addition, Brüchert et al. (2000) have shown that the sulphurization of organic matter is active in sediments at the continental slope off Namibia where it buffers

the rates of bacterial sulphate reduction and thereby sustains sulphide-free, suboxic environments that are inhabited by well-adapted benthic communities. This particular effect of organic matter sulphurization is also observable at site GeoB 1711 where our solid phase data indicate sulphurization over the whole length of the core though the sulphide concentrations are low in the upper pore water samples (Fig. 2.2, Fig. 2.3).

We propose that the incorporation of Zn, Cu, Ni, and Mo into organic sulphur compounds can proceed via both the complexation with sulphur containing functional groups of low-molecular-weight compounds and the cross-linking by sulphur in macromolecular organic matter. In this context the reaction with thiol groups is of particular concern. On the one hand the already mentioned investigation of Adam et al. (2000) demonstrates that polysulphide-bound unsaturated thiols are intermediates formed during the first sulphurization steps. They occur soon after deposition and are rapidly transformed in the course of early diagenesis. On the other hand the process study of Vairavamurthy et al. (2000) points out the importance of interactions between thiols and metals. These authors have investigated the complexation of Cd by 3-mercaptoproprionic acid (MPA) taking Cd as a typical soft acid and potential pollutant and MPA as a simple model for thiols. Their study identifies the thiol group of MPA as the primary functional group that binds the metal ion. It also shows that the affinity of the Cd ion for the thiolate ion is very high and leaves the dissociation of the thiol group ($RSH \rightarrow RS^- + H^+$) to be of minor importance. At the same time the excess of either metal or ligand determines the type of complex that is formed: in case the concentration of Cd ions is equal to or in excess of the concentration of MPA a monothio complex is formed while in case the thiol occurs in excess of the Cd ion a Cd-dithio complex is produced. If we transfer these findings to the incorporation of Zn, Cu, Ni, and Mo into organic sulphur compounds the formation of a monothio complex might be an equivalent for a reaction of the metal ions with the thiol group of a low-molecular-weight compound. Similarly the formation of a dithio complex might be a model for the incorporation of the metal ions into the polysulphide bridges of vulcanized organic macromolecules. However, further research is needed to identify the mechanisms and sites for trace metal binding in low- and high-molecular weight organic sulphur compounds.

2.5. Conclusions

Our geochemical investigation of an Fe and Mn depleted, sulphidic sediment in the upwelling region off Namibia reveals that two groups of trace elements can be distinguished: while Ce, Co, Cr, Fe, Ga, K, La, Mg, Mn, Nd, Pb, Sc, Sm, Ti, V, Yb, and Zr are dominated by their detrital concentration in the terrigenous sediment fraction, Cu, Mo, Ni, and Zn show a close relation to the C_{org} content of the sediment. We propose that this relation is not due to the primary input of the latter elements with the detritus of marine organisms. Instead, it is formed in the sediment during the early diagenetic sulphurization of organic matter.

These findings underline the important role of organic matter and sulphur for the fate of trace elements in marine environments. It is well known, that the decomposition of organic substances goes along with the release of incorporated trace metals and that it induces their redox cycling in the sediment. Our data indicate that organic matter can in addition also be involved in the fixation of trace elements to the solid phase of the sediment if the availability of sulphide supports the sulphurization of organic compounds.

We conclude that in the future more attention should be paid to the role of organic matter as a potential sink for trace elements in sulphidic sediments; in particular since the organic carbon related trace metal cycles work opposed to Mn cycling. While under oxic conditions trace elements are released from decomposing organic matter they are adsorbed to Mn oxides. As opposed reducing pore water conditions cause the release of trace metals from dissolving Mn oxides while they enable a further fixation to organic matter in the course of sulphurization.

Acknowledgements - We thank the crew and scientists aboard R.V. METEOR for their help with coring and sampling operations during cruise M 20/2 to the South Atlantic. The processing and analysis of the numerous solid phase samples would have been impossible without the committed assistance of Sigrid Hinrichs, Kerstin Diercks, Susanne Siemer, Silvana Hessler and Karsten Enneking. The preparation of the manuscript benefitted from constructive discussions with Matthias Zabel, Christian Hensen, Thomas Wagner, Volker Brüchert, and Jaap Sinnighe Damsté. This research was funded by the Deutsche Forschungsgemeinschaft (contribution no. of Special Research Project SFB 261 at the University of Bremen).

Chapter 3: Trace elements reflecting primary production, degradation, and preservation of organic matter in sediments from the Niger deep sea fan, equatorial Atlantic

Verena Heuer, Sabine Kasten, Horst D. Schulz
Fachbereich Geowissenschaften, Universität Bremen, Postfach 330 440, D-28334 Bremen

Abstract

This study deals with the relation of trace elements to primary production, degradation and preservation of organic matter in the solid phase of marine sediments. Presented data result from the solid phase analysis of a 20.3 m long gravity core that was taken from the Niger deep sea fan. In this core the identification of trace element patterns benefitted from a particularly large vertical extension of single redox zones.

With respect to the solid phase, two groups of trace elements could be distinguished. The distribution of Fe, Ce, Cr, Ga, La, Li, Nd, Pb, Pr, Sc, and V (group A) is characterised by a close correlation to Al which represents the lithogenic sediment fraction. In contrast, total solid phase contents of Cu, Ni, Zn, and Mo (group B) contain large, non-lithogenic excess fractions. Within the oxic and post-oxic sediment section excess fractions of Cu, Ni, and Zn agree well with the paleoproductivity pattern given by biogenic Ba. This correspondence confirms the primary input of Ni, Cu, and Zn with biogenic carrier phases and supports the reliability of biogenic Ba as a proxy for paleoproductivity. At the same time, neither biogenic Ba nor the trace elements are directly connected to the amount of preserved organic carbon (C_{org}). In the sulphidic zone, Ni, Cu, and Zn correspond to the preserved C_{org} content but they show no affinity to the concentration profile of Ba. We suggest that Ni, Cu, and Zn match the distribution of C_{org} in the sulphidic zone due to their early diagenetic complexation with organic sulphur compounds.

The distribution of Ba indicates either a period of enhanced productivity during the penultimate glacial/interglacial transition (Termination II) or a redistribution of barite during a past period of enhanced methane flux. In the former case, changes in productivity could have initiated non-steady state diagenesis and in particular downward progressing reaction fronts. In the latter case, a higher methane flux would not only have caused a redistribution of barite at the sulphate/methane transition but also an enhanced production of sulphide. Both scenarios are discussed with respect to their potential impact on the distribution of trace elements in the solid phase.

3.1. Introduction

In the marine environment many trace elements are related to the biogeochemical cycles of organic carbon (C_{org}), manganese, iron, and sulphur. They are drawn into the food chain by marine primary production until the decomposition of organic matter releases them again (Martin and Knauer, 1973; Brewer, 1975; Bruland, 1983; Collier and Edmond, 1984). They are adsorbed to particulate Mn and Fe oxides (Goldberg, 1954; Daesslé et al., 2000; Glasby, 2000) until the reduction of Mn and Fe mobilises them in post-oxic environments (Graybeal and Heath, 1984; Glasby, 2000). Finally, under sulphidic conditions they are fixed by the precipitation of insoluble sulphides (Elderfield et al., 1981; Kasten and Jørgensen, 2000). These interactions have received considerable attention. Mn crusts were investigated as potential economic resources for Ni, Cu, and Co (Mero, 1965) and the links of trace metals to productivity and anoxia have promising indications for the reconstruction of paleoenvironments (e.g., Finney and Lyle, 1988; Shaw et al., 1990; Calvert and Pedersen, 1993). However, the interpretation of the sedimentary record requires a clear understanding of the coupling between trace elements and the different biogeochemical cycles that are active in sediments.

In this context, the biogeochemical cycle of C_{org} is of overriding importance since the degradation of organic matter acts in two ways. On the one hand it goes along with the release of trace elements in a nutrient-type fashion. On the other hand it fuels a variety of redox reactions that control the valency state of trace metals, the availability of adsorption sites on Mn and Fe oxides and the formation of sulphides (Froelich et al., 1979). The presence of sulphide, in turn, does not only influence the cycling of Mn and Fe (e.g., Thamdrup et al., 1994; Schippers and Jørgensen, 2002) but also affects the degradation of C_{org}. Sulphurization, i.e. the reaction of organic matter with reduced inorganic sulphur species (H_2S and/or polysulphides), works as an antagonist to remineralization since the intra- and intermolecular incorporation of sulphur supports the preservation of organic compounds (e.g., Sinninghe Damsté et al., 1989; 1998; Sinninghe Damsté and de Leeuw, 1990; Kohnen et al., 1991; Schouten et al., 1994b; Lückge et al., 1999; Werne et al., 2000).

Of all the biogenic material that is produced in the euphotic zone only a small fraction reaches the seafloor (e.g., Berger et al., 1989; Wakeham and Lee, 1993). Yet, the twofold effects of the C_{org} cycle are particularly obvious in sediments where the degradation of organic matter causes a vertical succession of redox zones. While close to the sediment surface C_{org} is preferentially oxidised by oxygen, its oxidation proceeds in the oxygen depleted post-oxic zone utilising Mn oxides, nitrate, and Fe oxides as the next most efficient electron acceptors. Thereafter, dissolved sulphate is reduced in the sulphidic zone by both the degradation of C_{org} and the oxidation of methane that originates from fermentation or thermogenic processes in deeper parts of the sediment (e.g., Froelich et al., 1979; Berner, 1981; Jørgensen, 1982; 2001; Iversen and Jørgensen, 1985; Schulz et al., 1994; Niewöhner et al., 1998; Fossing et al., 2000).

Similarly, the major part of organically bound trace elements is already lost from the biogenic detritus while the latter is degraded in the water column (Kumar et al., 1996). Nevertheless, the emission of trace metals from decomposing organic matter continues in the upper, oxic part of the sediment where numerous adsorption sites and in particular Mn and Fe oxides prevent the quantitative release of the dissolved metals from the sediment (e.g., Heggie et al., 1986; Westerlund et al., 1986; Zhang et al., 1995). However, on entering the post-oxic zone Mn and Fe oxides are reduced and associated elements are released into pore water. As a result, trace metals are redistributed to the oxic zone where they are adsorbed again to Mn and Fe oxides as well as to the sulphidic zone where they are trapped as sulphides (Klinkhammer, 1980).

In this manner, variations in productivity do not only change the input of C_{org} and biogenic trace metals. They also affect the intensity of metal cycling that decouples trace elements from their initial carrier phases. Consequently, regional variations in productivity result in different trace metal signatures of the sedimentary record (Shaw et al., 1990). Moreover, temporal variations in productivity, bottom water oxygen level or bulk sedimentation rate change the burial rate of organic matter. As a result, early diagenesis is forced into a non-steady state. Under these circumstances redox zones can remain at a particular sediment depth for a prolonged period of time and distinct enrichments of trace elements can evolve in the solid phase of the sediment (Kasten et al., subm.). Such secondary signals have been documented for turbidites (e.g., Colley et al., 1984; Wilson et al., 1985; 1986b; Thomson et al., 1993; 1998a; 1998b), sapropels (e.g., Pruysers et al., 1993; Thomson et al., 1995; Passier et al., 1996; 1998: van Santvoort et al., 1996; 1997) and glacial/interglacial transitions (e.g., Thomson et al., 1984b; 1996; Wallace et al., 1988; Kasten et al., 1998; 2001).

As the degradation of organic matter has manifold effects on the distribution of trace metals, the question arises whether sediments retain any direct relation between trace elements and the primary production or preservation of C_{org}. Many solid phase and pore water studies indicate that this is not the case (e.g., Westerlund et al., 1986; Pruysers et al., 1993; Thomson et al., 1993; 1995; Zhang et al., 1995). However, these studies usually

focus on the sediment-water interface or on sediment sequences that were deposited under non-steady state conditions. In the former case, a shallow sampling depth and a close succession of redox zones over depth may not allow to identify any relation of trace elements to C_{org}, Mn, Fe or S in the solid phase of the sediment. In the latter case, distinct secondary enrichments dominate the distribution of trace elements in sediments.

In this study the relation of trace elements to primary production, degradation and preservation of organic matter is investigated in the solid-phase of a 20.3 m long gravity core taken from the Niger deep sea fan. In this long and undisturbed sediment core, the investigation of a coupling between trace elements and biogeochemical cycles benefits from a particularly large vertical extension of redox zones. Our pore water data reveal oxic and post-oxic conditions in the upper 12.5 m of sediment while free hydrogen sulphide is observed in the lower 7.8 m of the core. Since the sedimentary record covers the last 245,000 years, an impact of glacial/interglacial changes on the distribution of trace elements can be examined as well.

3.2. Sampling Sites and Core Descriptions

Site GeoB 4901 (Fig. 3.1) is located at the southern flank of the Niger deep sea fan (02°40.7'N, 06°43.2'E) and was sampled in February 1998 during RV Meteor cruise M 41/1 to the eastern South Atlantic (Schulz et al., 1998). The 20.3 m long gravity core GeoB 4901-8 was recovered from the continental slope at a water depth of 2184 m. A parallel core (GeoB 4901-9) of similar length was taken for pore water analysis. Visual inspection and smear slide analysis of the sediment gave no indication of perturbations. According to the age model established from the benthic foraminifera *C. wuellerstorfi* the sedimentary record of GeoB 4901-8 covers the last 245,000 years and terminates at the transition to oxygen isotope stage 8 (Adegbie et al., subm.). The corresponding sedimentation rates vary between 5 and 12 cm/ka.

The sediment mainly consists of clay-bearing diatomaceous nannofossil oozes and is characterised by the input of terrigenous material from the River Niger (Schulz et al., 1998). Zabel et al. (2001) have shown that a combination of riverine nutrient supply and zonal trade wind intensity drives a regional pattern of ocean fertility at site GeoB 4901. Carbonate concentrations and flux rates generally increase during cold periods that go along with a high total sediment discharge. However, the positive effect of fluvial input on marine productivity is difficult to distinguish from wind-induced upwelling of nutrient-rich subsurface waters.

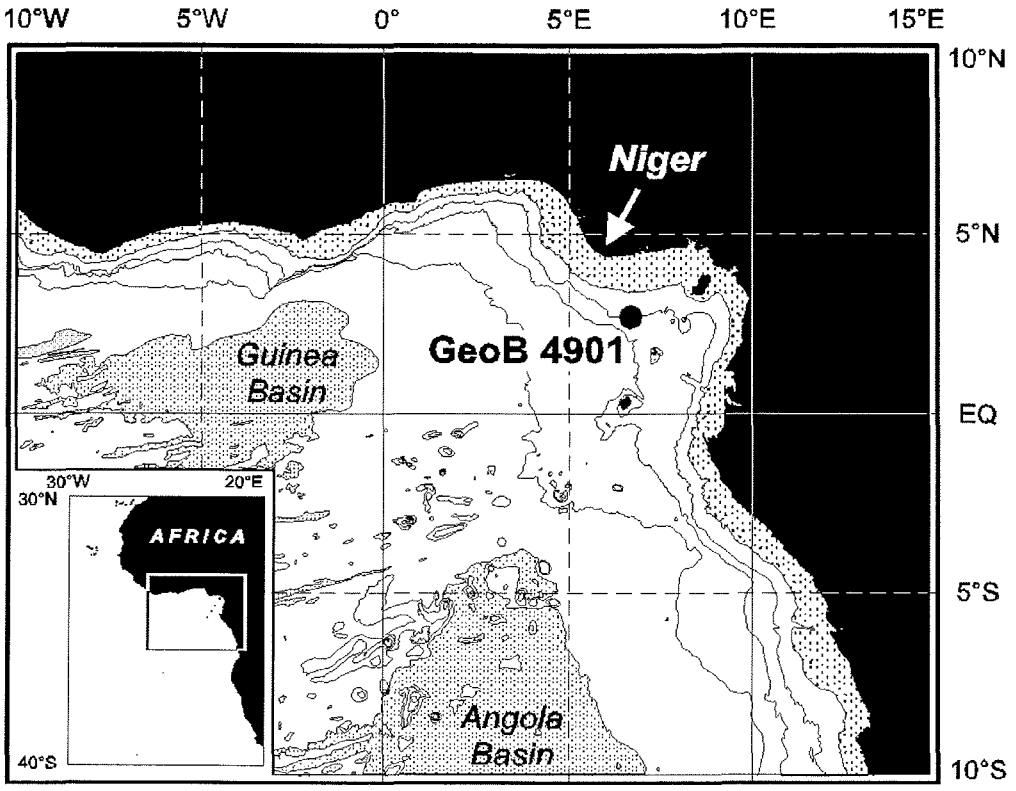

Fig. 3.1: Map showing the location of site GeoB 4901 at the southern flank of the Niger deep sea fan (02°40.7'N, 06°43.2'E; water depth: 2184 m)

3.3. Methods

3.3.1. Geochemical Analysis

Directly after recovery gravity core GeoB 4901-9 was cut into 1 m segments and taken to a refrigerated on-board laboratory (4°C) where pore water was extracted in the inert atmosphere of an argon filled glove-box. Subsequently sulphide was measured potentiometrically by an Ag/AgS electrode and sulphate was determined by ion chromatography. Both methods have been described earlier (Schulz et al., 1994; Niewöhner et al., 1998; Schulz et al., 1998). Subsamples of pore water were preserved for the analysis of Mn that was determined on land by ICP-AES.

Solid phase analysis was carried out on archived core material that is kept at the Department of Geosciences, University of Bremen, Germany. The whole length of gravity core GeoB 4901-8 was sampled every 10 cm. Samples (ca. 10 cm^3) were freeze-dried and ground in an agate mortar prior to further processing.

For bulk solid phase analysis 50 mg of dry sediment were digested in a microwave system (MLS - MEGA II and MLS - ETHOS 1600) with a mixture of concentrated nitric (3 ml), hydrofluoric (2 ml) and hydrochloric (2 ml) acids of supra-pure quality at a temperature of ~200°C and a pressure of 30 kbar. The digestion solutions were evaporated to dryness, redissolved in 0.5 ml concentrated nitric acid and 4.5 ml deionized water (MilliQ), homogenised and finally made up to a volume of 50 ml.

Major, minor and trace elements were analysed by inductively coupled plasma atomic emission spectrometry (ICP-AES) using a Perkin Elmer Optima 3300RL. For the measurement of trace elements an ultrasonic nebulizer was employed in order to improve the detection limit. The precision of the ICP-AES determination (three consecutive measurements on the same solution) was better than 1% for major and minor elements and in the range of 1-4% for trace elements. The accuracy of the analytical procedure was checked using standard reference material USGS MAG-1 (Gladney and Roelandts, 1988). For all elements the difference between the measured element contents and the certified concentration ranges was less than 10% and standard deviations of 17 replicates were less than 5%.

A detailed description of the used methods is also available at our homepage (http://www.geochemie.uni-bremen.de).

3.3.2. Normative Calculation of Element Fractions

In order to distinguish between different potential carrier phases of trace elements we employed a normative calculation of element fractions. This calculation is based on the assumption that the total measured element concentration TE_{tot} consists of a lithogenic fraction TE_{lith} and an additional excess fraction TE_{xs} (Eq. 1). The lithogenic fraction, i.e. the detrital part present in aluminosilicates, can be calculated from a constant element-aluminium ratio k(TE/Al) and the measured total aluminium content Al_{tot} (Eq. 2). Consequently, the excess fraction results from the difference between the total measured element concentration and the calculated lithogenic fraction (Eq. 3).

$$(1) \quad TE_{tot} = TE_{lith} + TE_{xs}$$

$$(2) \quad TE_{lith} = k(TE/Al) \cdot Al_{tot}$$

$$(3) \quad TE_{xs} = TE_{tot} - k(TE/Al) \cdot Al_{tot}$$

For the calculation of lithogenic element fractions we applied the constant element-aluminium ratios k(TE/Al) that result from the average composition of the continental crust as given by Wedepohl (1995) (Table 3.1).

	TE_{tot}			TE/Al				TE_{xs}
	mean	SD	r(Al)[a]	mean	SD	k(TE/Al)[b]	enrichment[c]	mean[d]
	[g/kg]	[%]		[g/g]	[%]	[g/g]		[%]
Al	77.0	13						
Ba	0.630	21	-0.37	0.0084	27	0.004[e]	2.1	49
Ca	63.7	48	-0.92					
C_{org}	13.9	17	-0.09					
Mn	1.48	44	0.08					
S	7.57	34	0.28					
group A:								
Fe	40.8	12	0.88	0.532	6	0.543	1.0	-2
	[mg/kg]	[%]		[mg/g]	[%]	[mg/g]		
Ce	76.8	11	0.84	1.0	7	0.75	1.3	25
Cr	62.7	12	0.96	0.816	4	1.58	0.5	-48
Ga	19.0	15	0.98	0.247	3	0.188	1.3	24
La	35.8	12	0.82	0.467	7	0.38	1.2	19
Li	72.8	16	0.94	0.943	6	0.226	4.2	76
Nd	32.9	11	0.80	0.430	8	0.34	1.3	21
Pb	21.9	12	0.85	0.287	10	0.186	1.5	35
Pr	17.0	12	0.82	0.221	8	0.084	2.6	62
Sc	11.0	12	0.94	0.144	5	0.20	0.7	-29
V	100	12	0.85	1.31	7	1.23	1.1	5
group B:								
Cu	42.5	10	0.15	0.560	14	0.314	1.8	43
Mo	5.13	25	0.14	0.0679	31	0.014	4.9	78
Ni	80.7	12	0.30	1.06	15	0.704	1.5	32
Zn	105	11	0.40	1.38	14	0.817	1.7	40

(a) Spearman correlation coefficient
(b) average continental crust value according to Wedepohl (1995)
(c) ratio between the TE/Al ratio in gravity core GeoB 4901 and the continental crust value k(TE/Al)
(d) relative contribution of the excess fraction to the total solid phase content
(e) Ba/Al ratio in aluminosilicates according to Gingele and Dahmke (1994)

Table 3.1: *Average composition of gravity core GeoB 4901-8: total solid phase contents of major, minor and trace elements (TE_{tot}) in group A and B; correlation coefficients r(Al) for the correlation between total solid phase contents of trace elements and Al; mean trace element - Al ratios (TE/Al) in the solid phase of gravity core GeoB 4901-8 and their enrichment with respect to the average continental crust values k(TE/Al); relative contribution of the excess fractions (TE_{xs}) to the total solid phase contents.*

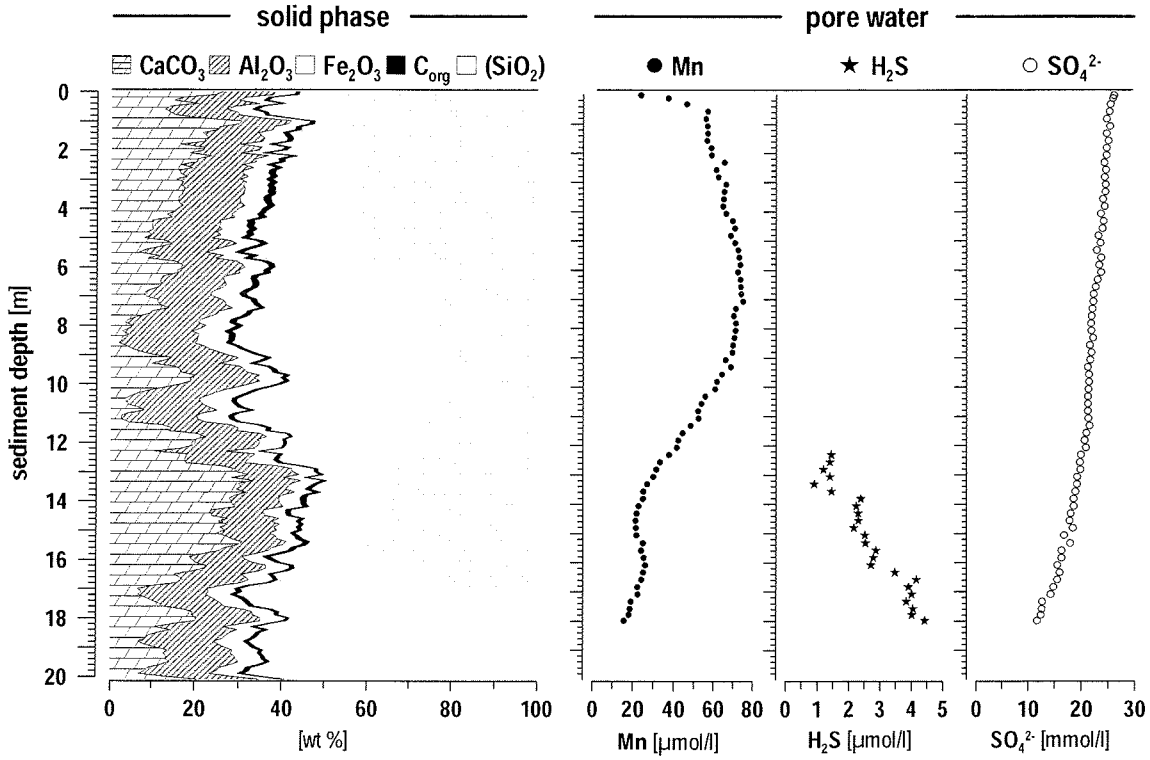

Fig. 3.2: *Overall sediment characteristics of site GeoB 4901: bulk solid phase and porewater chemistry. Ca and Al data according to Zabel et al. (2001), C_{org} data according to Kolonic et al. (in prep).*

3.4. Results and Discussion

The geochemical results for gravity core GeoB 4901-8 are summarised in Table 3.1. In addition, the full data set is available via the geological and environmental data network Pangaea (http://www.pangaea.de).

3.4.1. Overall Sediment Characteristics

At site GeoB 4901 the overall composition of the sediment (Fig. 3.2) is characterised by a large terrigenous fraction (Al_2O_3: 20.5 – 36.3 wt%) and relatively low carbonate contents ($CaCO_3$: 0.1 – 36.1 wt%) (Zabel et al., 2001). A significant input and preservation of organic matter is documented by a mean C_{org} content of 1.4 wt% (Kolonic et al., in prep.). In addition, Fe and Mn contribute on average 6 wt% in terms of Fe_2O_3 and 0.2 wt% in terms of MnO_2. Thus, the mass balance leaves a rest of about 62 wt% for silicate phases that were not accessible with the employed methods.

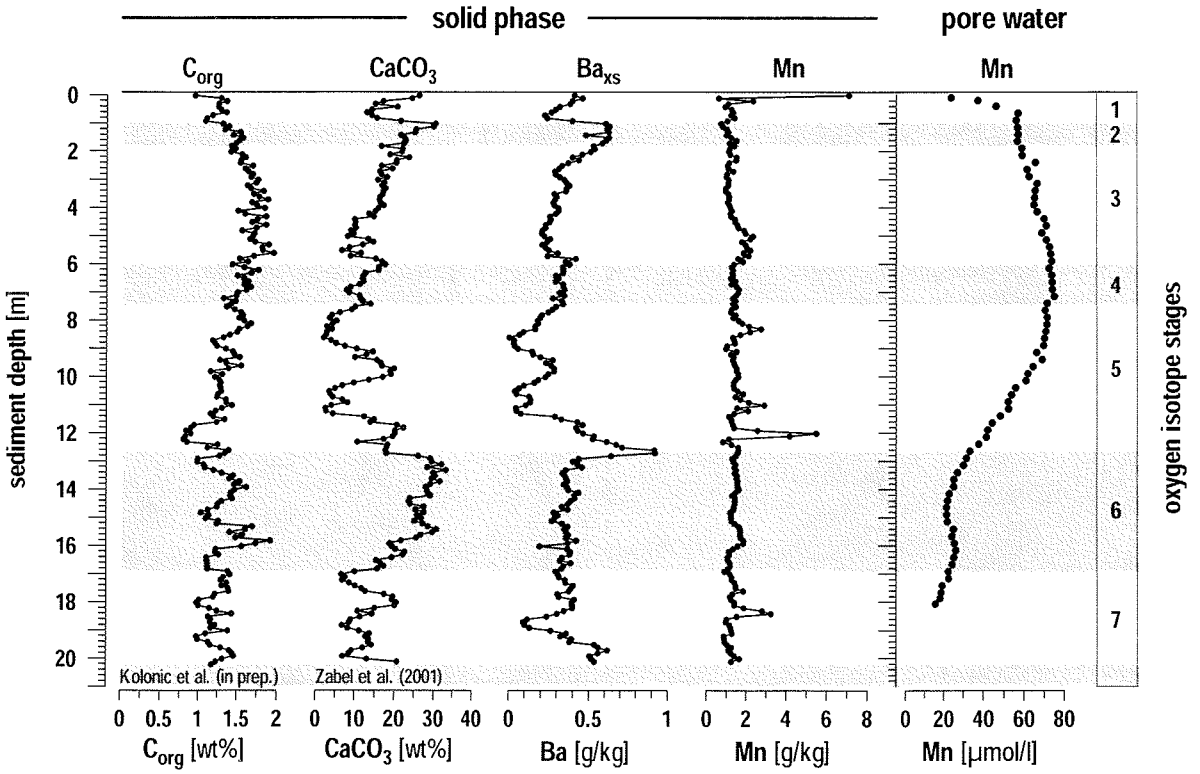

Fig. 3.3: *Distribution of C_{org}, $CaCO_3$, Ba_{xs}, and Mn in the solid phase of gravity core GeoB 4901-8. The pore water profile of dissolved Mn illustrates the extension of the post-oxic redox zone in the parallel core GeoB 4901-9. All results are presented on a linear depth scale. The corresponding age model (Adegbie et al., in prep.) is depicted in the figure on a non-linear age scale.*

Our pore water data reflect the following redox zonation (Fig. 3.2): the upper 10 cm of the sediment are oxic and host a distinct, currently forming Mn enrichment in the solid phase (cf. Fig. 3.3). The post-oxic zone extends from 0.1 m to 12.5 m below the sediment surface. In this zone pore water shows high concentrations of dissolved Mn that result from the reduction of Mn oxides contained in the solid phase. Below 12.5 m free hydrogen sulphide is present in pore water and marks the sulphidic zone. In addition, sulphate concentrations decline with depth. The pore water profile points to a complete consumption of sulphate in a deep sulphate reduction zone that was not penetrated by the gravity core. Given sulphate concentrations decrease linearly throughout the sulphidic zone, a complete consumption of sulphate and thus the top end of the methanic zone should be met at an estimated depth of 26.7 m.

This redox zonation results from a degradation of organic matter that can be observed in the solid phase, as well. Preserved C_{org} contents are not related to the paleoproductivity patterns given by $CaCO_3$ and biogenic barium (Ba_{xs}) (Fig. 3.3). This is true for the whole length of the core.

During the last two decades biogenic Ba has received increasing attention as a proxy for paleoproductivity (e.g., Dehairs et al., 1980; Bishop, 1988; Dymond et al., 1992; Francois et al., 1995; Gingele et al., 1999). Although its biogeochemical relation to productivity is not completely understood biogenic Ba offers one major advantage over other productivity related parameters like C_{org} and $CaCO_3$. It forms discrete barite ($BaSO_4$) crystals that are well preserved in the sediment due to their highly refractive nature (Dehairs et al., 1980; Gingele and Dahmke, 1994). In principle, there is only one important diagenetic process that alters the sedimentary Ba record and limits its use as a proxy for paleoproductivity: the dissolution of barite in sulphate-depleted sediments and the corresponding precipitation of barite in authigenic fronts located slightly above the sulphate/methane transition (e.g., Torres et al., 1996; Gingele et al., 1999; Dickens, 2001).

At site GeoB 4901 the reliability of biogenic Ba (Ba_{xs}) as a proxy for paleoproductivity is supported by its good agreement with the $CaCO_3$ record in the upper 12.4 m of the sediment (Fig. 3.3). However, the close correlation between Ba_{xs} and $CaCO_3$ is not found below this depth. While the Ba_{xs} contents increase to a maximum value of 920 ppm at 12.7 m below surface the $CaCO_3$ contents do not show a corresponding maximum. Instead, $CaCO_3$ suggests a higher productivity than Ba_{xs} in the underlying sediment section (Fig. 3.3).

In principle, the discrepancy between Ba_{xs} and $CaCO_3$ could be due to the early diagenetic dissolution and/or precipitation of both barite and carbonate (e.g., Adler et al., 2001; Pfeifer et al., in press). If we focus on biogenic Ba as the more reliable proxy for paleoproductivity, the question arises whether the Ba_{xs} maximum was caused by a productivity event or whether it results from an authigenic enrichment. Based on our pore water data we can exclude that barite is presently precipitating at 12.7 m sediment depth. Throughout the sampled gravity core no dissolved Ba is detectable in the pore water while sufficient sulphate is present to prevent substantial barite dissolution. Instead, precipitation of authigenic barite is a likely process at the current sulphate/methane transition at greater sediment depth (ca. 26.7 m). However, the Ba_{xs} maximum at 12.7 m sediment depth might be a fossil diagenetic enrichment that formed under different redox conditions in the past. In this manner, the Ba_{xs} front would mark a previous position of the sulphate/methane transition that had been closer to the sediment surface during a period of increased upward methane flux.

Both a period of enhanced productivity and a change in methane flux can have considerable effects on the redox conditions of the sediment. While redox zones adjust to a new rate of organic matter or methane oxidation, early diagenesis is not in a steady state. Such periods of non-steady state can produce distinct enrichments of redox sensitive trace elements in the solid phase of the sediment (e.g., Pruysers et al., 1993; Thomson et al., 1993; van Santvoort et al., 1996). In fact, 0.3 m above the Ba_{xs} maximum of gravity core GeoB 4901 a distinct solid phase enrichment of Mn is observed at 12.4 m sediment depth (Fig. 3.3). This Mn maximum is presently not forming a sink or source for dissolved Mn as can be seen in

the pore water profile (Fig. 3.3). Instead, it is a paleo peak that indicates non-steady state diagenesis during an earlier period of time.

In summary, we need to consider that the formation of the Ba_{xs} maximum goes along with a complex geochemical change of the depositional environment. This point gains further support from the fact that the Ba_{xs} maximum, the Mn peak, and the changing relation between Ba_{xs} and $CaCO_3$ coincide with the penultimate full glacial/interglacial transition (Termination II) at the boundary between oxygen isotope stages 6 and 5. Moreover, long-lasting effects can even be seen in the present day redox zonation: the Ba_{xs} maximum, the Mn peak, and the changing relation between Ba_{xs} and $CaCO_3$ do not only coincide with Termination II but also with the present transition from post-oxic to sulphidic redox conditions at 12.5 m sediment depth. Since this major geochemical change within gravity core GeoB 4901 also affects the distribution patterns of trace elements it will be discussed in more detail below.

3.4.2. Trace Elements

In the solid phase of gravity core GeoB 4901 two groups of trace elements can be distinguished. Group A consists of Ce, Cr, Ga, La, Li, Nd, Pb, Pr, Sc, and V. Like Fe, these elements show no correspondence to the present redox zonation and their close correlation to Al indicates an association with the lithogenic sediment fraction. In contrast, the distribution patterns of Cu, Ni, Zn, and Mo are related to the change in geochemical conditions at 12.5 m sediment depth. These elements form group B.

Group A: Ce, Cr, Ga, La, Li, Nd, Pb, Pr, Sc, and V

Throughout the whole length of gravity core GeoB 4901 total solid phase contents of Fe, Ce, Cr, Ga, La, Li, Nd, Pb, Pr, Sc, and V are closely correlated to the total Al contents that represent the lithogenic sediment fraction (Table 3.1, examples are given in Fig. 3.4). According to the Spearman analysis correlation coefficients r range from 0.98 to 0.84. Moreover, element-aluminium ratios are almost constant with standard deviations of only 3 – 10% (Table 3.1). While the mean Fe/Al and V/Al ratios closely resemble the composition of the continental crust, Sc/Al and Cr/Al ratios are depleted by 29 and 48% compared to the continental crust values (Wedepohl, 1995) (Table 3.1). As opposed, total solid phase contents of Ce, Ga, La, Li, Nd, Pb, and Pr are enriched with respect to the continental curst (Table 3.1). However, the fairly constant excess of these elements indicates that the applied normative calculation of lithogenic element fractions has systematically underestimated the content of the respective trace elements in the aluminosilicates of the source area.

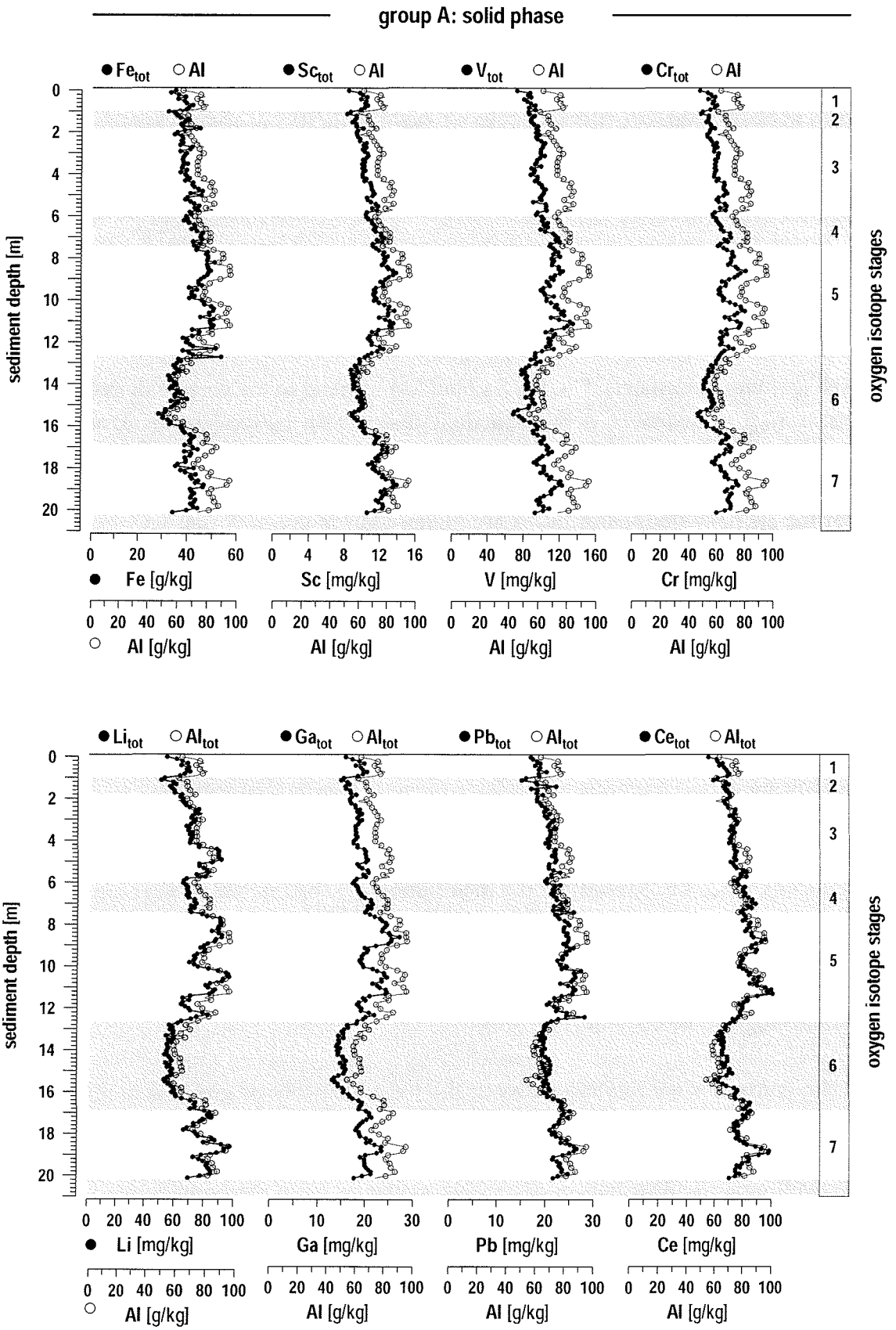

Fig 3.4: *Relation between total solid phase contents of group A elements and Al in gravity core GeoB 4901-8. Aluminium data according to Zabel et al. (2001). All results are presented on a linear depth scale. The corresponding age model (Adegbie et al., in prep.) is depicted in the figure on a non-linear age scale.*

The close correlation between group A elements and Al is in sharp contrast to the distribution patterns of Ti, K, and Zr which have been examined by Zabel et al. (2001). The latter elements are not redox-sensitive and we would expect them to belong to group A. Nevertheless, they have a completely different type of distribution that resembles neither group A nor group B. Instead their occurrence within the sediment is driven by continental weathering conditions (Zabel et al., 2001).

Group B: Cu, Ni, Zn, and Mo

As opposed to group A elements, Cu, Ni, Zn, and Mo respond to the change in geochemical conditions at 12.5 m sediment depth and their distribution pattern is not given by the lithogenic sediment fraction alone. The total solid phase contents of Cu, Ni, Zn, and Mo show a weak relation to total Al (r = 0.40 - 0.14) (Table 3.1). Similarly, the standard deviations of the element-aluminium ratios are higher than in group A and vary between 14 and 31%. In addition, the mean total element-aluminium ratios are 1.8- to 4.9-fold enriched with respect to the average composition of the continental crust (Table 3.1). Our normative calculation of element fractions illustrates that the deviations between the total measured element contents (Ni_{tot}, Cu_{tot}, Zn_{tot}, Mo_{tot}) and the estimated lithogenic element fractions (Ni_{lith}, Cu_{lith}, Zn_{lith}, Mo_{lith}) are not constant but vary over depth (Fig. 3.5). Hence, the observed enrichments do not result from a systematic underestimation of the trace element contents in the lithogenic fraction. Instead, the solid phase contents of Ni, Cu, Zn, and Mo include significant excess fractions which have separate distribution patterns.

In the oxic and post-oxic upper 12.5 m of gravity core GeoB 4901 excess fractions of Ni, Cu, and Zn (Ni_{xs}, Cu_{xs}, Zn_{xs}) resemble the distribution of biogenic Ba (Ba_{xs}) (Fig. 3.6) and the corresponding correlation coefficients are 0.75, 0.68 and 0.33, respectively. However, at greater sediment depth the correlation between Ni_{xs} and Ba_{xs} is sharply reduced (r = 0.46) while the excess fractions of Cu (r = 0.22) and Zn (r = -0.02) do not show any similarity with the biogenic Ba content (Fig. 3.6).

The opposite is true for the relation between the trace elements of group B and C_{org} (Fig. 3.7). Excess fractions of Ni, Cu, Zn, and Mo do not match to preserved C_{org} contents in the upper 12.5 m of the sediment (r = -0.11 - 0.26). In contrast, their concentration profiles agree very well with the distribution of organic matter in the underlying sulphidic part of the sediment where the correspondence to C_{org} yields correlation coefficients r of 0.71, 0.58, 0.51, and 0.38 for Zn_{xs}, Cu_{xs}, Mo_{xs}, and Ni_{xs}, respectively .

While the concentration profiles of group B elements obviously correspond to either the productivity proxy Ba_{xs} or the preserved C_{org} content there is no direct relation between the excess fractions of Ni, Cu, Zn, and Mo and the solid phase content of Mn (Fig. 3.8). Based on a correlation analysis over the total length of gravity core GeoB 4901 Mn_{xs} and the

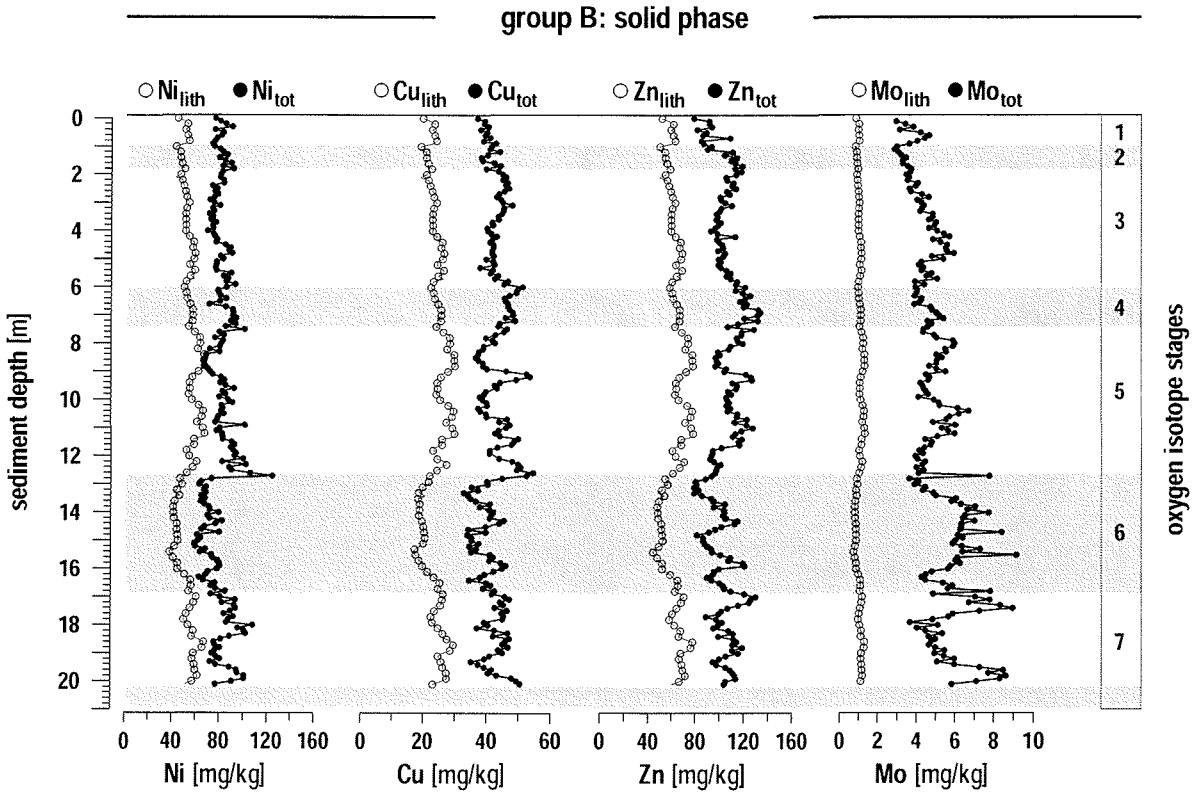

Fig. 3.5: *Calculated lithogenic element fractions (TE_{lith}) and analysed total solid phase contents (TE_{tot}) of group B elements in gravity core GeoB 4901-8. The total solid phase contents of Ni, Cu, Zn, and Mo do not alone result from the lithogenic element fractions present in aluminosilicates. All results are presented on a linear depth scale. The corresponding age model (Adegbie et al., in prep.) is depicted in the figure on a non-linear age scale.*

excess fractions of group B elements have correlation coefficients in the range of 0.04 to 0.26. Similarly, total solid phase contents of Fe have a weak or negative correlation to the excess fractions of group B elements (r = 0.07 to -0.39). The same is true for sulphur. Excess fractions of Ni, Cu, and Zn are not related to the total sulphur contents of the solid phase (r = 0.01 to –0.20) (Fig. 3.9). However, there is a significant correlation between the total sulphur contents and the excess fraction of Mo (r = 0.72) (Fig. 3.9).

3.4.3. Trace Elements and the Biogeochemical Cycle of C_{org}

Our findings in the deposits of the Niger deep sea fan stress the overriding importance of C_{org} for the distribution of trace elements in the solid phase of marine sediments. Ni, Cu, and Zn are known for their nutrient-type distribution in the water column (Bruland, 1983).

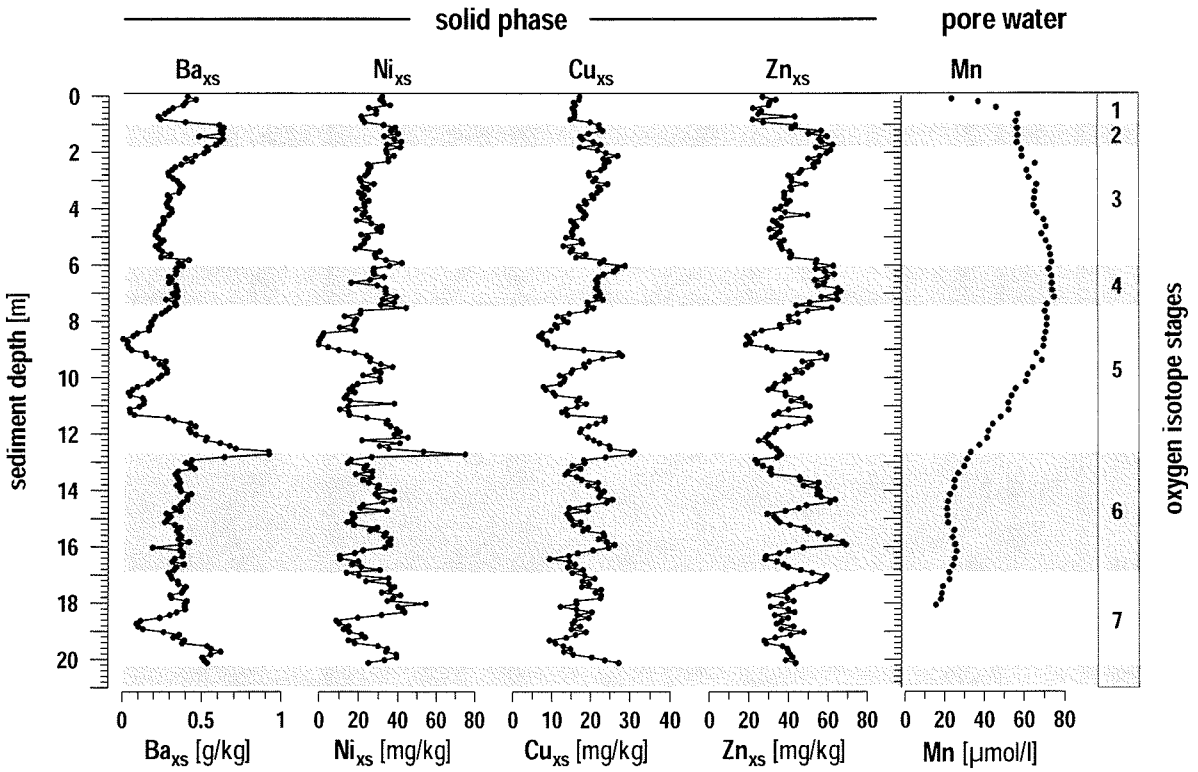

Fig. 3.6: *Excess fractions of Ni, Cu, and Zn and their relation to excess Ba in the solid phase of gravity core GeoB 4901-8. The pore water profile of dissolved Mn illustrates the extension of the post-oxic redox zone. All results are presented on a linear depth scale. The corresponding age model (Adegbie et al., in prep.) is depicted in the figure on a non-linear age scale.*

Now our data show a close correspondence between these elements and the productivity proxy Ba_{xs} in the upper 12.5 m of the sediment (Fig. 3.6) and suggest a productivity related occurrence within oxic and post-oxic sediment sections, as well. In contrast, the distribution patterns of Ni, Cu, and Zn do not correspond to the solid phase contents of Mn (Fig. 3.8), Fe or S (Fig. 3.9). However, it is the presence of dissolved Mn or sulphide in the pore water that determines whether the solid phase records of Ni, Cu, and Zn are related to either primary production or preservation of C_{org}. The presence of dissolved Mn or sulphide, in turn, is finally controlled by organic matter degradation and anaerobic methane oxidation.

The response of Ni, Cu, and Zn to the redox zonation of gravity core GeoB 4901 suggests an early diagenetic influence on the trace metals' distribution in the solid phase. In addition, neither primary production nor preservation of organic matter can explain the solid phase contents of Ni_{xs}, Cu_{xs}, and Zn_{xs} consistently throughout the core. With a continuously progressing degradation of biogenic carrier phases, we would expect a primary link between trace metals and C_{org} to decrease with sediment depth. The opposite is true at site GeoB 4901. Ni, Cu, and Zn are not associated with the distribution of organic matter in the

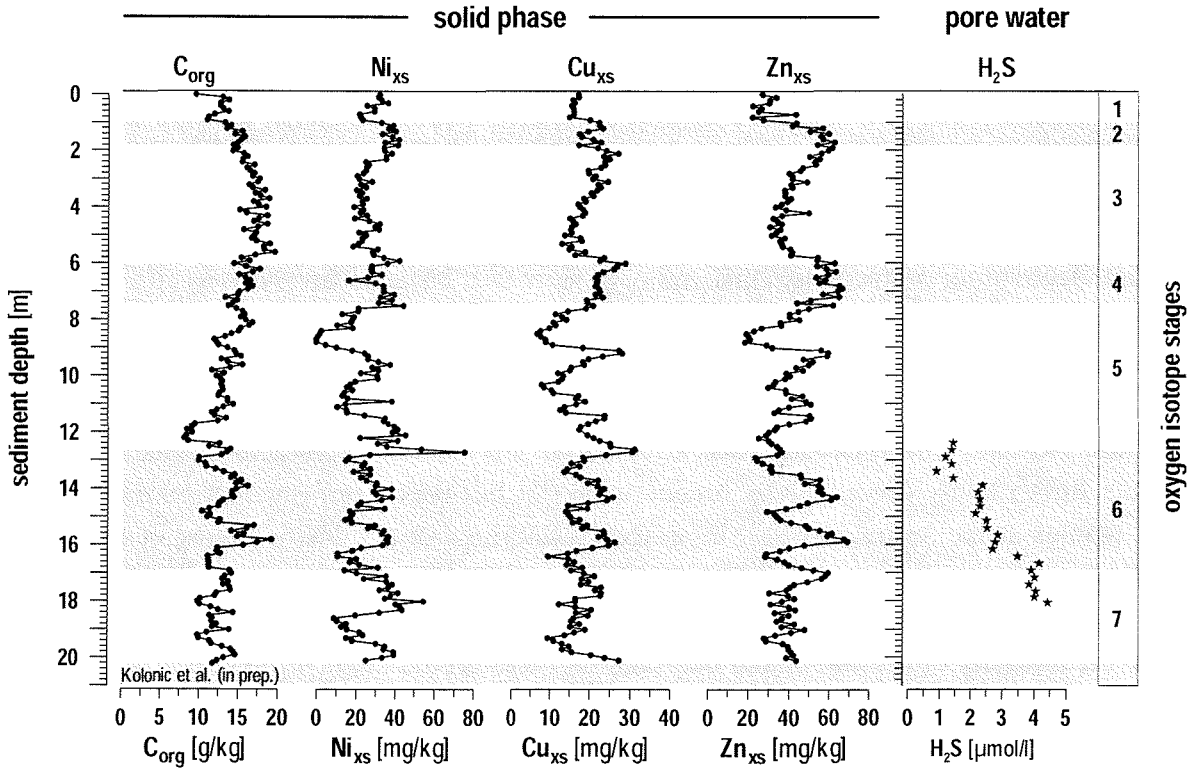

Fig. 3.7: *Excess fractions of Ni, Cu, and Zn in the solid phase of gravity core GeoB 4901-8 and their relation to the amount of preserved organic carbon (C_{org}). The pore water profile of dissolved hydrogen sulphide illustrates the extension of the sulphidic redox zone. All results are presented on a linear depth scale. The corresponding age model (Adegbie et al., in prep.) is depicted in the figure on a non-linear age scale.*

upper meters of the gravity core. Instead, their correspondence to the amount of preserved C_{org} is increased below 12.5 m sediment depth (Fig. 3.7). Similarly, we expect Ba_{xs} to bear a longer lasting relation to the trace elements than C_{org} since barite is a more refractory proxy for productivity than C_{org}. However, Ni, Cu, and Zn stop to resemble the distribution of Ba_{xs} in the lower half of gravity core GeoB 4901 (Fig. 3.6) in spite of their simultaneous correspondence to C_{org} (Fig. 3.7).

Supposed the distribution patterns of the trace metals are influenced by early diagenesis, two questions require further discussion; namely (a) what controls the relation between the solid phase contents of Ni, Cu, Zn and the preserved amounts of C_{org}? And (b) why is the similarity between these trace metals and Ba_{xs} lost? In the following discussion of the trace metals' relation to C_{org} and Ba_{xs}, we will consider the present redox zonation as well as possible consequences of a past change in productivity or methane flux.

Present Redox Zonation

In the oxic and post-oxic sections of gravity core GeoB 4901 the observed discrepancy between the investigated trace metals and preserved C_{org} agrees well with previous findings. For example, a rapid and extensive release of Cu and Ni from particulate C_{org} has been shown by the exposure of sediment traps in the water column (Kumar et al., 1996). An overall decoupling of trace elements and organic matter has also been observed in the solid phase of sediments. So, Thomson et al. (1984a) have found authigenic metal fluxes that are independent of the accumulation rates of the sediment. These authors suggest that the trace metal contents emanate from biogenic particles that are no longer present in the sediment because they have been decomposed after burial. Furthermore, the actual release of trace metals from rapidly decomposing organic material has been confirmed in pore water and flux studies at the sediment-water interface (Westerlund et al., 1986; Zhang et al., 1995). However, the dissolved metals interact with the sediment's numerous adsorption sites and this secondary fixation to the solid phase decouples the pore water fluxes of Cu, Ni, and Zn from the intensity of organic matter degradation (Westerlund et al., 1986).

While the remineralization of organic matter has probably destroyed the link between C_{org} and biogenic trace elements in the upper 12.5 m of gravity core GeoB 4901 (Fig. 3.7), the solid phase contents of Ni_{xs}, Cu_{xs}, and Zn_{xs} are still related to the productivity proxy Ba_{xs} (Fig. 3.6). These findings do not only confirm the input of excess Ni, Cu, and Zn with biogenic carrier phases. They also suggest that the productivity related input of Ni, Cu, and Zn has been preserved whereas the original biogenic carrier phases have been decomposed. Moreover, the trace elements' adsorption to the solid phase is not hindered by the current reduction and dissolution of Mn oxides. Likewise, the solid phase contents of Ni, Cu, and Zn do not correspond to Mn enrichments indicating past redistribution processes (Fig. 3.8).

Under sulphidic conditions the distribution patterns change. We suggest that the observed correspondence between the trace metals and C_{org} results from an early diagenetic reaction that is mediated by sulphide. Both the trace elements and organic matter are known to react with sulphide. Ni, Cu, and Zn precipitate as sulphides in anoxic environments (e.g., Francois, 1988; Calvert and Pedersen, 1993; Sternbeck et al., 2000) and organic molecules incorporate reduced inorganic sulphur species (H_2S and/or polysulphides) into sulphur containing structural units and (poly)sulphide linkages of low- and high-molecular-weight organic sulphur compounds, respectively (e.g., Sinninghe Damsté and de Leeuw, 1990; Kohnen et al., 1991; Schouten et al., 1994b; Lückge et al., 1999; Werne et al., 2000). Moreover, trace metals can also react with organic sulphur compounds. Among other sulphur containing structural units thiol groups are known to play an important role in the formation of organic trace metal complexes and the complexation of trace metals with high-molecular-weight and particle-bound thiols will probably bind the metals to the particulate phase (Vairavamurthy et al., 2000).

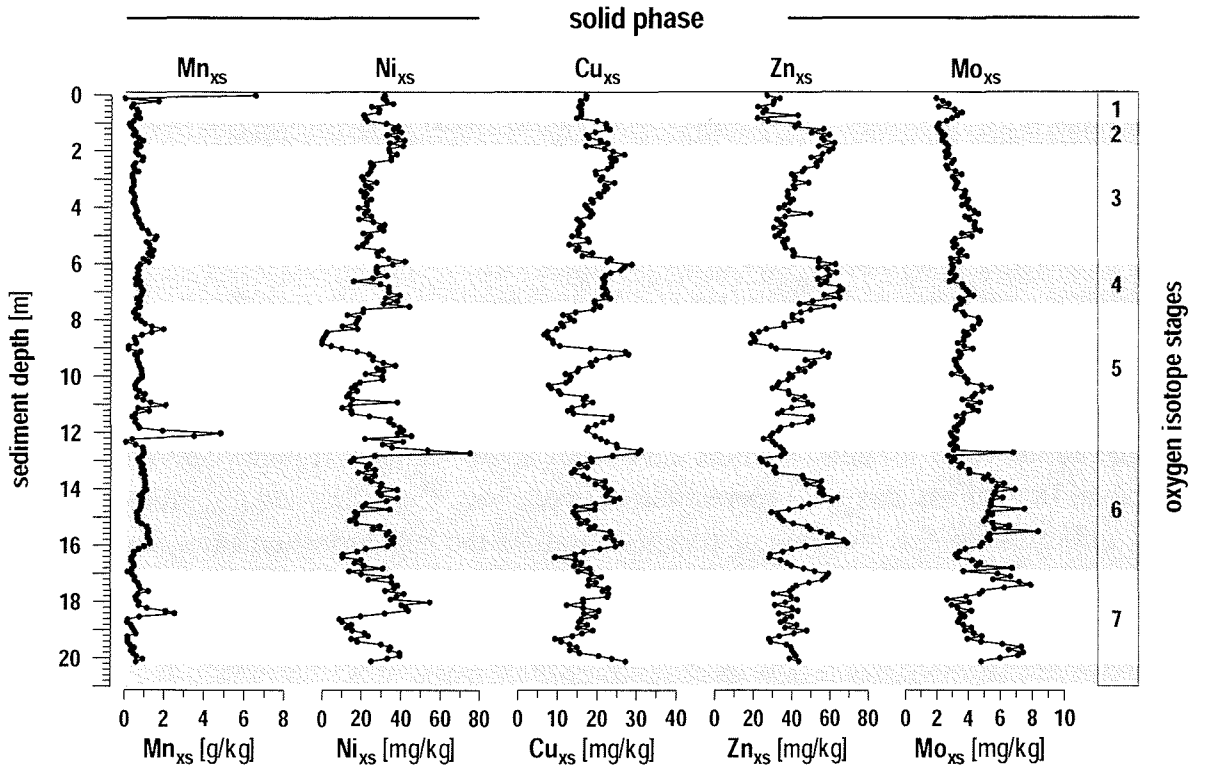

Fig. 3.8: *Excess fractions of Ni, Cu, Zn, and Mo and their relation to the total Mn content in the solid phase of gravity core GeoB 4901-8. All results are presented on a linear depth scale. The corresponding age model (Adegbie et al., in prep.) is depicted in the figure on a non-linear age scale.*

Further support for a sulphide mediated binding of trace metals to organic matter comes from observations at the continental slope off Namibia (Heuer et al., subm.-b). In this region, sediments contain only little Fe and Mn but high amounts of C_{org} and intense early diagenetic processes give rise to sulphidic conditions even close to the sediment-water interface. The investigation of a 10.7 m long sulphidic gravity core revealed trace element patterns that are comparable to those found in the lower, sulphidic part of gravity core GeoB 4901: solid phase contents of Ni_{xs}, Cu_{xs}, Zn_{xs} and Mo_{xs} are closely correlated with the amounts of preserved C_{org} but they do not match the distribution of Ba_{xs}. Moreover, in the Fe limited sediment at the continental slope off Namibia, both the trace metals and C_{org} were closely correlated to the solid phase contents of S_{tot}. This correspondence suggests a complexation of Ni, Cu, Zn, and Mo with sulphurised organic matter in the solid phase of the sediment (Heuer et al., subm.-b).

As opposed to the sediments at the continental slope off Namibia, the sediments of the Niger deep sea fan are rich in Fe. In the presence of abundant H_2S sulphur can still be incorporated into organic matter (Hartgers et al., 1997) but the formation of Fe sulphides

has to be considered as well (Canfield, 1989). Given inorganic sulphides make up a significant part of the total sulphur content in gravity core GeoB 4901, no correlation is observable between the solid phase contents of S_{tot} and C_{org}. However, in the sulphidic sediment section the similar distribution patterns of C_{org}, Ni_{xs}, Cu_{xs}, and Zn_{xs} suggest that the formation of organic sulphur complexes is more important for the trace metals' fixation to the solid phase than their precipitation as inorganic sulphides (Fig. 3.7, Fig. 3.9).

These findings have considerable implications for the reconstruction of paleoenvironments. The good correlation between Ni_{xs}, Cu_{xs}, Zn_{xs}, and Ba_{xs} supports the interpretation of biogenic Ba as a proxy for paleoproductivity. At the same time, this correlation might become an indicator for non-sulphidic conditions in the sediment if pore water data are not available. In contrast, the good correlation between Ni_{xs}, Cu_{xs}, Zn_{xs} and C_{org} might be used as an indicator for the presence of free H_2S and for the sulphurization of organic matter. However, further investigations are required to confirm the proposed mechanisms and the general applicability of our findings from the Niger deep sea fan.

Past Change in Productivity or Methane Flux

An early diagenetic reaction of trace metals with organic sulphur compounds might have changed the distribution of Ni_{xs}, Cu_{xs}, and Zn_{xs} to the effect that these elements do not resemble the productivity related pattern of Ba_{xs} in the sulphidic section of gravity core GeoB 4901 (Fig. 3.6). Vice versa, an early diagenetic redistribution of barite might have caused the observed discrepancy as well. Thus, the changing relation between trace metals and Ba_{xs} drives once more attention to the question whether the Ba_{xs} maximum at 12.7 m sediment depth was caused by a productivity event or whether it results from an authigenic enrichment. In the following, we will discuss both scenarios and their implications for the redox conditions of the sediment.

The productivity scenario is supported by the particular position of the Ba_{xs} maximum in gravity core GeoB 4901 (Fig. 3.3). Plotted on a time scale, the absolute Ba_{xs} maximum coincides with the penultimate full glacial/interglacial transition (Termination II) at the boundary between oxygen isotope stages 6 and 5. Similar Ba peaks at glacial terminations have been documented for several sites (e.g., Matthewson et al., 1995; Schwarz et al., 1996; Thomson et al., 2000; Kasten et al., 2001). Originally, the formation of Ba spikes at glacial/interglacial transitions was explained by an increased deposition of Ba due to changes in global ice volume and ocean circulation (Matthewson et al., 1995; Schwarz et al., 1996), but Thomson et al. (2000) reported simultaneous maxima of the productivity indicators C_{org}, Ba/Al and diatom abundance for a piston core from the Portuguese margin. They concluded that the Ba peaks arise from short-duration high productivity episodes that occurred during major glacial/interglacial transitions. Recently, Kasten et al. (2001) postulated that the 'productivity explanation' is also applicable to other Ba peaks at

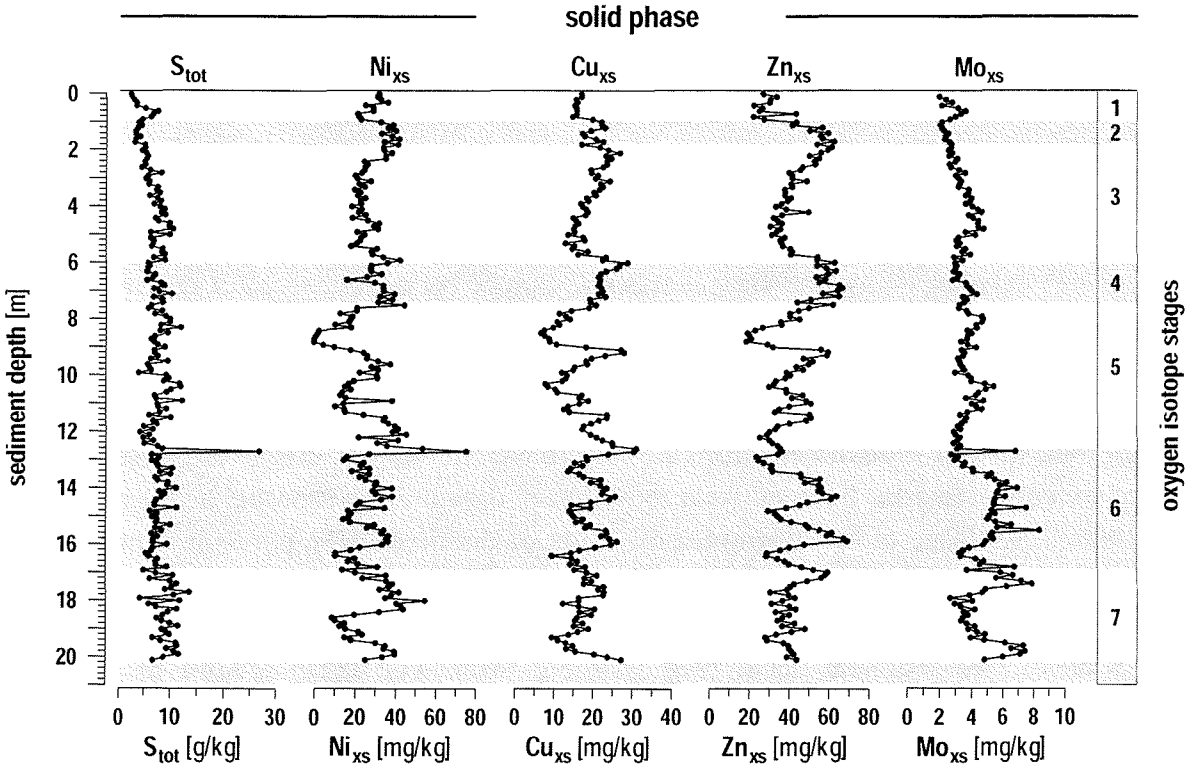

Fig. 3.9: *Excess fractions of Ni, Cu, Zn, and Mo and their relation to the total sulphur content in the solid phase of gravity core GeoB 4901-8. All results are presented on a linear depth scale. The corresponding age model (Adegbie et al., in prep.) is depicted in the figure on a non-linear age scale.*

glacial/inter-glacial transitions. Kasten et al. (2001) argue that the initial coincidence between Ba_{xs} and C_{org} does no longer exist since a downward progressing oxidation front has caused an effective post-depositional degradation of C_{org} during the early interglacial. Evidence for the action of a downward progressing oxidation front comes from the concurrent redistribution of trace elements. Kasten et al. (2001) have found a distinct peak of Mn slightly above the Ba_{xs} maximum at Termination II as well as coincident peaks of Fe and As below the Ba_{xs} maximum. This succession of element peaks is also known to occur at active oxidation fronts along sapropels in the eastern Mediterranean (Thomson et al., 1995; van Santvoort et al., 1996).

At site GeoB 4901 the Ba_{xs} maximum is not accompanied by any other productivity indicator. In fact, C_{org} contents are particularly low between 11.7 and 12.3 m below surface. However, 0.3 m above the Ba_{xs} maximum a distinct solid phase enrichment of Mn is observed at 12.4 m sediment depth (Fig. 3.3). This Mn peak suggests that a downward progressing oxidation front might have altered the C_{org} record after a productivity event at Termination II as proposed by Kasten et al. (2001). Thus, the Mn enrichment supports the productivity scenario. Nevertheless, if the Ba_{xs} maximum at 12.7 m sediment depth is re-

lated to productivity, the discrepancy between Ba_{xs} and $CaCO_3$ and the loss of correspondence between Ba_{xs} and the solid phase contents of Ni_{xs}, Cu_{xs}, and Zn_{xs} still remain to be explained for both the Ba_{xs} maximum and the underlying sediment.

At present, the close relation between Ni_{xs}, Cu_{xs}, Zn_{xs} and Ba_{xs} is not notably affected by the dissolution of Mn oxides in the post-oxic section of gravity core GeoB 4901. Thus, the loss of this relation below the Ba_{xs} maximum cannot be explained by a downward progressing oxidation front that initiated a redistribution of trace metals at the oxic/post-oxic transition of that time, i.e. ca. 120 kyrs ago. Instead, the question arises whether the postulated productivity event could have caused sulphidic conditions that mediated a redistribution of trace metals. In sediments from the eastern Mediterranean, downward sulphidisation fronts are known to arise from sulphate reduction in organic-rich sapropel layers (Passier et al., 1996; 1999). Due to the downward diffusion of dissolved HS^-, pyrite is formed in the horizon immediately below the organic-rich sediment (Berner, 1969; Passier et al., 1996). In fact, the Ba_{xs} maximum of gravity core GeoB 4901 coincides with distinct peaks of Fe and S at 12.7 m sediment depth (Fig. 3.4, Fig. 3.9). The latter suggest an enhanced precipitation of iron sulphides at the base of an organic-rich layer. These findings agree well with the observations in sapropels and support the proposed productivity scenario. However, they also indicate that the precipitation of sulphides stopped the downward progressing sulphidisation front at 12.7 m sediment depth. Thus, this scenario does not explain that Ni, Cu, and Zn do not correspond to the productivity proxy Ba_{xs} in the underlying sediment.

Alternatively, we will now consider the scenario of an authigenic redistribution of Ba in the lower half of gravity core GeoB 4901. In marine sediments, the formation of 'barite fronts' is a long known process (e.g., Goldberg and Arrhenius, 1958; Brumsack, 1986; Torres et al., 1996). During sediment burial barite ($BaSO_4$) starts to dissolve once it enters the zone of sulphate-depleted pore water below the sulphate/methane transition. This process is of particular significance since the dissolution of barite limits the use of biogenic Ba as a potential proxy for paleoproductivity (e.g., Von Breymann et al., 1992). Dissolved Ba^{2+}, in turn, diffuses upward from sulphate depleted to sulphate rich pore water where it reprecipitates as barite. As a result, a diagenetic enrichment of barite can form in the solid phase of the sediment at or above the sulphate/methane transition (e.g., Heuer et al., subm.-a). Such barite fronts can be used to track changes in diagenesis. For example, Dickens (2001) has recently applied sedimentary Ba records in order to assess variations in the upward methane flux out of the Blake Ridge gas hydrate reservoir during the late Pleistocene. His approach is based on the observation that diagenetic enrichments of barite mark present and past depths of complete sulphate depletion in marine sediments. Complete sulphate consumption, in turn, is thought to result from anaerobic methane oxidation and its position below the sediment surface is given by the upward methane flux. Consequently, diagenetic enrichments of barite can be used for the reconstruction of methane fluxes provided the barite fronts have always stayed at or above the sulphate/methane transition. These

conditions are met at sites where decreasing methane fluxes have lowered the sulphate/methane transition down into the sediment in the course of time (Dickens, 2001).

Based on our pore water data we can exclude a currently active Ba cycling within gravity core GeoB 4901. However, the Ba_{xs} maximum at 12.7 m sediment depth might be an early diagenetic enrichment that was formed in the past during a period of increased upward methane flux. A redistribution of barite would not only explain the Ba_{xs} maximum as a result of barite precipitation on top of a formerly shallower sulphate/methane transition. A redistribution of barite would also imply dissolution of barite in the underlying sediment that used to be sulphate-depleted at that time. In fact, the distribution pattern of Ba_{xs} is levelled out below the Ba_{xs} maximum. Solid phase contents of Ba_{xs} remain rather constant between 13 and 18 m sediment depth. Thus, a past period of increased upward methane flux would explain that a relation of Ba_{xs} to $CaCO_3$ and to the nutrient-type distributed trace elements Ni, Cu, and Zn is no longer preserved in the lower half of gravity core GeoB 4901.

Moreover, a period of increased methane flux would not only have moved the position of the sulphate/methane transition towards the sediment surface. An enlarged supply of methane would also have enhanced the production of sulphide. At the sulphate/methane transition sulphate is completely consumed by reduction. However, at this particular location, reduction of sulphate is not fuelled by the continuous degradation of biogenic detritus. Instead, it results from an anaerobic oxidation of methane that is assumed to be mediated by a consortium of methane consuming archaea and sulphate-reducing bacteria in a distinct sulphate/methane transition zone (Boetius et al., 2000). In fact, anaerobic methane oxidation can consume the total net diffusive sulphate flux in sediments (e.g., Niewöhner et al., 1998; Zabel and Schulz, 2001). Hence, the upward methane flux is an important source for the production of sulphide. In this manner, a former period of increased upward methane flux could have provided sufficient dissolved sulphide for the sulphurization of organic matter and for the accompanying fixation of Ni, Cu, and Zn at site GeoB 4901.

A previously enhanced production of sulphide at the sulphate/methane transition could also have formed the distinct peaks of Fe and S_{tot} that coincide with the Ba_{xs} maximum at 12.7 m sediment depth (Fig. 3.4, Fig. 3.9). A modern analogue of this process has already been documented for the iron-dominated sediments on the Amazon Fan, where the immediate precipitation of sulphides forms a distinct enrichment of iron sulphides slightly below the current depth of the sulphate/methane transition (Kasten et al., 1998).

More evidence for a previously enhanced production of sulphide comes from the solid phase profile of Mo_{xs} (Fig. 3.9). The enrichment of Mo in sulphidic sediments is driven by the precipitation of dissolved Mo diffusing from the water column into the sediment (Francois, 1988). Thus, at site GeoB 4901 the considerable enrichment of Mo below 12.5 m sediment depth suggests that more dissolved sulphide used to be present in this sediment section during an earlier stage of sedimentation.

In summary, a productivity event at Termination II would account for the occurrence of distinct Mn and Fe peaks above and below the Ba_{xs} maximum at 12.7 m sediment depth. Changes in C_{org} burial can initiate periods of non-steady state diagenesis and in particular downward progressing oxidation or sulphidisation fronts. The latter are known to produce trace metal enrichments in the solid phase of the sediment. However, a productivity event alone gives neither an explanation for the loss of relation between Ba_{xs} and $CaCO_3$ nor for the discrepancy between Ba_{xs} and the excess fractions of Ni, Cu, and Zn below the Ba_{xs} peak at 12.7 m sediment depth.

A period of enhanced methane flux, in turn, could have initiated a redistribution of barite at the sulphate/methane transition. A redistribution of barite would explain the particular concentration profile of Ba_{xs} as well as its deviation from Ni_{xs}, Cu_{xs}, Zn_{xs} and $CaCO_3$ below the Ba_{xs} peak at 12.7 m sediment depth. Moreover, the accompanying anaerobic oxidation of methane would have produced large amounts of sulphide. Thus, a period of enhanced methane flux would have enabled the sulphurization of organic matter as well as a secondary binding of Ni, Cu, and Zn to organic matter and the distinct enrichments of enrichment of Fe, S_{tot} and Mo. In contrast, there is no straightforward explanation for the enrichment of Mn in the vicinity of a diagenetic Ba_{xs} front.

3.5. Conclusions

Our findings underline the importance of organic matter for the distribution of trace elements in the solid phase of marine sediments. Within the oxic and post-oxic section of the investigated gravity core, Ni_{xs}, Cu_{xs}, and Zn_{xs} show a close correspondence to the productivity proxy Ba_{xs}. This relation suggests that the productivity driven input of these trace elements is still recorded in the sediment though organic matter has been degraded intensely. In contrast, neither the trace elements nor Ba_{xs} are directly connected to the preserved C_{org} contents.

In the sulphidic zone, the type of relation changes. Ni_{xs}, Cu_{xs}, and Zn_{xs} are related to the amount of preserved C_{org} but they do not reveal any similarity with the distribution of Ba_{xs}. We suggest that under sulphidic conditions a correspondence between trace metals and preserved C_{org} might result from an early diagenetic complexation of Ni, Cu, and Zn with organic sulphur compounds.

These findings have promising implications for the reconstruction of paleoenvironments. On the one hand, the good correlation between Ni_{xs}, Cu_{xs}, Zn_{xs}, and Ba_{xs} under oxic and post-oxic conditions supports the reliability of biogenic Ba as a proxy for paleoproductivity. Moreover, this relation might become a promising indicator for non-sulphidic conditions in the sediment if pore water data are not available. On the other hand, the good correlation between Ni_{xs}, Cu_{xs}, Zn_{xs}, and C_{org} under sulphidic conditions might be used as

an indicator for the presence of dissolved sulphide in pore water and for the sulphurization of organic matter.

Furthermore, the solid phase contents of Ba_{xs} suggest either a period of enhanced productivity during the penultimate glacial/interglacial transition (Termination II) or a redistribution of barite during a period of enhanced methane flux at site GeoB 4901. In the former case, changes in productivity along with non-steady state diagenesis could have formed the observed enrichments of Mn and Fe in the vicinity of the Ba_{xs} maximum. In the latter case, a higher methane flux would not only have caused a redistribution of barite at the sulphate/methane transition but also an enhanced production of sulphide. Thereby, methane would have enabled the sulphurization of organic matter and the observed distribution pattern of Ni, Cu, and Zn, as well. While at present none of both scenarios can be discarded completely, our findings clearly stress the potential impact of the upward methane flux on the pore water and solid phase of sediments.

This study points to the important role of reactions that occur at the sulphate/methane transition of marine sediments. In this context, the observed correspondence of trace elements to either Ba_{xs} or (sulphurized) C_{org} needs further investigation since a better understanding of the governing processes might allow to distinguish between productivity and methane as driving forces for early diagenesis.

Acknowledgements - We thank the crew and scientists aboard R.V. METEOR for their help with coring and sampling operations during cruise M 41/1 to the South Atlantic. The processing and analysis of the numerous solid phase and pore-water samples would have been impossible without the committed assistance of Sigrid Hinrichs, Joseph Hell, Silvana Hessler, Susanne Siemer, and Karsten Enneking. We are also grateful to Sadat Kolonic and Adesina Adegbie who provided the unpublished C_{org} data set and the age model of gravity core GeoB 4901-8, respectively. The preparation of the manuscript benefited from constructive discussions with Matthias Zabel, Christian Hensen, Thomas Wagner, and Gert de Lange. This research was funded by the Deutsche Forschungsgemeinschaft (contribution no. of Special Research Project SFB 261 at the University of Bremen).

Chapter 4: Early diagenesis at the sulphate/methane transition: (re)distribution of barium and other trace elements in sediments on the continental slope off Namibia, Southeast Atlantic

Verena Heuer, Sabine Kasten, Christian Hensen*, Horst D. Schulz
Fachbereich Geowissenschaften, Universität Bremen, Postfach 330 440, D-28334 Bremen
** present address: GEOMAR, Wischhofstr. 1-3, D-24148 Kiel, Germany*

Abstract

Below the highly productive upwelling region off Namibia, anaerobic oxidation of methane is known to consume all sulphate from the pore water at fairly shallow sediment depth. Our pore water and solid phase analyses of a 13.7 m long gravity core document the redistribution of barite ($BaSO_4$) at the present sulphate/methane transition as well as further effects of anaerobic methane oxidation.

The precipitation of diagenetic barite fronts can be used for the reconstruction of temporal variations in the upward methane flux. At the sulphate/methane transition of the investigated sediment, the solid phase enrichment of Ba and the observed flux of dissolved Ba^{2+} indicate that the present steady state of upward methane and downward sulphate fluxes has been fairly constant for at least 23,900 years.

Due to methane driven sulphate reduction and low Fe-reactivity pore waters are sulphidic throughout the analysed gravity core. These conditions facilitate the sulphurization of organic matter. In the investigated gravity core, solid phase contents of Cu, Ni, and partly Zn resemble the distribution of C_{org} and S_{tot}. We suggest that the trace metals' correspondence to C_{org} and S_{tot} does not result from the primary input of Ni, Cu, and Zn with organic matter but from an early diagenetic redistribution, i.e. from a complexation of these trace metals with either sulphur containing functional groups or polysulphide bridges that result from the intra- and intermolecular incorporation of sulphur into organic matter. In contrast Ce, Co, Cr, Fe, Ga, K, La, Mg, Mn, Nd, Pb, Pr, Sc, Sm, Ti, V, and Yb are closely correlated to Al and their total solid phase contents are controlled by terrigenous aluminosilicates.

4.1. Introduction

Early diagenesis is known to affect the geochemical composition of marine sediments in several ways. The degradation of organic matter does not only obscure any relation between the productivity in surface waters and the preservation of organic carbon (C_{org}) in sediments (e.g., de Lange et al., 1994; Rullkötter, 2000). The remineralization process fuels also a variety of redox reactions which can alter the composition of the solid phase (e.g., Froelich et al., 1979; Berner, 1980; 1981). In particular, Mn and Fe are dissolved and mobilised by the reduction of Mn(IV) and Fe(III) oxides in post-oxic environments whereas the precipitation of sulphides binds metals to the solid phase in sulphidic sediment sections (e.g., Shaw et al., 1990). Moreover, reduced sulphur species (H_2S and/or polysulphides) can also react with organic matter. This sulphurization of organic matter works as an antagonist to remineralization since the intra- and intermolecular incorporation of sulphur supports the preservation of organic compounds (e.g., Sinninghe Damsté et al., 1989; 1998; Sinninghe Damsté and de Leeuw, 1990; Kohnen et al., 1991; Schouten et al., 1994b; Lückge et al., 1999; Werne et al., 2000).

While the early diagenetic decay and alteration of organic matter limits the use of the amount and composition of sedimentary C_{org} as proxies for past productivity and other ocean properties, the early diagenetic redistribution of trace elements forms new signals that are related to the redox conditions of the sediment. Thus, the solid phase record of trace elements can be used for the reconstruction of depositional environments. In this context particular attention has been paid to metal enrichments that form during periods of non-steady state diagenesis (e.g., Kasten et al., subm.).

Non-steady state diagenesis can arise from temporal variations of productivity, bottom water oxygen level or bulk sedimentation rate that change the burial rate of organic matter. During the transition from one depositional environment to another geochemical reaction fronts develop. These fronts can either be fixed at particular sediment levels for a prolonged period of time or move downwards into the sediment (Kasten and Jørgensen, 2000). They are accompanied by dissolution and reprecipitation processes that can lead to distinct enrichments of trace elements in the solid phase of the sediment. For example, downward progressing oxidation fronts can cause the precipitation and enrichment of Mn and Fe by the oxidation of dissolved Mn(II) and Fe(II) species that emanate from the reductive dissolution of Mn(IV) and Fe(III) oxides in the underlying post-oxic zone (e.g., Wilson et al., 1985; 1986a; 1986b; Wallace et al., 1988). Similarly, downward progressing sulphidisation fronts can form distinct iron sulphide enrichments due to the precipitation of upward diffusing, dissolved Fe(II) (e.g., Berner, 1969; Passier et al., 1996; Kasten et al., 1998). In this way, secondary enrichments of trace metals record geochemical changes in the depositional environment that can result from the deposition of turbidites (e.g., Colley et al., 1984; Wilson et al., 1985; 1986b; Thomson et al., 1993; 1998a; 1998b), from the formation of sapropels (e.g., Pruysers et al., 1993; Thomson et al., 1995; Passier et al., 1996; 1998; van

Santvoort et al., 1996; 1997) or at glacial/interglacial transitions (e.g., Thomson et al., 1984b; 1996; Wallace et al., 1988; Kasten et al., 1998).

Heterogeneity in the preservation of a primary signal introduces large uncertainties into a reconstruction of marine productivity that is based on the C_{org} content of sediments. Thus, additional proxies are required for more reliable estimations of paleoproductivity (e.g., Rühlemann et al., 1999; Wefer et al., 1999). During the last two decades biogenic Ba has received increasing attention as a potential proxy for primary productivity (e.g., Dehairs et al., 1980; Bishop, 1988; Dymond et al., 1992; Francois et al., 1995; Gingele et al., 1999). Although its biogeochemical relation to productivity is not completely understood biogenic Ba offers one major advantage over other productivity related parameters like C_{org} and $CaCO_3$. It forms discrete barite ($BaSO_4$) crystals that are well preserved in the sediment due to their highly refractive nature (Dehairs et al., 1980; Gingele and Dahmke, 1994). In principle, there is only one important diagenetic process that alters the sedimentary Ba record and limits its use as a proxy for paleoproductivity: the dissolution of barite in sulphate-depleted sediments (e.g., Brumsack, 1986; von Breymann et al., 1992; Torres et al., 1996; Dickens, 2001).

Complete sulphate depletion is a prominent feature of the transition from sulphidic to methanic conditions in deeper parts of marine sediments. The consumption of sulphate at the sulphate/methane transition results from anaerobic methane oxidation (e.g., Iversen and Jørgensen, 1985; Jørgensen et al., 2001) and this process is assumed to be mediated by a consortium of methane consuming archaea and sulphate-reducing bacteria in a distinct sulphate/methane transition zone (Boetius et al., 2000). Niewöhner et al. (1998) have shown that anaerobic methane oxidation accounts for up to 100% of deep sulphate reduction within the sulphate/methane transition zone and consumes the total net diffusive sulphate flux in sediments from the highly productive upwelling area off Namibia.

While numerous studies have demonstrated the effects of reaction fronts acting at the oxic/post-oxic redox boundary and at the interface between post-oxic and sulphidic conditions, only few investigations focus on the sulphate/methane transition. Nevertheless, the formation of 'barite fronts', i.e. the diagenetic mobilisation of barium and reprecipitation in the depth range of near zero pore-water sulphate, is a long known process (e.g., Goldberg and Arrhenius, 1958; Brumsack, 1986) and additional mechanisms that enhance the accumulation of barite have been discussed as well (Torres et al., 1996). Von Breymann et al. (1992) have pointed out that Ba remobilisation does not only degrade the paleoproductivity signal. Instead, buried and partially dissolved diagenetic barite fronts might also offer a novel way of tracking changes in diagenesis. In fact, Dickens (2001) has recently applied sedimentary Ba records in order to assess changes in the upward methane flux out of the Blake Ridge gas hydrate reservoir during the late Pleistocene. His approach is based on the assumption that diagenetic enrichments of barite mark present and past depths of complete sulphate depletion in pore water. Complete sulphate consumption, in

turn, is thought to result from anaerobic methane oxidation. Thus, the upward methane flux can be reconstructed from diagenetic barite enrichments marking the depth of zero pore water sulphate.

In this contribution, we present detailed solid phase and pore-water data that describe a sulphate/methane transition in a core from the continental slope off Namibia. Considering the potential alteration of the solid phase record at this reaction front we will address the relation of barium enrichments to present and past methane fluxes and the formation of further secondary signals in the solid phase of the sediment.

4.2. Sampling Sites and Core Descriptions

Site GeoB 3718 is located south of Walvis Bay at the continental slope off Namibia (24°53.6'S, 13°09.8'E) and was sampled in February 1996 during RV Meteor cruise M 34/2 to the eastern South Atlantic (Fig. 4.1). The 13.71 m long gravity core GeoB 3718-9 was recovered from a water depth of 1312 m. According to the shipboard geological analysis

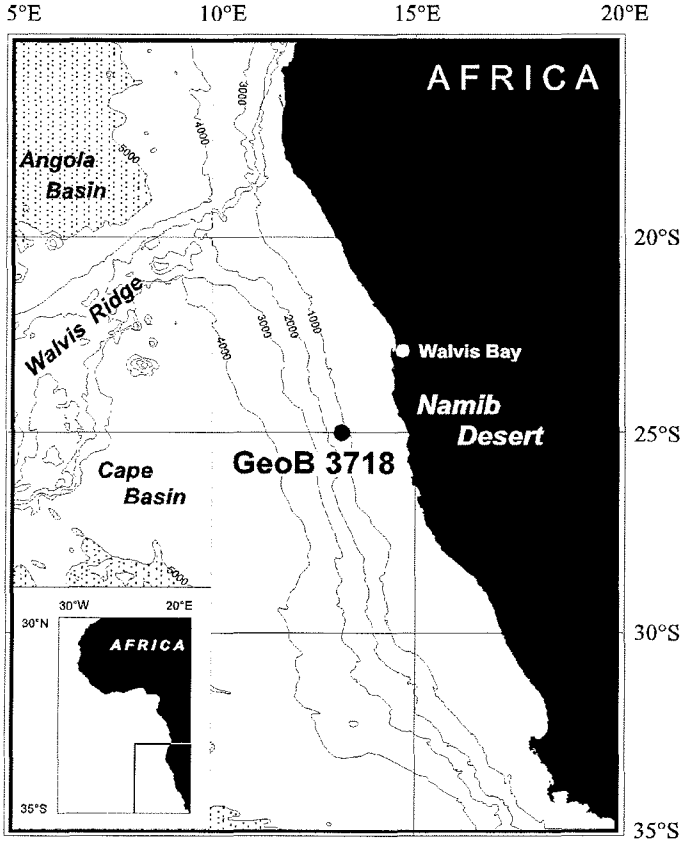

Fig. 4.1: *Map showing the location of site GeoB 3718 at the continental slope off Namibia (24°53.6'S, 13°09.8'E; water depth: 1312 m)*

the recovered sediment is a nannofossil ooze with minor to major amounts of clay. Foraminifera were found in the top five meters while in the sediment section between 7 and 11 m a great abundance of diatoms was observed which partly even exceeded the abundance of calcareous nannofossils (Schulz et al., 1996). For site GeoB 3718 sedimentation rates of 8-11 cm/ka can be adopted from adjacent sampling sites at similar water depths (Donner and Giese, 1992).

Due to the lack of large rivers terrigenous input is of minor importance at site GeoB 3718 and terrigenous material reaches the continental slope off Namibia mainly via the aeolian pathway (Lisitzin, 1996). At present Southeast-Northwest trade winds cause the upwelling of nutrient-rich water masses in this area (Wefer and Fischer, 1993) and thus enhance the primary productivity within the surface waters and the organic matter export to the sediment (Embley and Morley, 1980; Gingele, 1992). As a result, intense remineralization of C_{org} takes place in the sediment and methanogenesis becomes a significant process even at shallow sediment depths (Niewöhner et al., 1998; Hensen et al., 2000).

4.3. Methods

4.3.1. Geochemical Analysis

Directly after recovery gravity core GeoB 3718-9 was cut into 1 m segments and taken to a refrigerated on-board laboratory (4°C) where pore water was extracted in the inert atmosphere of an argon filled glove-box. In addition to the analyses of sulphide, sulphate, and methane (Niewöhner et al., 1998) subsamples of pore water were preserved for the analysis of Ba that was determined on land by ICP-AES.

Solid phase analysis was carried out on archived core material that is kept at the Department of Geosciences, University of Bremen, Germany. Over the whole length of gravity core GeoB 3718-9 discrete samples were taken at intervals of 5 to 30 cm. Samples (ca. 10 cm^3) were freeze-dried and ground in an agate mortar prior to further processing.

For bulk solid phase analysis, 50 mg of dry sediment were digested in a microwave system (MLS – MEGA II and MLS – ETHOS 1600) with a mixture of concentrated nitric (3 ml), hydrofluoric (2 ml) and hydrochloric (2 ml) acids of supra-pure quality at a temperature of ~200°C and a pressure of 30 kbar. The digestion solutions were evaporated to dryness, redissolved in 0.5 ml concentrated nitric acid and 4.5 ml deionized water (MilliQ), homogenised and finally made up to a volume of 50 ml.

Subsequently, major, minor and trace elements were analysed by inductively coupled plasma atomic emission spectrometry (ICP-AES) using a Perkin Elmer Optima 3300RL. For the measurement of trace elements an ultrasonic nebulizer was employed in order to improve the detection limit. The precision of the ICP-AES determination (three consecutive measurements on the same solution) was better than 1% for major and minor elements and in the range of 1-3% for all trace elements except for Co (5%) and Pb (15%). The accuracy of the analytical procedure was checked using standard reference material USGS MAG-1 (Gladney and Roelandts, 1988). For all elements the difference between the measured element contents and the certified concentration ranges was less than 4% and standard deviations of eight replicates were less than 5%.

In addition, total amounts of organic carbon (C_{org}) were determined in subsamples of the freeze-dried and ground solid phase samples with a LECO CS-300 Carbon-Sulphur analyser after careful removal of inorganic carbon by 0.25 N HCl. A detailed description of the used methods is available at our homepage (http://www.geochemie.uni-bremen.de).

4.3.2. Normative Calculation of Element Fractions

In order to distinguish between different potential carrier phases of trace elements we employed a normative calculation of element fractions. This calculation is based on the assumption that the total measured element concentration TE_{tot} consists of a lithogenic fraction TE_{lith} and an additional excess fraction TE_{xs} (Eq. 1). The lithogenic fraction, i.e. the detrital part present in aluminosilicates, can be calculated from a constant element-aluminium ratio k(TE/Al) and the measured total aluminium content Al_{tot} (Eq. 2). Consequently, the excess fraction results from the difference between the total measured element concentration and the calculated lithogenic fraction (Eq. 3).

(1) $TE_{tot} = TE_{lith} + TE_{xs}$

(2) $TE_{lith} = k(TE/Al) \cdot Al_{tot}$

(3) $TE_{xs} = TE_{tot} - k(TE/Al) \cdot Al_{tot}$

For the calculation of lithogenic element fractions we applied the constant element-aluminium ratios k(TE/Al) that result from the average composition of the continental crust as given by Wedepohl (1995) (Table 4.1).

				TE/Al				TE_{xs}
	mean	SD	r(Al)[a]	mean	SD	k(TE/Al)[b]	enrichment[c]	mean[d]
	[g/kg]	[%]		[g/g]	[%]	[g/g]		[%]
Al	36.7	16						
Ba	1.17	117	0.01	0.033	116	0.004[e]	8.3	77
Ca	134	30	-0.35					
C_{org}	81.6	18	0.33					
S	18.3	19	0.44					

	TE_{tot}			TE/Al				TE_{xs}
group A:	mean	SD	r(Al)[a]	mean	SD	k(TE/Al)[b]	enrichment[c]	mean[d]
	[g/kg]	[%]		[g/g]	[%]	[g/g]		[%]
Fe	23.2	17	0.96	0.631	3	0.543	1.2	14
K	11.5	15	0.98	0.314	3	0.269	1.2	14
Mg	10.6	10	0.89	0.294	10	0.276	1.1	5
Ti	1.76	16	0.91	0.048	5	0.050	1.0	-5
	[mg/kg]	[%]		[mg/g]	[%]	[mg/g]		
Ce	29.9	14	0.93	0.74	7	0.75	1.0	0
Co	4.68	15	0.82	0.128	7	0.301	0.4	-57
Cr	129.6	18	0.73	3.54	9	1.58	2.2	45
Ga	10.4	18	0.89	0.282	6	0.19	1.5	33
La	15.5	14	0.88	0.426	8	0.38	1.1	11
Mn	138.8	14	0.92	3.81	6	8.99	0.4	-57
Nd	15.3	13	0.87	0.423	10	0.34	1.2	19
Pb	7.10	18	0.80	0.196	11	0.186	1.1	3
Pr	4.84	18	0.96	0.132	4	0.084	1.6	36
Sc	9.26	15	0.94	0.254	5	0.20	1.3	21
Sm	3.13	14	0.89	0.086	7	0.067	1.3	22
V	54.6	14	0.91	1.50	8	1.23	1.2	18
Yb	1.97	12	0.67	0.055	14	0.025	2.2	53

	TE_{tot}			TE/Al				TE_{xs}
group B:	mean	SD	r(Al)[a]	mean	SD	k(TE/Al)[b]	enrichment[c]	mean[d]
	[mg/kg]	[%]		[mg/g]	[%]	[mg/g]		[%]
Cu	75.6	16	0.56	2.09	15	0.314	6.7	85
Mo	35.5	28	0.18	0.977	29	0.014	70.7	98
Ni	92.0	15	0.52	2.54	15	0.704	3.6	72
Zn	99.8	17	0.65	2.74	13	0.817	3.4	70

(a) Spearman correlation coefficient
(b) average continental crust value according to Wedepohl (1995)
(c) ratio between the TE/Al ratio in gravity core GeoB 3718 and the continental crust value k(TE/Al)
(d) relative contribution of the excess fraction to the total solid phase content
(e) Ba/Al ratio in aluminosilicates according to Gingele and Dahmke (1994)

Table 4.1: *Average composition of gravity core GeoB 3718-9: total solid phase contents of major, minor and trace elements (TE_{tot}) in group A and B; correlation coefficients r(Al) for the correlation between total solid phase contents of trace elements and Al; mean trace element - Al ratios (TE/Al) in the solid phase of gravity core GeoB 3718-9 and their enrichment with respect to the average continental crust values k(TE/Al); relative contribution of the excess fractions (TE_{xs}) to the total solid phase contents.*

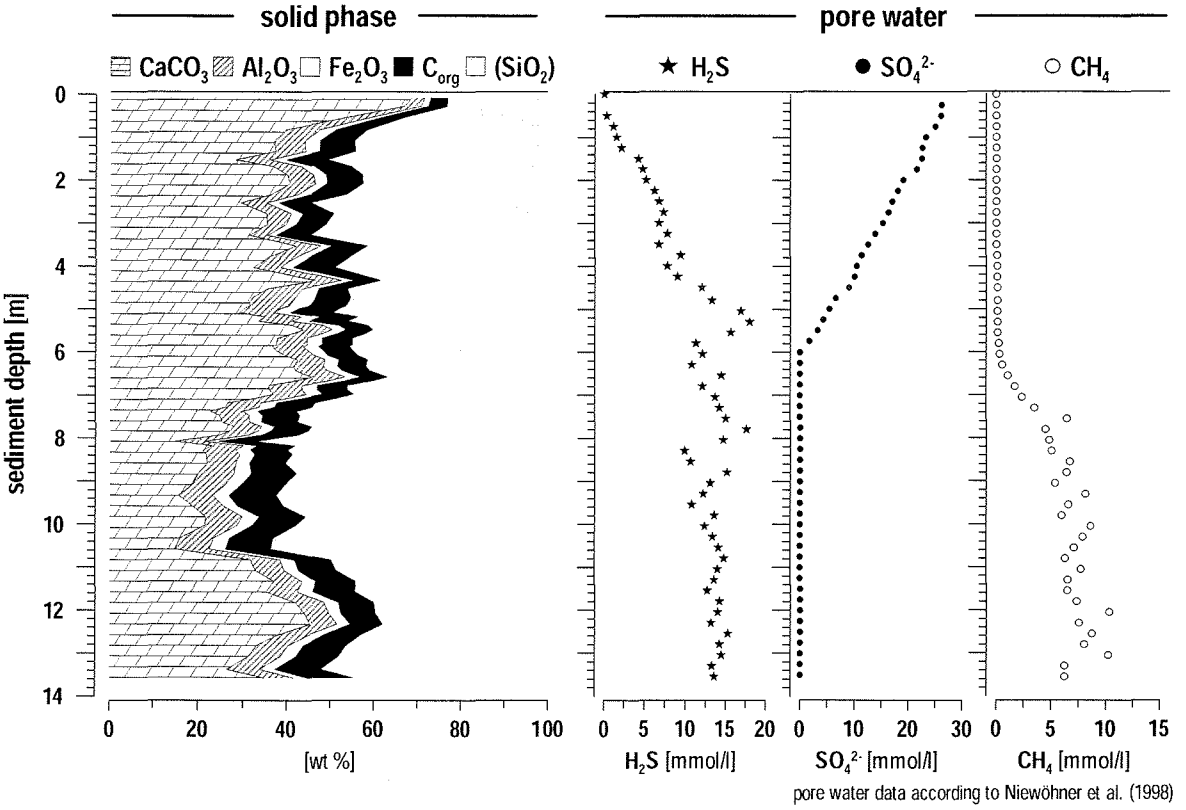

Fig. 4.2: *Overall sediment characteristics of site GeoB 3718: bulk solid phase and pore water chemistry. Pore water data according to Niewöhner et al. (1998).*

4.4. Results

The geochemical results for gravity core GeoB 3718-9 are summarised in Table 4.1. In addition, the full data set is available via the geological and environmental data network Pangaea (http://www.pangaea.de).

4.4.1. Overall Sediment Characteristics

In gravity core GeoB 3718-9 $CaCO_3$ presents 15 to 69 wt% of the solid phase while the terrigenous sediment fraction is of minor importance contributing an Al_2O_3 content of 3 to 10 wt%. The high organic carbon content (C_{org}) makes up 4 to 11 wt% whereas Fe presents only 1 to 5 wt% in terms of Fe_2O_3. On total, the mass balance leaves a rest of about 48 wt% for silicate phases that were not accessible with the employed methods (Fig. 4.2).

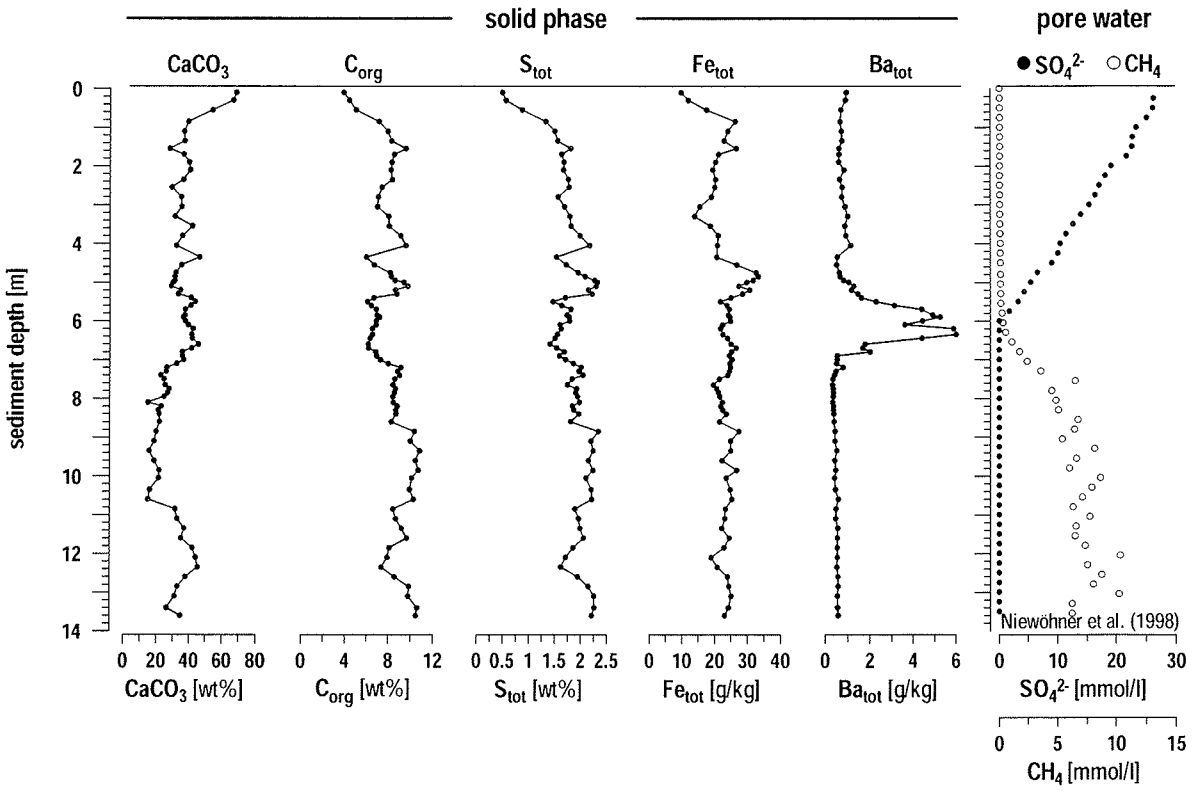

Fig. 4.3: *Distribution of $CaCO_3$, C_{org}, S_{tot}, Fe_{tot}, and Ba_{tot} in the solid phase of gravity core GeoB 3718-9. Pore water profiles of sulphate and methane indicate the sulphate/methane transition at 6 m below sediment surface. Pore water data according to Niewöhner et al. (1998).*

In the solid phase the concentration profiles of carbonate ($CaCO_3$), organic carbon (C_{org}), total sulphur (S_{tot}), and total iron (Fe_{tot}) show only little variation over sediment depth (Fig. 4.3). Moreover, the increase of C_{org}, S_{tot}, and Fe_{tot} within the upper 2 meters corresponds well to decreasing $CaCO_3$ contents and points to carbonate dilution. Yet, the distribution of Fe_{tot} differs distinctly from the concentration profiles of C_{org} and S_{tot}. While the amounts of preserved C_{org} and the S_{tot} contents are closely correlated to each other with a correlation coefficient r of 0.88, Fe_{tot} shows only low correspondence to S_{tot} (r = 0.45) and C_{org} (r = 0.28).

4.4.2. Barium

The solid phase analysis of gravity core GeoB 3718-9 shows a distinct enrichment of barium in the vicinity of the sulphate/methane transition at 6.0 mbsf (Fig. 4.3). Total solid phase contents of barium (Ba_{tot}) invariably exceed 750 ppm in the sediment section between

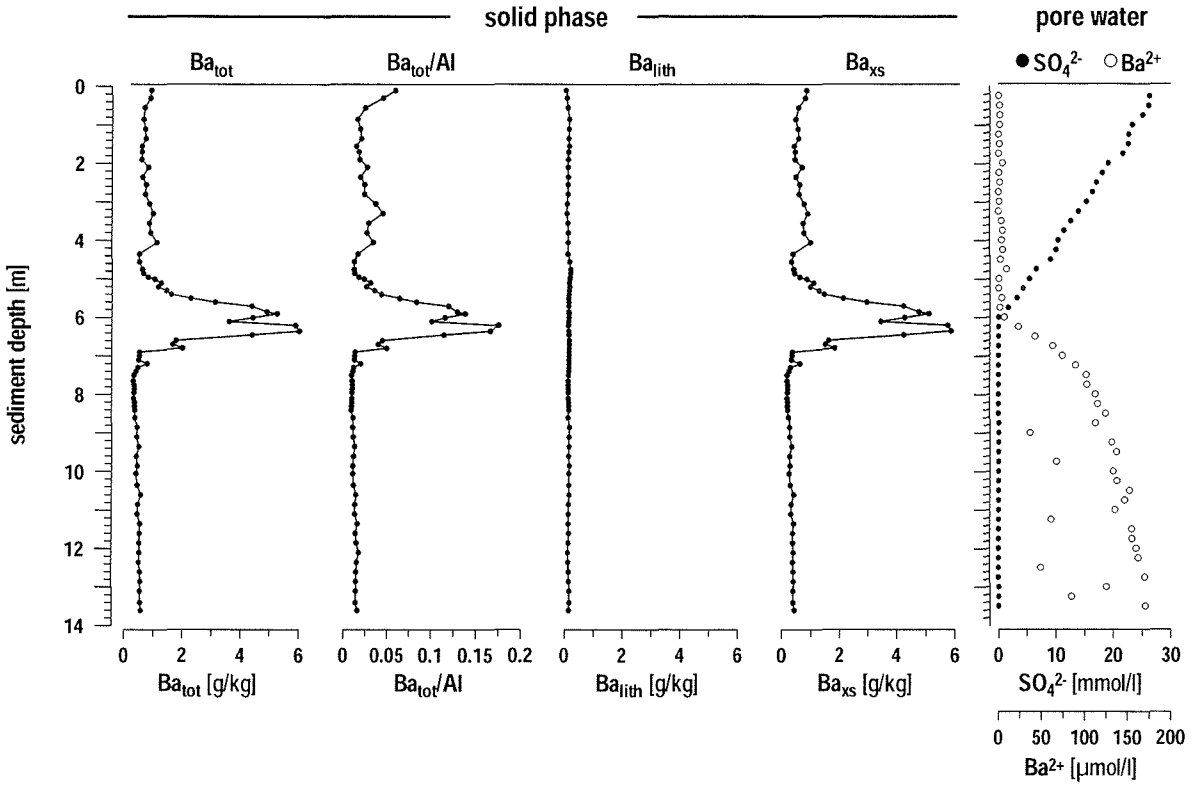

Fig. 4.4: *Distribution of Ba_{tot}, Ba/Al, Ba_{lith} and Ba_{xs} in the solid phase of gravity core GeoB 3718. The pore water profiles of Ba^{2+} and sulphate illustrate the dissolution of barite in sulphate depleted sediment section below 6 m sediment depth. Suphate data according to Niewöhner et al. (1998).*

5.0 and 6.8 mbsf and peak Ba_{tot} concentrations amount up to 6020 ppm at 6.4 mbsf and 5260 ppm at 5.9 mbsf. In contrast, a mean Ba_{tot} content of only 750 ppm is observed in the upper 5.0 m of sediment. Moreover, the sulphate depleted sediment section between 7.0 and 13.6 mbsf contains even lower and nearly constant amounts of Ba_{tot} that average around 470 ppm.

Across the barium front, the distribution of primary sediment components does not change significantly (Fig. 4.3). Consequently, the normalisation of Ba_{tot} to Al yields a Ba/Al profile that closely resembles the concentration profile of Ba_{tot} (Fig. 4.4). The similarity of both profiles suggests that the prominent barium front represents a secondary, diagenetic accumulation of barium at the sulphate/methane transition. Moreover, the normative calculation of barium fractions shows the governing role of an excess fraction in gravity core GeoB 3718-9 (Fig. 4.4). Provided the immobile barium fraction in aluminosilicates (Ba_{lith}) is given by a constant lithogenic Ba/Al ratio of 0.004 (Gingele and Dahmke, 1994), an additional excess fraction of barium (Ba_{xs}) makes up 57-98% of the total solid phase content Ba_{tot}.

Finally, our pore water data confirm the precipitation of barium at the sulphate/methane transition (Fig. 4.4). While dissolved Ba^{2+} is negligible in the sulphate containing pore water throughout the upper 6.0 m of sediment, the dissolution of barite has produced up to 170 µmol/l dissolved Ba^{2+} in the sulphate depleted pore water of the underlying sediment section. The convex-shaped concentration profile points to a decreasing dissolution rate of barium in a system that is controlled by diffusion. Following upward diffusion pore water Ba^{2+} become zero due to the precipitation of barite in sulphate rich pore water.

4.4.3. Minor and Trace Elements

In analogy to the fairly homogenous distribution of major sediment components in gravity core GeoB 3718-9, solid phase contents of minor and trace elements show only little variation over depth. Yet, two groups of minor and trace elements can be distinguished. Group A (Ce, Co, Cr, Fe, Ga, K, La, Mg, Mn, Nd, Pb, Pr, Sc, Sm, Ti, V, Yb) is governed by the lithogenic sediment fraction that is represented by Al (Fig. 4.5). Group B (Cu, Ni, Mo, Zn) shows a separate distribution pattern (Fig. 4.6) and is closely related to the distribution of both C_{org} (Fig. 4.7) and S_{tot} (Fig. 4.8).

Group A: Ce, Co, Cr, Fe, Ga, K, La, Mg, Mn, Nd, Pb, Pr, Sc, Sm, Ti, V, Yb

In the solid phase of gravity core GeoB 3718-9, the overall distribution of Group A elements is characterised by a close correlation of the total element contents and the total Al content. According to the Spearman analysis the correlation coefficients r range from 0.98 to 0.80 except for Cr (r = 0.73) and Yb (r = 0.67) (Table 4.1). Moreover, element-aluminium ratios are almost constant with standard deviations of only 3 to 14% (Table 4.1).

A further feature of this element association is the dominating contribution of the lithogenic fraction to the total element content in the solid phase (Fig. 4.5). According to our normative estimation, lithogenic fractions present 81 - 100% of the total element contents of Nd, V, Fe, K, La, Mg, Pb, and Ce and 47 - 78% of the total element contents of Yb, Cr, Pr, Ga, Sc, and Sm (Table 4.1). With respect to Ti, the calculated lithogenic fraction overestimates the total content by 5%. For Ce, Pb, Mg, and Ti, we observe a constant deviation of 0 - 5% between analysed total contents and calculated contents in the lithogenic fraction. This disagreement is within the accuracy of the analytical procedure. Fe, K, V, Sc, Ga, Cr and the REE have larger excess fractions which represent 14 - 53% of the total element contents. However, the relative contribution of the excess fractions remains constant throughout the core. This constancy suggests that the continental crust values that were used for the normative calculation of the lithogenic element fractions (Table 4.1) systematically underestimate the content of the respective trace elements in the

aluminosilicates of the source region. In other words, the Fe/Al, K/Al, V/Al, Sc/Al, Ga/Al, Cr/Al and REE/Al ratios of the sediment are 1.2- to 2.2-fold enriched compared to the average continental crust values (Table 4.1). The opposite is true for Mn and Co. These elements are depleted with respect to the estimated lithogenic element contents. For both Mn and Co a relative deficiency of 57% was observed throughout the core and indicates that the used average continental crust values (Table 4.1) systematically overestimate the contents of Mn and Co in the terrigenous aluminosilicate fraction.

Group B: Cu, Ni, Mo, Zn

Group B shows a notably lower correspondence to the terrigenous sediment fraction than group A. Total solid phase contents of group B elements and of Al are correlated with correlation coefficients r ranging from 0.65 to 0.18. Likewise, the standard deviations of the element-aluminium ratios are higher than in group A and vary between 13 and 29% (Table 4.1).

Furthermore, the normative calculation of element fractions illustrates the minor contribution of the lithogenic element fractions to the total element contents (Fig. 4.6). As opposed to group A the excess fractions dominate in the solid phase of the sediment (Table 4.1). They make up 70 - 98% of the total element contents and increase in the order Zn < Ni < Cu < Mo. The corresponding total element-aluminium ratios are 3.4 to 71-fold enriched with respect to the average continental crust values (Table 4.1). In addition, the deviation between the total element contents and the lithogenic element fractions is not constant but varies over depth (Fig. 4.6). Therefore, the excess does not result from a systematic underestimation of trace element contents in aluminosilicates. Instead, it is associated with at least one further carrier aside from the terrigenous sediment fraction.

As can be seen in Figure 4.7 excess fractions of copper (Cu_{xs}) and nickel (Ni_{xs}) have a similar distribution pattern as the preserved C_{org} content with corresponding correlation coefficients r of 0.91 and 0.87, respectively. The concentration profile of excess zinc (Zn_{xs}) partly resembles the distribution of C_{org} but differs in the interval between 5.2 and 7.0 m sediment depth. The overall correlation between Zn_{xs} and C_{org} yields a correlation coefficient r of 0.38. Similarly, the excess fractions of Cu and Ni are closely related to S_{tot} (Fig. 4.8) with corresponding correlation coefficients r of 0.85 and 0.82, respectively, while the correlation between Zn_{xs} and S_{tot} is reduced (r = 0.44). In contrast, Mo_{xs} shows no correlation to C_{org} (r = 0.15) or S_{tot} (r = 0.18).

As opposed to C_{org} and S_{tot}, total Fe contents show only little correspondence to the excess fractions of Cu (r = 0.44) and Ni (r = 0.25) (Fig. 4.9). Similarly, the correlation between Fe_{tot} and Mo_{xs} is low (r = 0.21). However, the distribution of Zn_{xs} is more similar to Fe_{tot} (r = 0.52) than to C_{org} (r = 0.38) or S_{tot} (r = 0.44).

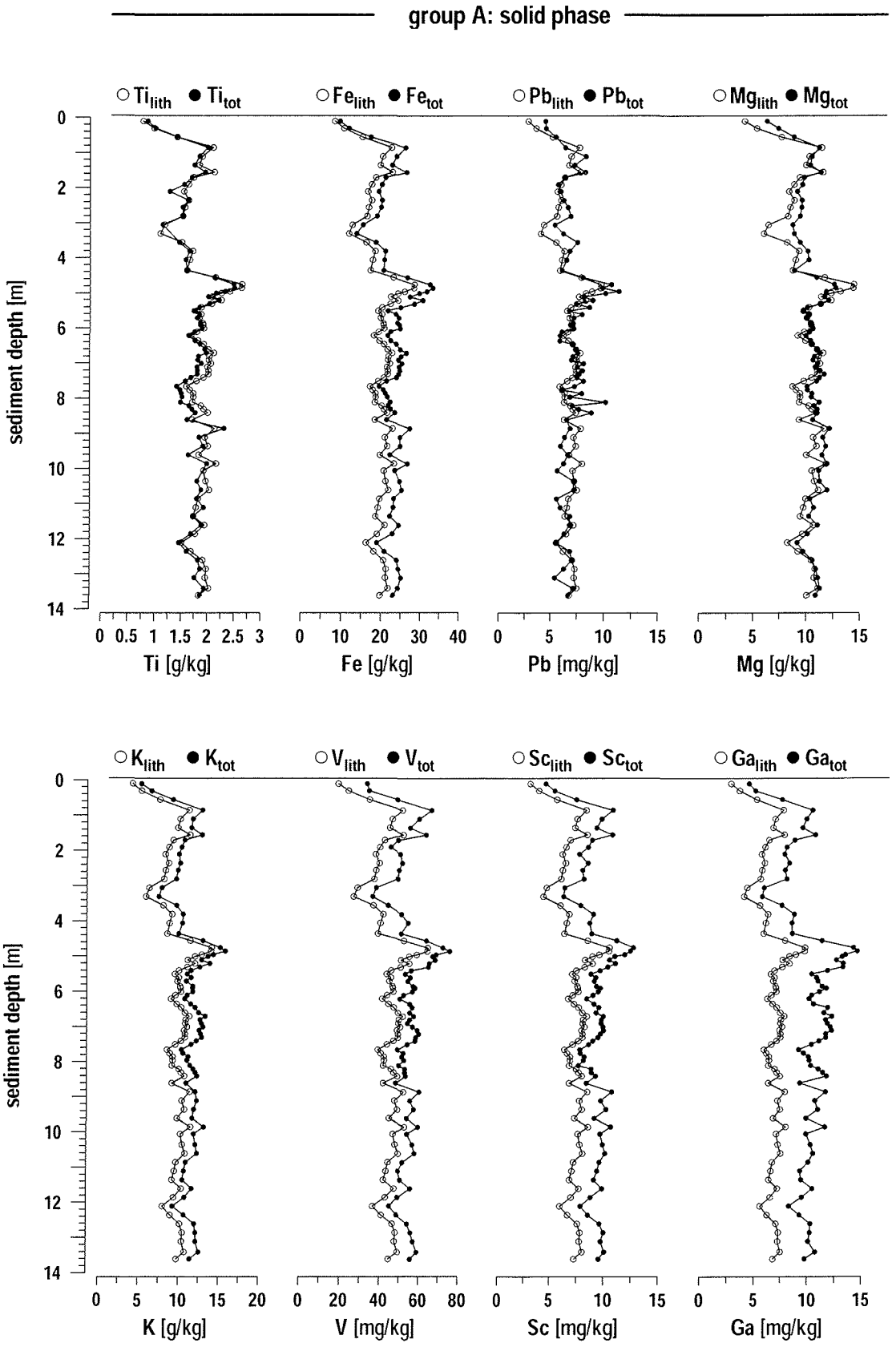

Fig 4.5: *Calculated lithogenic element fractions and analysed total solid phase contents of group A elements in gravity core GeoB 3718. For Ti, Fe, Pb, Mg, K, and V there is only a small deviation between total element contents (Ti_{tot}, ...) and lithogenic fractions (Ti_{lith}, ...)*

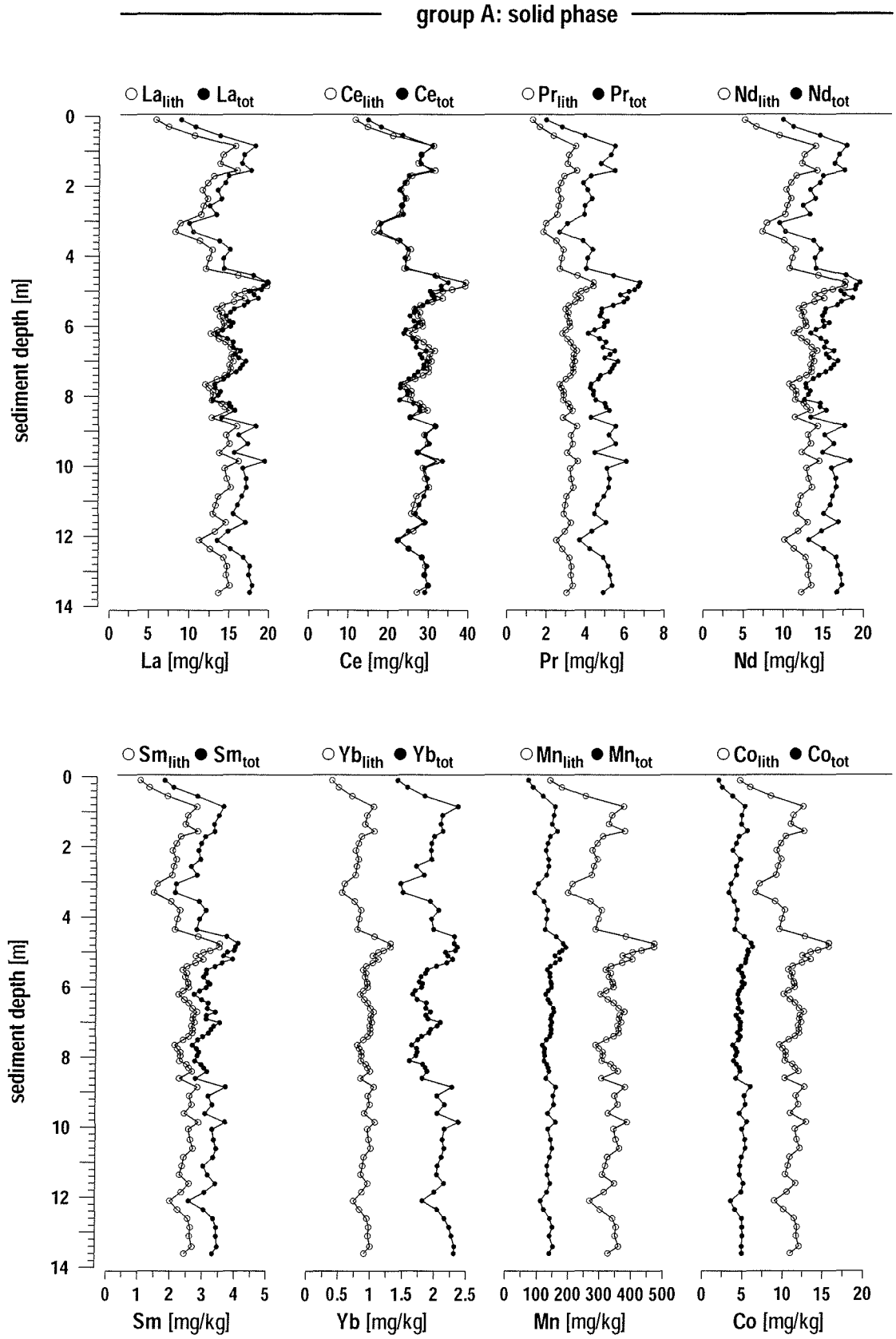

Fig 4.5 (continued): *For Mn and Co, total element contents are deficient with respect to the estimated lithogenic input.*

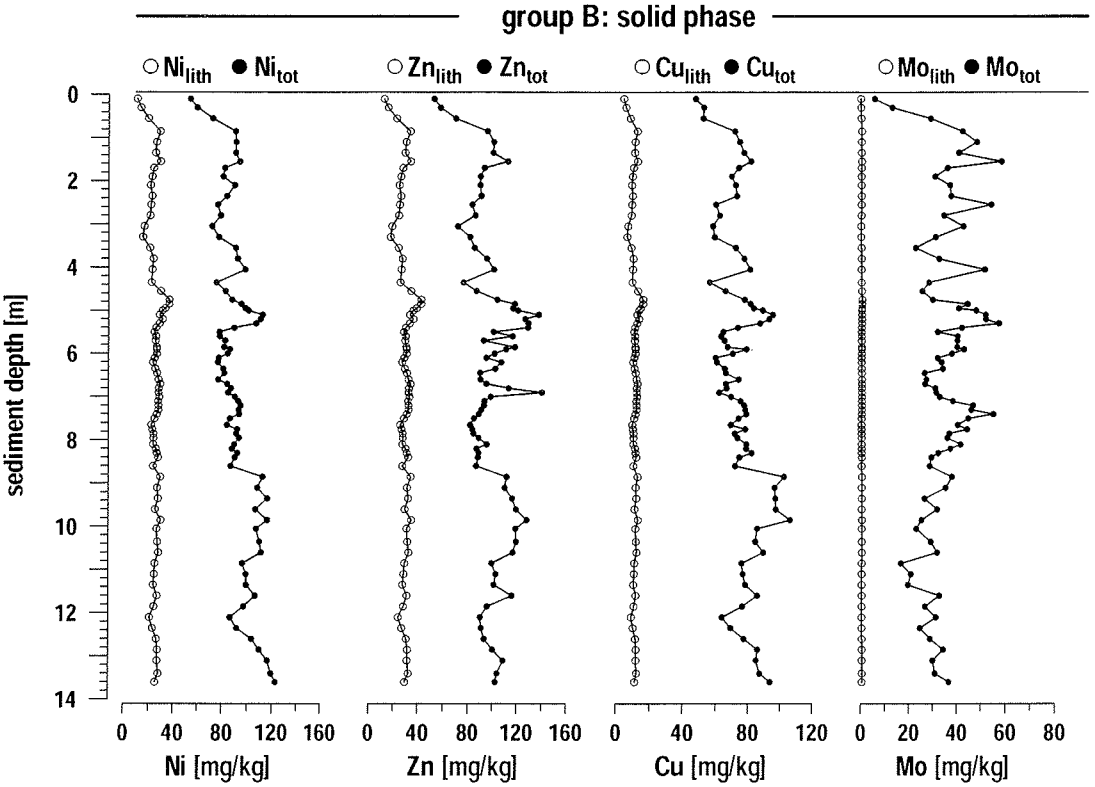

Fig 4.6: *Calculated lithogenic element fractions and analysed total solid phase contents of group B elements in gravity core GeoB 3718. The total solid phase contents of Ni, Zn, Cu, and Mo do not alone result from the lithogenic element fractions present in aluminosilicates.*

4.5. Discussion

The observed distribution patterns of trace elements in the solid phase of gravity core GeoB 3718-9 raise two major questions, namely: (a) How is the barium enrichment related to present and past methane fluxes? - and (b) Do group B elements correspond to both C_{org} and S_{tot} due to primary production and preservation of organic matter or due to early diagenetic processes in the presence of sulphide? In the following, both questions will be discussed with respect to their potential implications for the reconstruction of paleoenvironments.

4.5.1. Barium at the Sulphate/Methane Transition

According to Dickens (2001) sedimentary Ba records can be used to assess changes in upward methane flux. His approach is based on the assumption that diagenetic enrichments of barite mark present and past depths of complete sulphate depletion in the pore water of

marine sediments. Complete sulphate consumption, in turn, is thought to result from anaerobic methane oxidation and the depth of complete sulphate depletion is given by the upward methane flux. Consequently, diagenetic enrichments of barite can be used for the reconstruction of methane fluxes provided the barite fronts have always stayed at or above the sulphate/methane transition. These conditions are met at sites where decreasing methane fluxes have lowered the sulphate/methane transition down into the sediment in the course of time. The approach of Dickens (2001) offers one particular advantage. Barite fronts record a time-integrated signal of sulphate depletion whereas the present pore water profiles of sulphate could have had a complex history.

At site GeoB 3718, pore water investigations have shown that the consumption of sulphate by anaerobic methane oxidation is presently in a steady state. Sulphate concentrations decrease linearly with depth and the diffusive fluxes of sulphate and methane (30.2 mmol·m^{-2}·a^{-1}) are balanced (Niewöhner et al., 1998). In the following, we will use the solid phase enrichment of Ba in order to estimate how long the current methane flux has already been active.

Our pore water data confirm active barium cycling at the present sulphate/methane transition (Fig. 4.4). During sediment burial, barite moves downward from sulphate rich to sulphate depleted pore water where it dissolves. In turn, dissolved Ba^{2+} diffuses upward from sulphate depleted to sulphate rich pore water where it precipitates as barite. Since a considerable Ba enrichment has formed in the solid phase of the sediment, upward Ba^{2+} diffusion must have exceeded downward barite burial over a long period of time. Based on the present flux of dissolved Ba^{2+} across the sulphate/methane transition we can estimate the minimum time that is required for the formation of the authigenic Ba enrichment in gravity core GeoB 3718-9.

The authigenic enrichment of Ba can be quantified with the following assumptions: (a) Authigenic Ba contents result from the amount of Ba that is present in excess of a given background value. For site GeoB 3718 we adopt a background concentration of 750 ppm from the average barium content in the upper 5.0 m of the sediment. (b)The total amount of authigenic Ba is given by both the authigenic Ba contents and the thickness of the barite front. In gravity core GeoB 3718-9 the depth interval between 5.0 and 6.8 mbsf yields an integrated authigenic Ba peak of $3.79 \cdot 10^5$ ppm·cm. With an assumed average grain density of 2.7 g·cm^{-3} and a measured mean porosity of 82%, the amount of authigenic Ba in the 1.8 m thick barite front totals up to 0.220 g·cm^{-2}, or $1.61 \cdot 10^{-3}$ moles of Ba for a 1 cm^2 vertical column of sediment.

For steady state conditions, the diffusive flux of Ba^{2+} across the sulphate/methane transition can be calculated from the present concentration gradient of dissolved Ba^{2+} using the following adaption of Fick's first law of diffusion to the pore water volume of sediments (e.g., Berner, 1980; Boudreau, 1997; Schulz, 2000):

$$J_{sed} = -\Phi \cdot D_{sed} \cdot \frac{\delta C}{\delta x}$$

where J_{sed} is the flux in sediment, Φ is porosity, D_{sed} is the diffusion coefficient in sediment, C is concentration, and x is depth. According to shipboard analysis porosity was 82% at the sulphate/methane transition of site GeoB 3718 and the temperature was 6 °C. For these conditions a diffusion coefficient D_{sed} of $3.46 \cdot 10^{-10}$ $m^2 \cdot s^{-1}$ can be adopted for Ba^{2+} (Schulz, 2000). With an observed concentration gradient of $75.4 \cdot 10^{-10}$ $mmol \cdot m^{-3} \cdot m^{-1}$, the Ba^{2+} flux comes up to $2.14 \cdot 10^{-8}$ $mmol \cdot m^{-2} \cdot s^{-1}$ or $6.74 \cdot 10^{-8}$ $mol \cdot cm^{-2} \cdot a^{-1}$.

A Ba^{2+} flux of this magnitude would allow to build up the observed Ba enrichment ($1.61 \cdot 10^{-3}$ $moles \cdot cm^{-2}$) within 23,900 years. Consequently, the Ba enrichment at site GeoB 3718 suggests that the present methane flux and thus the depth of complete sulphate depletion have been similar over at least 23,900 years - provided diagenesis has always been in a steady state.

Nevertheless, the vertical extension and profile of the barium front indicate slight variations in the position of the sulphate/methane transition. In gravity core GeoB 3718, the barium enrichment is not confined to a distinct layer but extends over the whole sediment section between 5.0 and 6.8 mbsf while the present sulphate/methane transition is located at 6.0 mbsf. Thus, the authigenic enrichment of barium can be found both above and below the current depth of zero pore water sulphate. In particular, peak solid phase contents of barium are situated both at 5.9 mbsf, i.e. on top of the present sulphate/methane transition, and at 6.4 mbsf, i.e. within the sulphate depleted zone. The overlap between the authigenic barium enrichment and the present extension of the sulphate depleted zone points to a recent upward shift of the sulphate/methane transition, i.e. to a recently increased methane flux.

In summary, the quantity of the Ba enrichment can be explained by steady state diagenesis as observed today. However, the extension of the barite front and the multiple peaks can also be attributed to slight changes in the depth of zero pore water sulphate. Nevertheless, the absence of barite fronts in the upper 5.0 m of sediment indicates that in the past methane fluxes were not drastically larger than they are today for a significant period of time. As opposed, smaller methane fluxes cannot be completely excluded since a subsequent upward shift of the sulphate/methane transition could have induced the dissolution of old Ba enrichments at greater sediment depths.

On the whole, our findings at the continental slope off Namibia agree well to the Ba fronts and methane fluxes in sediments on the Blake Ridge (Dickens, 2001). At the Blake Ridge, Ba fronts exist within 0.7 - 3.0 m above the depth of pore water sulphate depletion. The fronts are diffusely distributed, have multiple peaks and extend over a depth interval of 2.6 to 3.0 m. Moreover, their accumulation has required approximately 18,000 years (Dickens, 2001).

4.5.2. Cu, Ni, Zn and the Sulphurization of Organic Matter

At the sulphate/methane transition of gravity core GeoB 3718-9, the anaerobic oxidation of methane does not only consume all sulphate but also produces high concentrations of pore water sulphide (Fig. 4.2) (Niewöhner et al., 1998). Thereby methane oxidation provides the means for the sulphurization of organic matter (cf., Sinninghe Damsté and de Leeuw, 1990; Kohnen et al., 1991; Schouten et al., 1994b). The reaction of organic matter with dissolved sulphide and polysulphides is of particular importance in sediments with high C_{org} contents and a small supply of reactive Fe that prevents the complete trapping of sulphide as iron sulphides (e.g., Mossmann et al., 1991; Werne et al., 2000). Consequently, a significant formation of secondary organosulphur compounds has also been observed at the continental slope off Namibia (e.g., Adam et al., 2000; Brüchert et al., 2000).

At site GeoB 3718, there are strong indications for the sulphurization of organic matter. The close correlation between S_{tot} and C_{org} ($r = 0.88$) suggests that organic sulphur represents the dominant sulphur species in the solid phase (Fig. 4.3). In contrast, iron sulphides are of minor importance and thus there is only little correspondence in the distribution of S_{tot} and Fe_{tot} ($r = 0.45$). These findings reflect the prevalence of C_{org} over Fe_{tot} in the overall composition of the sediment. On a weight basis, C_{org} makes up 4 to 11 wt% of the solid phase while Fe presents only 1 to 3 wt% (Fig. 4.3). On a molar basis, the dominance of C_{org} gets even more obvious. C_{org} yields an average molar ratio of 12 C_{org}/S_{tot} while iron does not even balance the sulphur content of the solid phase as can be seen from mean molar Fe_{tot}/S_{tot} and Fe_{xs}/S_{tot} ratios of only 0.75 and 0.10, respectively. It has to be noted that in this context the distribution of barite is negligible since the sulphur content of barite contributes on average only 1.5 % to the total sulphur content S_{tot}.

Due to the sulphurization of organic matter, the solid phase contents of Ni_{xs}, Cu_{xs}, and Zn_{xs} correspond closely to the distribution of both C_{org} and S_{tot} (Fig. 4.7, Fig. 4.8). In principle, the observed resemblance could result either from the input of Ni, Cu, and Zn with organic matter or from a precipitation of these elements as sulphides.

Ni, Cu, and Zn are known for their interactions with marine organisms and they have a nutrient-type distribution in the water column (Bruland, 1983). Consequently, a productivity based relation between these trace elements and organic matter might also continue in the sediment. However, there is also considerable evidence that Ni, Cu, and Zn lose their association with C_{org} before or while the biogenic detritus is buried in the sediment. For example, a rapid and extensive release of Cu and Ni from particulate C_{org} has been measured in the water column (Kumar et al., 1996). Furthermore, an overall decoupling of trace elements and organic matter has also been observed in the solid phase of sediments and is attributed to a different retention of C_{org} and trace metals during their burial in the sediment (e.g., Thomson et al., 1984a). Finally, the actual release of trace metals from rapidly decomposing organic material has been confirmed in pore water and flux studies at

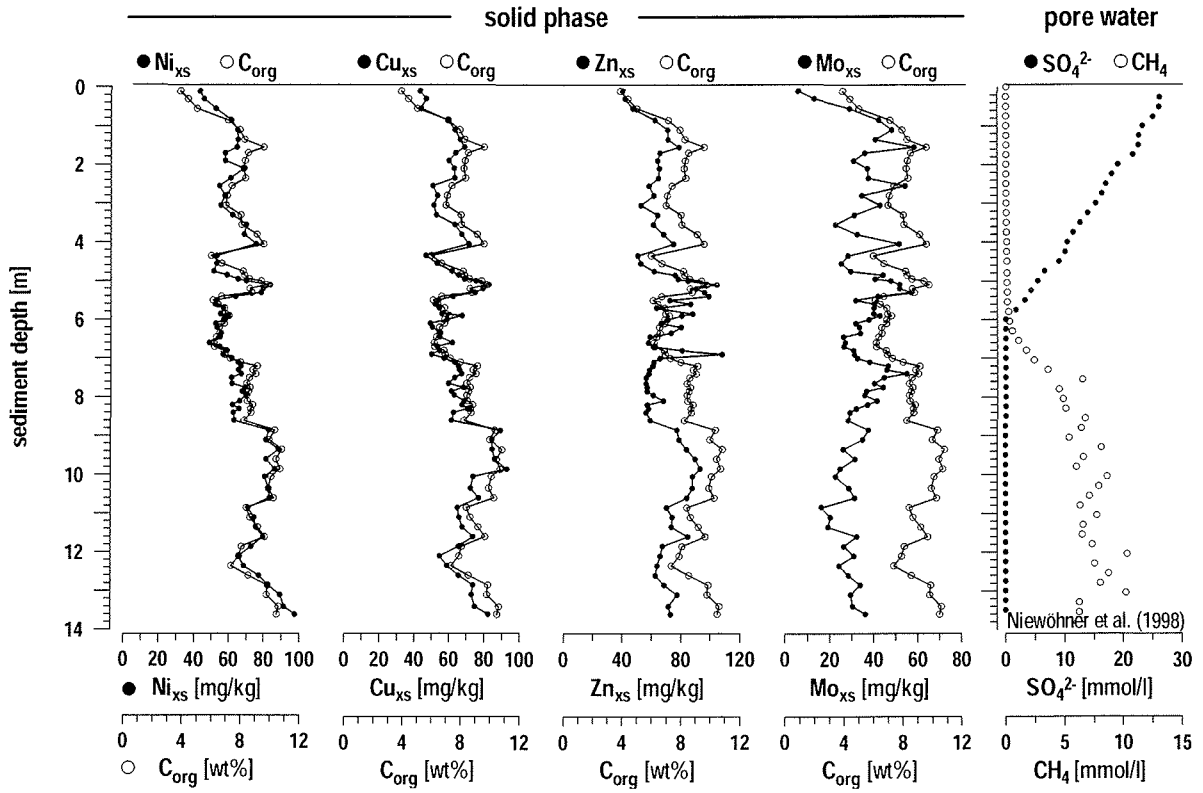

Fig. 4.7: *Excess fractions of Ni, Cu, Zn, and Mo in the solid phase of gravity core GeoB 3718 and their relation to the amount of preserved organic carbon (C_{org}). The pore water profiles illustrate the present sulphate/methane transition at 6 m below sediment surface. Pore water data according to Niewöhner et al. (1998).*

the sediment-water interface (Westerlund et al., 1986; Zhang et al., 1995). According to these studies, Cu, Ni, and Zn are clearly emitted during the oxidative breakdown of organic matter but there is no direct relationship between the metal fluxes and the degradation intensity since numerous adsorption sites prevent the quantitative release of the dissolved metals (Westerlund et al., 1986).

A decoupling between the solid phase contents of biogenic trace elements and C_{org} was also observed in the upper 12.5 m of a gravity core from the Niger deep sea fan. However, in the same core a close correspondence between Ni, Cu, Zn and C_{org} occurs under sulphidic conditions at greater sediment depth and suggests a secondary binding between trace metals and organic matter in the presence of sulphide (Heuer et al., subm.-c).

Ni, Cu, and Zn are known to form sulphides and their precipitation in anoxic environments has been reported in numerous studies (e.g., Francois, 1988; Huerta-Diaz and Morse, 1990; 1992; Calvert and Pedersen, 1993; Morse and Arakaki, 1993; Morse, 1994; Sternbeck et

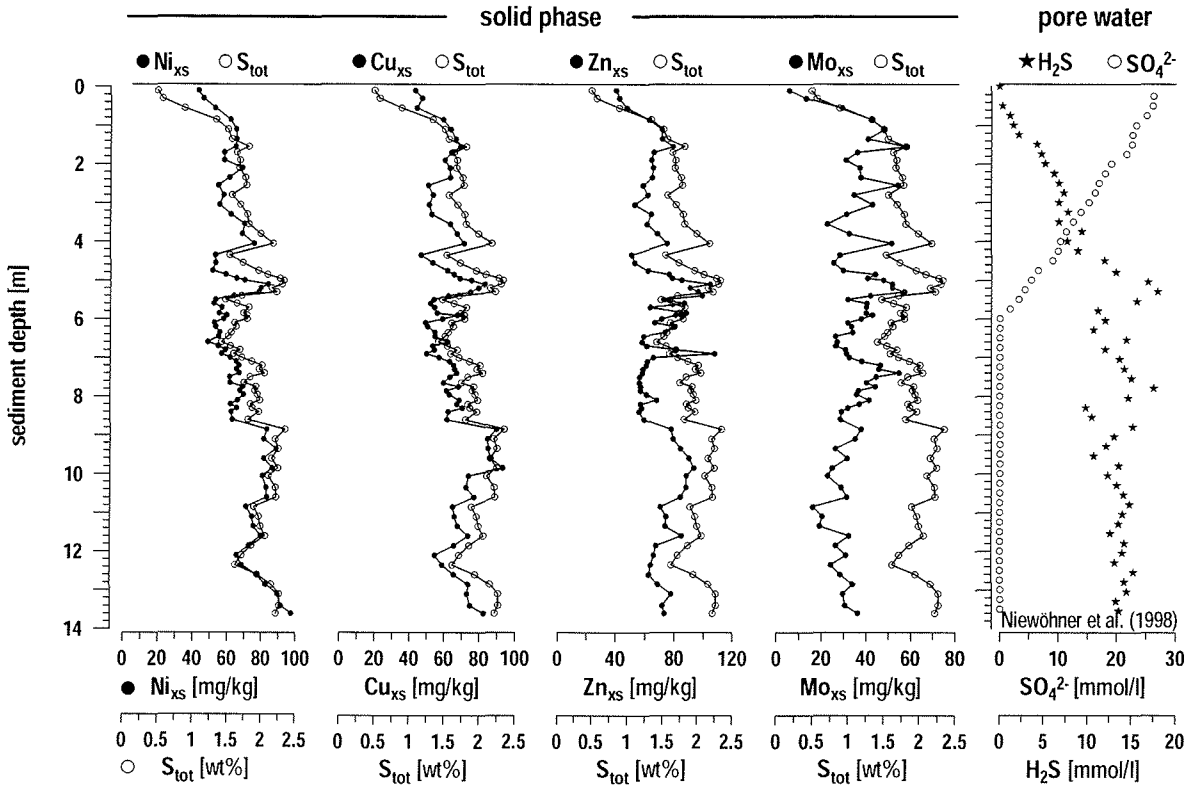

Fig. 4.8: *Excess fractions of Ni, Cu, Zn, and Mo in the solid phase of gravity core GeoB 3718 and their relation to the total solid phase content of sulphur (S_{tot}). The pore water profiles illustrate the current reduction of sulphate at the sulphate/methane transition and the presence of free hydrogen sulphide over the total length of the gravity core. Pore water data according to Niewöhner et al. (1998).*

al., 2000). However, in the iron limited sediment of site GeoB 3718 the precipitation of inorganic sulphides is of minor importance. Instead, organic sulphur compounds dominate the total sulphur content. Consequently, a coprecipitation of trace metals with iron sulphides cannot explain the obvious correspondence of Ni, Cu, and Zn to the total sulphur content of the sediment.

Alternatively, the correspondence between group B elements and both C_{org} and S_{tot} might result from an early diagenetic reaction of Cu, Ni, and Zn with secondary organosulphur compounds. On the one hand, sulphur containing structural units like thiol groups are known to play an important role in the formation of organic trace metal complexes (Vairavamurthy et al., 2000). In this way, high-molecular-weight and particle-bound thiols are thought to bind metals to the particulate phase (Vairavamurthy et al., 2000). On the other hand, polysulphide-bound unsaturated thiols have explicitly been identified as intermediates that form during the first sulphurization steps. They occur soon after deposition and are rapidly transformed in the course of early diagenesis (Adam et al., 2000).

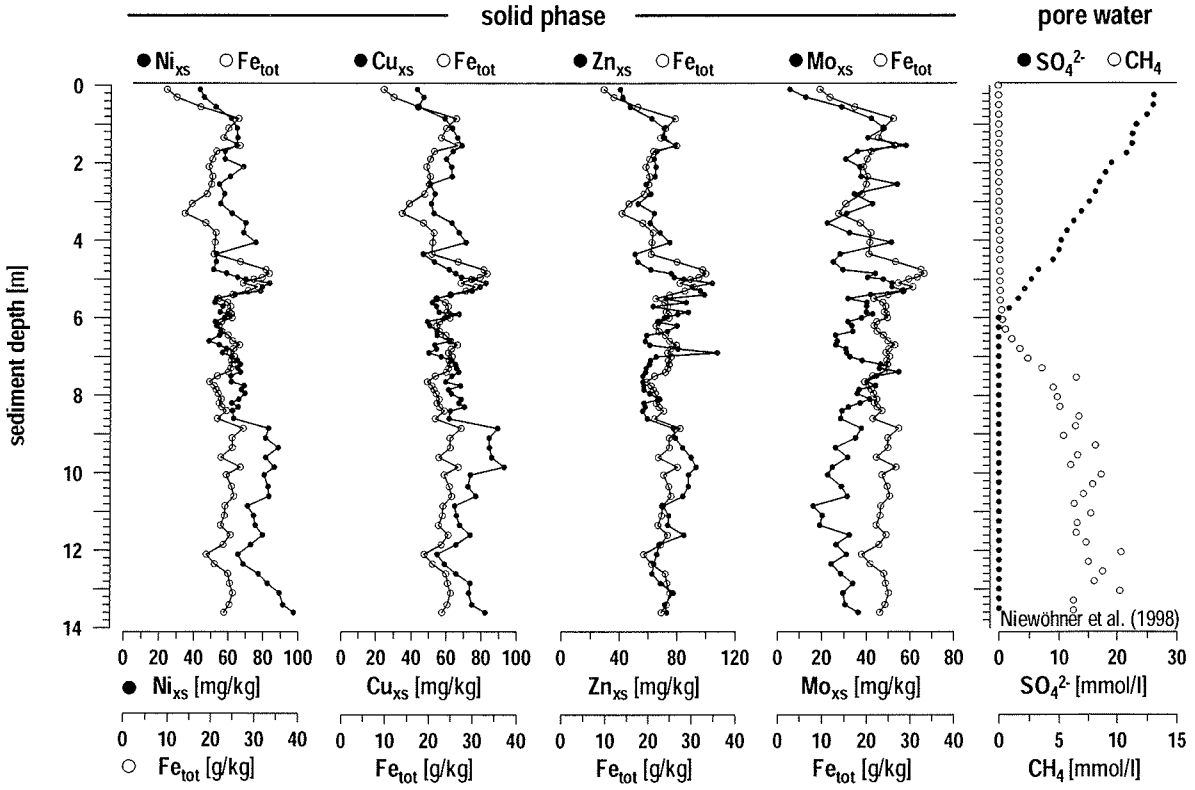

Fig. 4.9: *Excess fractions of Ni, Cu, Zn, and Mo in the solid phase of gravity core GeoB 3718 and their relation to the total solid phase content of Fe. The pore water profiles illustrate the present sulphate/methane transition at 6 m below sediment surface. Pore water data according to Niewöhner et al. (1998).*

The sulphurization of organic matter has been intensively studied during the last two decades and two primary classes of reactions have been distinguished. Firstly, intramolecular incorporation of sulphur leads to low-molecular-weight organic compounds with specific sulphur-containing functional groups and carbon skeletons that are related to biochemical precursors. Secondly, intermolecular sulphur incorporation or "natural vulcanisation" binds organic compounds into macromolecular material through (poly)sulphide linkages (e.g., Sinninghe Damsté et al., 1988; Sinninghe Damsté and de Leeuw, 1990; Kohnen et al., 1991; Adam et al., 1993; Schouten et al., 1994a). These reactions can already occur during the very early stages of diagenesis in the upper meters of sediment and even at the sediment-water interface (e.g., Mossmann et al., 1991; de Graaf et al., 1992; Eglinton et al., 1994; Wakeham et al., 1995; Adam et al., 2000).

We propose that the incorporation of Ni, Cu, and Zn into organic sulphur compounds can proceed via both the complexation with sulphur containing functional groups of low-molecular-weight compounds and the cross-linking by sulphur in macromolecular organic

matter. According to the process study of Vairavamurthy et al. (2000) complexation of trace metals by thiols can produce both monothio and dithio complexes. The formation of monothio complexes might be an equivalent for a reaction of metal ions with single thiol groups of low-molecular-weight compounds. Similarly, the formation of dithio complexes might be a model for the incorporation of metal ions into the polysulphide bridges of vulcanised organic macromolecules. However, further research is needed to identify the mechanisms and sites for trace metal binding in low- and high-molecular weight organic sulphur compounds.

Additional evidence for a secondary binding of trace metals to organic sulphur compounds comes from another investigation at the continental slope off Namibia (Heuer et al., subm.-b). In accordance to our findings at site GeoB 3718, solid phase contents of Ni, Cu, and Zn were closely correlated to both C_{org} and S_{tot} in the upper 10.7 meters of a sulphidic sediment. Moreover, Mo showed a close correlation to C_{org} and S_{tot}, as well. Mo has a conservative distribution in the water column (Bruland, 1983) and thus the observed correspondence of Mo to both C_{org} and S_{tot} was ascribed to a secondary binding in the sediment (Heuer et al., subm.-b). In gravity core GeoB 3718 the overall distribution of Mo_{xs} and the distinct enrichment of Zn_{xs} at 6.9 mbsf do not match the distribution of S_{tot} and C_{org} and cannot be explained on the basis of the available data set.

4.6. Summary and Conclusions

Our pore water and solid phase analyses have shown that the sulphate/methane transition is an important reaction front in sediments on the continental slope off Namibia. Anaerobic methane oxidation causes a complete depletion of pore water sulphate that initiates a redistribution of barite at the sulphate/methane transition. Moreover, the parallel production of sulphide has considerable impact on the solid phase of the sediment, as well. First, the supply of inorganic sulphides to the pore water facilitates the sulphurization of organic matter. Secondly, complexation of trace metals with organic sulphur compounds might also control the retention and accumulation of trace elements in the solid phase of the sediment.

The observed remobilization of Ba alters the sedimentary Ba record and limits the use of biogenic Ba as a proxy for paleoproductivity. However, a diagenetic barite front is a new signal that allows to assess changes in the upward methane flux. The solid phase enrichment of Ba at the sulphate/methane transition of gravity core GeoB 3718 and the observed flux of dissolved Ba^{2+} indicate that the present steady state of upward methane and downward sulphate fluxes has been fairly constant for at least 23,900 years.

While sulphate depletion and barite dissolution limit the use of biogenic Ba as a proxy for paleoproductivity, sulphide production and sulphurization of organic matter support the

preservation of C_{org}. In this context, the retention of biogenic trace elements might carry information about the degree of sulphurization and preservation. Consequently, the correlation of Ni, Cu, and Zn with both C_{org} and S_{tot} might become useful for the reconstruction of paleoproductivity. However, a better understanding is required of the processes that govern the fixation or redistribution of trace elements in the course of organic matter sulphurization.

On the whole, the upward methane flux has considerable impact on the composition of the solid phase. So far, a lot of attention has been paid to the respirative decomposition of organic matter that is known to initiate early diagenesis at the sediment/water interface. With respect to the distribution of trace elements, changes in the burial rate of C_{org} have been of particular interest since the accompanying non-steady state situations can produce distinct enrichments of trace elements in the solid phase of the sediment. Our data show that the fermentation of organic matter can initiate an early diagenetic alteration of the solid phase as well since the upward methane flux drives the reduction of sulphate at the sulphate/methane transition. This reaction front differs from reaction fronts that are related to productivity and burial of C_{org} since its position is ultimately controlled by processes in the underlying sediment. Moreover, a distinct enrichment of Ba can form at the sulphate/methane transition even under steady state conditions.

Acknowledgements - We thank the crew and scientists aboard R.V. METEOR for their help with coring and sampling operations during cruise M 34/2 to the South Atlantic. The processing and analysis of the numerous solid phase and pore water samples would have been impossible without the committed assistance of Sigrid Hinrichs, Karsten Enneking, Susanne Siemer, Kerstin Diercks, and Silvana Hessler. In particular, we would like to thank Thomas Wagner and Inka Ebert who carried out the analysis of C_{org}. The preparation of the manuscript benefited from the valuable discussions with Matthias Zabel, Thomas Wagner, and Jaap Sinnighe Damsté. This research was funded by the Deutsche Forschungsgemeinschaft (contribution no. of Special Research Project SFB 261 at the University of Bremen).

Chapter 5: Nonsteady-state diagenesis and its documentation and preservation in marine sediment/pore water systems

Sabine Kasten, Matthias Zabel, Verena Heuer, Christian Hensen[†]
Fachbereich Geowissenschaften, Universität Bremen, Postfach 330 440, D-28334 Bremen
[†] *present address: GEOMAR, Wischhofstr. 1-3, D-24148 Kiel*

Abstract

Our studies have revealed that nonsteady-state periods – induced by changes in depositional and geochemical conditions - were and are still widespread in sediments of the equatorial and South Atlantic Ocean. Typical diagenetic phenomena initiated during such nonsteady-state episodes comprise the fixation and downward progression of redox boundaries and reaction fronts. Intervals most severely altered by diagenetic overprint often occur cyclically within the sedimentary record and are mostly associated with full glacial/interglacial transitions. The extent of post-depositional oxidation of organic carbon as well as the dissolution and re-precipitation of minerals across these glacial terminations was shown to depend on the overall sedimentation rate and the magnitude of change encountered in the various depositional and geochemical factors. A sedimentation rate of about 2 cm/kyr was confirmed to be the critical value below which no significant amounts of non-refractory organic carbon are preserved.

The influence of climatically induced variations in environmental conditions is not restricted to the geochemical boundaries in the vicinity of the sediment surface (e.g. oxic/post-oxic and Fe redox boundary) but well extends into much deeper sediment sections – namely into the zone of anaerobic methane oxidation (AMO). In this way, processes within the zone of AMO can produce a further profound diagenetic alteration of the sediment composition several thousands of years after initial deposition and thus a significantly delayed chemical log-in. The long-term usability of all primary and secondary signals – also those formed and initially preserved across the oxic/post-oxic and Fe redox boundaries – is ultimately controlled by the geochemical processes within and below the sulfate/methane transition (SMT). While dissolution of authigenic and productivity-related barite takes place in sulfate-depleted sediment sections, iron sulfides as well as sulfurized

organic matter and associated trace elements have a high potential to survive burial below the SMT.

We could also demonstrate that nonsteady-state situations cannot only be triggered by changes in conditions at the sediment/water interface like TOC input, sedimentation rate or O_2 content of bottom water but also by processes in the underlying sediment – namely the formation and/or liberation of methane. Apart from the distinct overprint of the solid-phase, variations in the upward flux of methane also have a considerable impact on the shape of sulfate pore water profiles. Modelling the effects of such variations in methane flux on sulfate profiles has illustrated that considering possible nonsteady-state situations in the sediment/pore water system is of utmost importance for the interpretation of pore water data.

5.1. Introduction

While sedimentary conditions and biogeochemical processes in deep-sea sediments have long been assumed to be at - or close to - a steady-state, numerous studies published during the past two decades demonstrated that nonsteady-state depositional and diagenetic episodes are common even in deposits at greater water depths and/or with low organic carbon contents (e.g. Thomson et al. 1984-b, 1996; Wallace et al. 1988; Tarduno 1994; Tarduno and Wilkison 1996; Kasten et al. 1998). Nonsteady-state diagenesis can be initiated by any changes in the input of organic matter, in sedimentation rate and/or bottom water oxygen contents through time - i.e. any changes in organic carbon burial. While the sediment/pore water system adjusts to the new depositional and/or diagenetic conditions, the primary sediment composition can be efficiently modified. For example, organic carbon is oxidized to various degrees post-depositionally, (magnetic) minerals are dissolved, and redistribution processes cause distinct enrichments of elements and minerals in the solid phase.

The imprint that such nonsteady-state processes can leave on the sedimentary record has been extensively studied in cyclic sediments as e.g. along sapropel/hemipelagic transitions in the eastern Mediterranean (e.g. Pruysers et al. 1991, 1993; Higgs et al. 1994; Thomson et al. 1995; van Santvoort et al. 1996, 1997; Passier et al. 1996) or turbiditic/pelagic sequences in the Madeira and Nares Abyssal Plains (e.g. Colley et al. 1984; Wilson et al. 1985, 1986). Besides redistribution of elements along turbidite/hemipelagic or sapropel/hemipelagic sediment sequences, post-depositional redistributions of elements due to non-constant depositional conditions have also been reported for transitional sediment intervals from glacial to interglacial times. The most recent example is the Pleistocene/Holocene boundary (oxygen isotope stage boundary 2/1 or Termination I) where the diagenetic processes responsible for the formation of distinct solid phase element enrichments were shown to be still active (Thomson et al. 1984-b, 1990; Wallace et al. 1988; Kasten et al. 1998). Thomson et al. (1996) studied the penultimate full glacial/interglacial transition – i.e. Termination II - in Atlantic sediments as the fossil analogue of the Pleistocene/Holocene boundary. They

demonstrated that similar nonsteady-state diagenetic processes were also active along this penultimate climatic boundary.

Nonsteady-state diagenetic periods can also be induced by (giant) submarine landslides which were reported to be widespread along continental margins (e.g. Mienert et al. 1998; Rothwell et al. 1998; Zabel and Schulz 2001). The mechanisms that trigger such massive sediment movements (tectonics or climate-related destabilization of underlying gashydrates) as well as their feedback to climate (possible release of methane to the atmosphere) are still under dispute. Furthermore the impact of these nonsteady-state events on the shape of pore water profiles and the solid phase composition of sediments is not fully understood yet. Several studies relate the occurrence of authigenic carbonates (Bohrmann et al. 1998) or ikaites to the destabilization of gas hydrates (Schubert et al. 1997). Similarly, changes in the diffusive flux of methane or in advective fluid/gas migration have a strong potential to initiate non-steady state diagenesis from below.

The aim of this contribution is to describe the diagenetic processes which are initiated during non-constant depositional and diagenetic phases and to give an overview of related studies on nonsteady-state diagenesis in the frame of the SFB 261. We also intend to emphasize the potential of secondary sedimentary signals to reconstruct changes in paleoceanographic, depositional and geochemical conditions particularly focussing on changes in organic carbon burial and in methane fluxes from deeper sediment strata over time. These examples will demonstrate the potential of nonsteady-state diagenesis to overprint the primary sediment composition – with strongest modifications occurring across the Fe(II)/Fe(III) redox boundary and at the sulfate/methane transition, respectively. We will also present a modeling approach which gives evidence that particular shapes of sulfate pore water profiles which have been either unexplained until now or interpreted in different ways can result from changes in methane fluxes from below or from the emplacement of turbidites or submarine landslides – thus from a nonsteady-state geochemical or depositional situation.

5.2. Redox zones and redox boundaries (reaction fronts)

The microbial degradation/oxidation of organic matter in aquatic sediments by successive use of different terminal electron acceptors (TEA) leads to the establishment of a typical redox zonation. The concept of redox zonation is based on the assumption that the different electron acceptor processes for the oxidation of organic material are segregated into separate sediment intervals and that the succession of these zones is determined by the overall energy yield of the different reactions. The TEAs are generally used in the sequence oxygen, nitrate, manganese oxides, iron oxides, sulfate - followed by methane formation (Froelich et al.

1979). Redox zonation has also been used to classify the different early diagenetic environments in marine sediments (Froelich et al. 1979; Berner 1981) as indicated in Fig. 5.1.

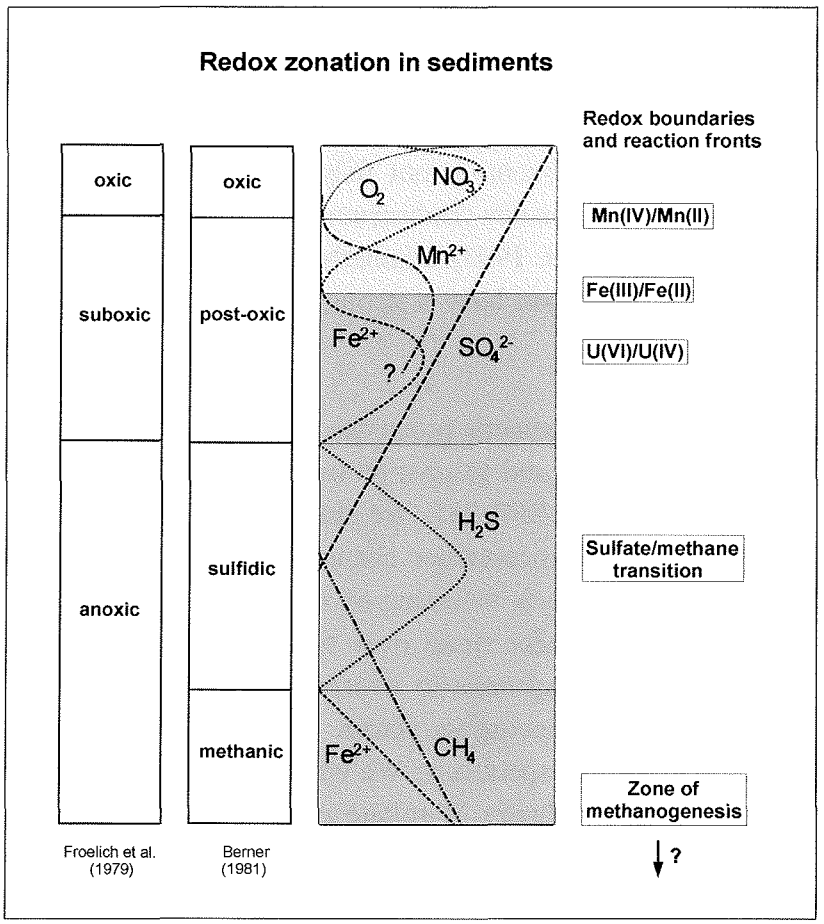

Fig. 5.1: *Schematic representation of redox zonation in marine sediments. The classifications of the different early diagenetic environments as given by Froelich et al. (1979) and Berner (1981) are shown on the left side. Pore water profiles of the dissolved terminal electron acceptors as well as products of the different TEA processes (Mn^{2+}, Fe^{2+}, HS^-) are depicted in the center. This illustration represents a particular situation in which the sulfate pore water profile is primarily shaped by the reaction with upward diffusing methane, i.e. by anaerobic methane oxidation. On the right side the redox boundaries of Mn, Fe and U are given as examples.*

The classical sequence of redox zones in marine sediments is depicted in Fig. 5.1 including schematized pore water profiles of the different dissolved TEAs (oxygen, nitrate, sulfate) as well as of the products of the particular TEA processes (Mn^{2+}, Fe^{2+}, HS^-). It has to be noted that this idealized model represents a specific situation in which the sulfate pore water profile is primarily shaped by the reaction of sulfate with upward diffusing methane, i.e. by anaerobic methane oxidation.

However, numerous studies in marine and lacustrine sediments as well as groundwater systems have demonstrated that the different terminal electron acceptor (TEA) processes are not necessarily separated into distinct zones. Moreover, the different reactions of organic matter degradation can occur simultaneously or the zones can even be reversed. As a general explanation for redox zonation the energy gain of the overall process has been given. In fact

it is known that the degradation of organic matter proceeds via at least two steps, i.e. a first fermentative step and a second TEA reaction step. In the first fermentative step organic material is degraded to small organic molecules like acetate and formate as well as hydrogen. These fermentation products are subsequently consumed by the different TEA processes.

As the TEA processes are much faster than fermentation they could be considered as approaching chemical equilibrium. Based on this line of argumentation Postma and Jakobsen (1996) developed the concept of 'partial equilibrium' in which fermentation determines the overall rate of organic matter oxidation, while equilibrium is approached by the different terminal electron acceptors. In other words: Postma and Jakobsen (1996) suggested that it is not the energy gain of the overall process but of the second step in the process of organic matter mineralization, i.e. the TEA process, that determines the sequence or overlapping of redox zones. In this way they offered a more plausible explanation for the segregation of TEA processes into different redox zones as well as for the often observed simultaneous occurrence of sulfate reduction and iron reduction or a reversal of different redox zones. Examples of such concurrently occurring degradation processes have been found in sediments of the Amazon Fan where Fe reduction was shown to continue in the methanic zone (Flood et al. 1995; Kasten et al. 1998). These findings are also confirmed by experimental studies of Schinzel et al. (1993) who demonstrated that methanogenesis and iron reduction can take place contemporaneously.

The vertical extension of the different redox zones depends on the input of organic matter to the sediment, the supply of TEAs (oxygen content of the bottom water, Mn and Fe (oxi)hydroxide content of the sediment) as well as the flux of reduced pore water constituents (e.g. methane) from greater sediment depth. The higher the amount of organic detritus settling to the seafloor and/or the higher the flux of reduced components from below the more condensed this zonation generally will be. The exact location of the different redox boundaries – e.g. the Fe and Mn redox boundary – with respect to the sediment surface therefore is a function of the balance between oxidants and reductants on the one hand and sedimentation rate on the other hand. We would like to emphasize the significance of redox boundaries and reaction fronts in the following because these are the sites where the strongest modifications of the primary sediment composition take place.

Figure 5.2 illustrates the most important early diagenetic processes which lead to an alteration of the primary sediment composition as well as to the formation of secondary signals in the sedimentary record. The most intense redistributions of elements between the solid phase and the pore water including dissolution and precipitation of (magnetic) minerals take place (1) in the surface sediment interval reaching from the oxic/suboxic (post-oxic) boundary (often also referred to as 'redoxcline') down across the Fe(II)/Fe(III) redox boundary and (2) across the sulfate/methane transition where hydrogen sulfide and carbon dioxide (bicarbonate) are produced through the anaerobic oxidation of methane.

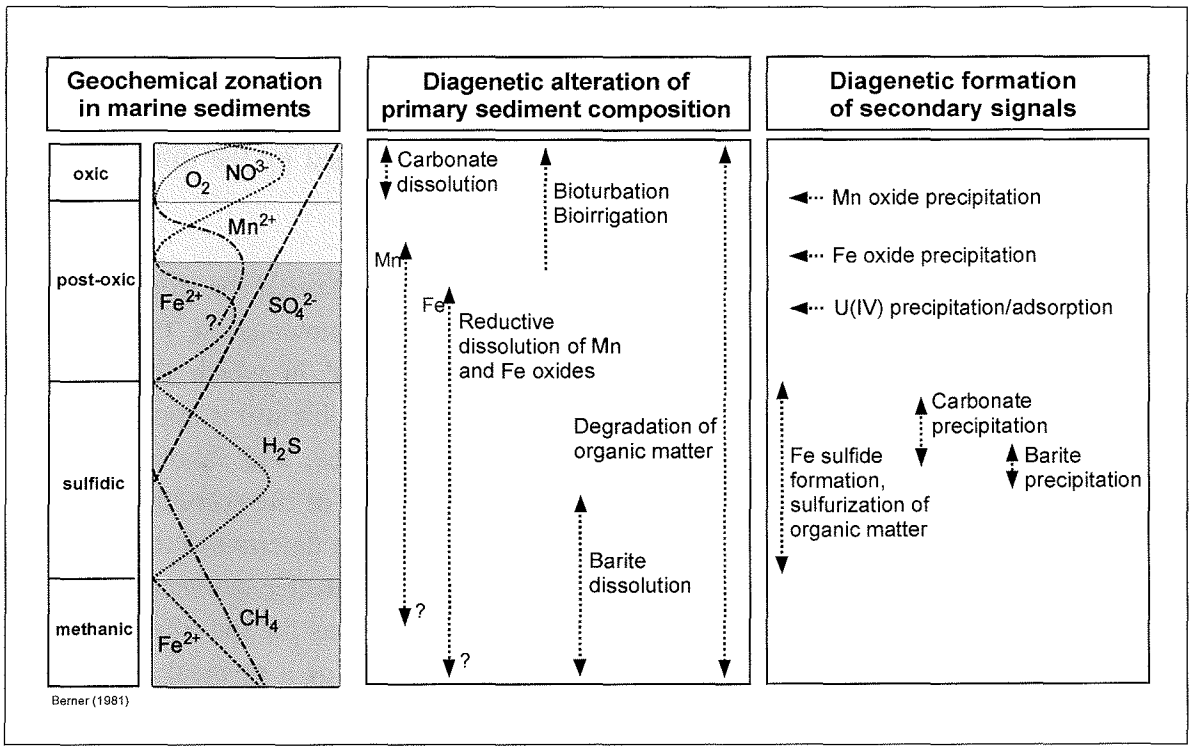

Fig. 5.2: *The most important early diagenetic processes for the alteration of the primary sediment composition as well as for the formation of secondary signals in the sedimentary record.*

Besides bioturbation and bioirrigation which can destroy the initial depth/age relation of sediment components, carbonate dissolution driven by the release of metabolic CO_2 during aerobic degradation of organic matter represents one of the most important diagenetic reactions in surface sediments. The significance of this process is discussed in detail by Adler et al. (2001), Pfeifer et al. (in press) and Hensen et al. (subm.-a). Moving deeper into the sediment, the reduction of Mn and Fe (oxi)hydroxides takes place both biotically and abiotically. This process can occur over considerable sediment depth sometimes even continuing within the methanic zone – as has been described above. Besides the redistribution of Fe and Mn in the sediment column and the pronounced alteration of the initial Fe and Mn mineralogy, reductive dissolution of ferric iron components also has a strong impact on the rock magnetic properties of the sediment. Funk et al. (subm.) demonstrate that in sediments of the equatorial Atlantic reductive dissolution below the Fe redox boundary under nonsteady-state conditions has extensively altered the magnetic mineral inventory of these deposits.

With respect to the diagenetic formation of secondary minerals, the sediment interval across the oxic/suboxic boundary hosts a suite of redox boundaries for different redox-sensitive elements like e.g. Mn, Fe and U (cf. Fig. 5.1). Correspondingly, the formation of

authigenic solid-phase enrichments of these elements – including precipitation of bacterial magnetite - occurs at different sediment depths as indicated in Fig. 5.2.

Within the zone of anaerobic methane oxidation the primary mineral which is most affected by diagenetic alteration is barite ($BaSO_4$) (Kasten and Jørgensen 2000). In the sediment interval below the sulfate/methane transition where interstitial sulfate is completely depleted, barite is undersaturated and consequently subject to dissolution. The Ba^{2+} ions liberated into the pore water by this process diffuse upwards and precipitate as secondary barite slightly above the sulfate penetration depth at a so-called authigenic barite front (cf. Fig. 5.2) (e.g. Brumsack 1986; von Breymann et al. 1992; Torres et al. 1996). This process is of particular significance since the dissolution and re-precipitation of barite limits the use of biogenic Ba as a potential proxy for paleoproductivity (for a review see Gingele et al. 1999). Besides authigenic barite, carbonates and iron sulfides are two other important secondary minerals precipitated within the sulfate/methane transition zone. Both mineral groups form as a direct consequence of anaerobic methane oxidation which produces large amounts of hydrogen sulfide and carbon dioxide (bicarbonate) according to equation (1).

(1) $$CH_4 + SO_4^{2-} \rightarrow HCO_3^- + HS^- + H_2O$$

Boetius et al. (2000) have shown recently that the anaerobic oxidation of methane by sulfate is mediated by a consortium of methane-consuming archaea and sulfate-reducing bacteria. Hydrogen sulfide liberated into the pore water by this process has at least a two-fold effect on the sedimentary solid phase as it initiates the precipitation of iron sulfides (e.g. Berner 1969, 1984) as well as the sulfurization of organic matter (e.g. Sinninghe Damsté and de Leeuw 1990; Schouten et al. 1994). Moreover, both iron sulfides and organic sulfur compounds affect the retention and accumulation of trace elements in the solid phase of sulfidic sediments (e.g. Huerta-Diaz and Morse 1992; Morse and Arakaki 1993; Heuer et al. subm.-a,b).

5.3. Nonsteady-state diagenesis

During steady-state diagenesis redox zones and redox boundaries establish at specific subsurface depths and remain at these constant relative distances with respect to the sediment surface over time. These depths are determined by a balance between fluxes of oxidants and reductants on the one hand and sedimentation rate on the other hand. A permanent steady-state condition - including permanent steady-state diagenesis - requires constant sedimentary and geochemical conditions over a long period of time. Only under such circumstances the relative depth positions of the redox boundaries and reaction fronts with respect to the sediment surface as well as the vertical extension of the redox zones remain constant too. However, as has already been pointed out by Pruysers et al. (1993) the

balance between fluxes and sedimentation rate is very delicate, and thus, a steady-state condition, persisting over a long period of time is very unlikely in any sedimentary environment.

A change in at least one of the depositional or geochemical parameters puts the sediment/pore water system out of balance. The time interval during which the system adjusts to the new conditions – in order to obtain a new balance and thus a steady state – is referred to as a nonsteady-state diagenetic situation. In the following we will show that especially such periods of nonsteady-state diagenesis have a strong potential for overprinting the primary sediment composition and for producing distinct secondary signals in the sedimentary record.

Typical depositional and geochemical "events" which can initiate nonsteady-state diagenetic episodes comprise (1) changes in organic carbon burial induced by variations in sedimentation rate, organic carbon input to the sediment and/or oxygen content of bottom water, (2) mass transfer events of sediments in the form of turbidites, debris flows or submarine landslides, (3) variations in the upward-directed diffusive flux of methane or other reduced components from greater sediment depth, and (4) fluctuations in the advective flow of pore water and fluids from deeper sources or across the sediment/water interface. A decrease in organic carbon burial or a surplus in the supply of oxidants over time will result in an extension of redox zones. In the opposite case, redox boundaries and reaction fronts will be shifted towards the sediment surface and the redox succession will be condensed.

The effects of increases in the input and burial of organic carbon over time - accompanied by an upward shift of the redox boundaries and reaction fronts – have been demonstrated by Finney et al. (1988), de Lange et al. (1994) and Passier et al. (1996). They showed that metastable element enrichments (e.g. Mn hydroxides) can be preserved after a sudden upward shift of the redox boundaries. Passier et al. (1996) described that downward sulfidization fronts can lead to the formation of distinct Fe sulfide enrichments below organic-rich layers like sapropels. In this contribution we will, however, focus on the opposite case – i.e. decrease in organic carbon burial and extension of redox zones over time – because it is the scenario which leads to the strongest diagenetic overprint of the primary sediment composition as we will demonstrate by means of the following schematic representations.

Figure 5.3 illustrates the potential of nonsteady-state diagenesis to produce distinct secondary element enrichments in the solid phase using Mn, Fe and U as examples. This illustration demonstrates that the redox boundaries of the elements under consideration are arranged in a typical depth succession across the Fe(II)/Fe(III) redox boundary. Under steady-state diagenetic conditions, the different redox boundaries and thus also the solid-phase enrichments of the elements will remain at constant depths with respect to the

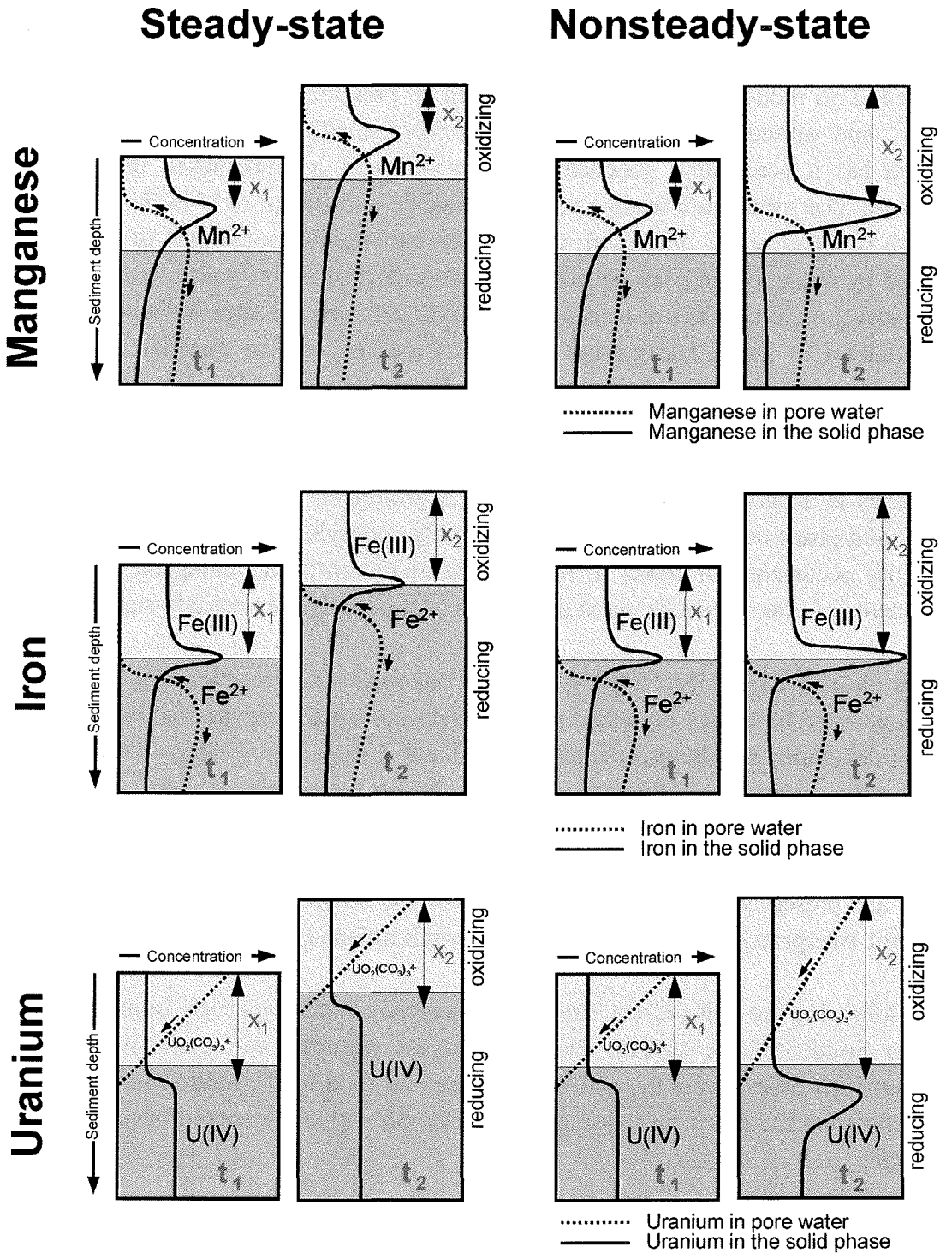

Fig. 5.3: *Model concept for the formation of solid-phase enrichments of manganese, iron and uranium under steady-state (left side) and nonsteady-state (right side) depositional and diagenetic conditions. Dotted lines represent pore water profiles, solid lines show solid-phase concentration profiles.*

sediment surface over time. With ongoing sedimentation the lower parts of the solid-phase enrichments of Fe and Mn move into more reducing conditions and are successively dissolved. This reductive dissolution is followed by preferential upward migration of Mn^{2+} and Fe^{2+} and subsequent re-precipitation as (oxi)hydroxides in the top part of the peak. Uranium has a contrasting geochemical behaviour and is immobilized under post-oxic conditions. The mechanism leading to the authigenic enrichment of U in the solid phase is diffusion of dissolved U species from seawater into the post-oxic part of the sediments followed by reduction and subsequent precipitation and/or adsorption to reactive surfaces. Under steady-state conditions, each sediment layer receives the same amount of authigenic U in addition to the U background content of the sedimenting material. In this way a constant U concentration level evolves in the sediments below the U redox boundary.

In contrast, a decrease in organic carbon burial over time causes a fixation of the redox boundaries at a particular sediment depth for a prolonged period of time thus producing higher solid-phase concentrations of the metal under consideration than during steady-state. Thus, the occurrence of peaks in the concentration profile of authigenic U and strong enrichments of other elements are indicative for past periods of nonsteady-state diagenesis.

Besides the above described fixation of redox boundaries and reaction fronts other typical nonsteady-state processes comprise progressively downward-moving oxidation fronts – a concept developed by Thomson et al. (1984-b) and Wilson et al. (1985, 1986) – as well as the already mentioned sulfidization fronts below sapropels (Passier et al. 1996). Furthermore, Funk et al. (subm.) demonstrate that redox boundaries can be trapped at or within sediment intervals in which elevated amounts of degradable/non-refractory organic carbon are preserved. In this way, these layers are subject to a much higher degree of diagenetic overprint compared to sediment intervals affected by steady-state diagenesis.

In the following we will present studies of nonsteady-state diagenesis from the equatorial and the South Atlantic Ocean. These works are grouped into those which focus on diagenetic processes across the oxic/suboxic boundary and the Fe redox boundary and those which illustrate the extent of diagenetic modification within the zone of anaerobic methane oxidation.

5.4. Redistribution of elements across the oxic/suboxic boundary and the Fe(II)/Fe(III) redox boundary

High-resolution solid-phase investigations have been performed along glacial Terminations in sediments of the central equatorial Atlantic Ocean (Reitz et al. in prep) and of the upwelling area off Morocco, NW Africa (Kasten et al. in prep). These sites were selected

because we expected strong nonsteady-state diagenetic overprint of the transitional sediment intervals across the glacial/interglacial boundaries. The aim of these studies was to identify the extent of post-depositional modification of the primary sediment composition during a fixation or a progressive downward movement of the redoxcline and the Fe redox boundary induced by deglacial changes in depositional and geochemical conditions. Furthermore we wanted to reveal which of the secondary element enrichments produced are preserved in the sedimentary record on further burial and can thus serve as valuable indicators for changes in organic carbon burial. For this purpose we compared the last glacial/interglacial transition – i.e. Termination I - where these nonsteady-state processes were shown to be still active with the fossil example – i.e. the penultimate glacial/interglacial transition or Termination II, respectively.

Central equatorial Atlantic Ocean – periphery of equatorial divergence

Gravity core GeoB 2908-7 (00°06,4'N; 23°19,6'W) was recovered from a water depth of 3809 m during RV Meteor cruise M 29/3 (Schulz et al. 1995). The core has a total length of 1094 cm and reaches into oxygen isotope stage 10 (OIS 10). Sedimentation rates are on average 4.3 cm/kyr during glacial periods and 2.3 cm/kyr during interglacials (Funk et al. subm.). The two core segments of interest – i.e. the intervals across the OIS boundaries 2/1 and 6/5 - are characterized by color changes from brown to grey/green (cf. Fig. 5.4). The most pronounced color change is found at a sediment depth of about 46 cm and is located 10 cm below the maximum of Termination I (age: about 13.4 ka). This colour change marks the position of the *active* Fe(II)/Fe(III) redox boundary at this site. Around the 6/5 OIS boundary, about 15 cm below the maximum of Termination II (age: about 128 ka) a less distinct colour change occurs at about 433 cm which represents the *fossil* analogue of the modern Fe(II)/Fe(III) redox boundary.

The results of high-resolution geochemical investigations at 1-cm intervals are shown in Fig. 5.4 and reveal a characteristic succession of the solid-phase peaks of Mn, Fe, V, Cd and U with depth across the active Fe redox boundary (Reitz et al. in prep). Along the fossil Fe redox boundary the same sequence of peaks is observed except for Mn. This depth succession of the enrichments of redox-sensitive elements is a characteristic result of nonsteady-state diagenesis and has also been observed by Thomson et al. (1996) in glacial/interglacial transition sediments of the northeast Atlantic Ocean. We suggest that - similar to the schematic representation shown in Fig. 5.3 – this depth arrangement of the peaks as well as their magnitude was caused by a sustained localization of the oxic/suboxic boundary and the Fe redox boundary at particular levels in the sediment. The conditions which are likely to have induced these nonsteady-state diagenetic periods are shifts to lower organic carbon input and sedimentation rates as well as to higher bottom water oxygen contents at the onset of enhanced NADW production during interglacials.

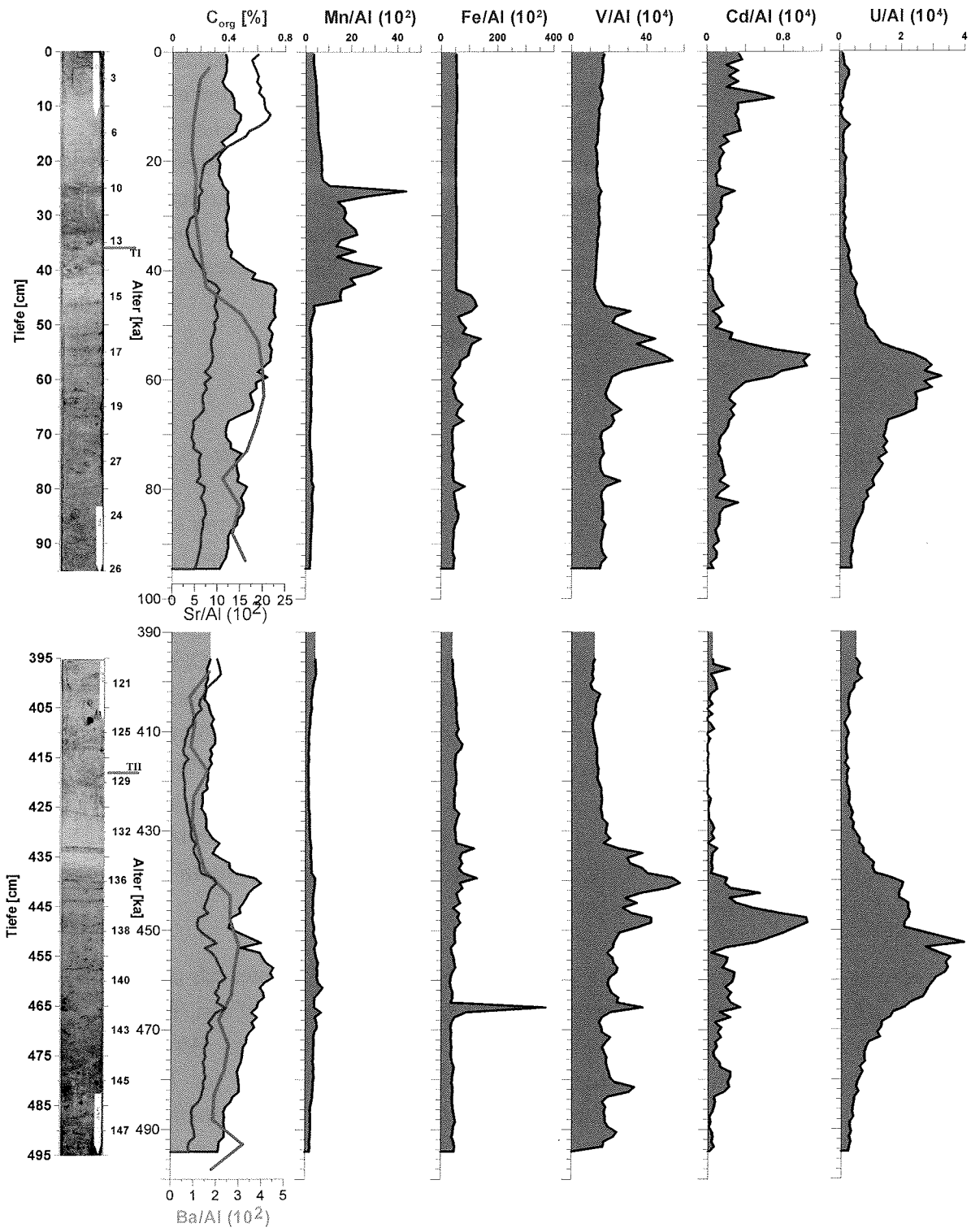

Fig. 5.4: *Al-normalized solid-phase concentrations of Mn, Fe, V, Cd and U versus sediment depth along the active (above) and the fossil (below) Fe redox boundary in gravity core GeoB 2908-7 from the central equatorial Atlantic Ocean. On the left side photographs of the two core segments as well as organic carbon (C_{org}) and Ba/Al and Sr/Al data are shown. Modified from Reitz et al. (in prep).*

The concentration profile of TOC displays higher preserved amounts within glacial intervals and illustrates that the modern Fe redox boundary is trapped at the top of the youngest TOC-enriched sediment interval at about 46 cm depth. This fixation of the active Fe(II)/Fe(III) redox boundary at the upper boundary of the most recent TOC pulse is a ubiquitous phenomenon in the equatorial Atlantic (cf. Funk et al. subm.). Compared to this active Fe redox boundary the peaks of the elements which form authigenic enrichments in post-oxic sediments (V, Cd, U) are still in place along the fossil Fe redox boundary at about 433 cm as also found by Thomson et al. (1996). The Mn spike which was initially located at the fossil oxic/suboxic boundary above Termination II has been mobilized by reduction during further burial and re-precipitated at the modern redoxcline in the form of a broad enrichment between 24 and 47 cm sediment depth. Although being similarly unstable under post-oxic and anoxic conditions, a relict of the Fe enrichment is still present at the fossil Fe redox boundary due to the slower reduction kinetics of Fe compared to Mn. The distinct Fe spike found at 468 cm depth represents an enrichment of authigenic iron sulfides.

A close look at the concentration profiles of TOC and solid-phase Ba in the vicinity of the two colour changes reveals a discrepancy between these two components immediately above the TOC-enriched sediment intervals. The relatively higher Ba contents at these depths suggest that there has not only been a fixation but a slight downward progression of the redox boundaries across the glacial/interglacial boundaries. This downward movement is likely to have caused an efficient post-depositional oxidation of the upper part of the TOC-enriched sediment interval leaving Ba as a relict.

Nonsteady-state diagenesis acting along these glacial terminations has not only led to the formation of distinct secondary element enrichments and the post-depositional oxidation of organic carbon, but has also caused a strong dissolution of magnetic Fe minerals below the Fe redox boundaries. The imprint on the magnetic mineral inventory is described in detail by Funk et al. (subm.) for sediment core GeoB 2908-7 as well as for numerous other sites in the equatorial Atlantic. The high-resolution geochemical and rock magnetic data demonstrate that the extent of diagenetic overprint of the primary sediment composition is proportional to the magnitude of change encountered in depositional and geochemical conditions. For this reason glacial/interglacial transitions, which represent time intervals of the most profound variations in environmental parameters are subject to the highest degree of diagenetic overprint in an undisturbed sedimentary sequence. With respect to the potential use of secondary signals as indicators for changes – or more precisely decreases - in organic carbon burial, those elements which form authigenic enrichments in post-oxic sediment sections are most promising as they are stable and thus preserved during further burial into more reducing conditions.

Upwelling-filament area off Morocco, NW Africa

Site GeoB 4216 is located offshore the upwelling area off Morocco and strongly influenced by Trade Wind driven filament activity (Freudenthal et al. 2002, subm.). The 1117 cm long gravity core GeoB 4216-1 (30°38'N, 12°24'W) was taken from a water depth of 2324 m during RV Meteor cruise M 37/1 (Wefer et al. 1997) and reaches into OIS 7. With an average value of 5 cm/kyr (Freudenthal et al. 2002), sedimentation rates at this site are slightly higher than at location GeoB 2908 in the central equatorial Atlantic. However – in accordance with site GeoB 2908 – sedimentation rates and preserved TOC contents are higher during glacial times than during interglacials.

The records of solid phase Ba and TOC across the 2/1 and the 6/5 oxygen isotope stage boundaries of core GeoB 4216-1 (Kasten et al. in prep) are depicted in Fig 5.5. Like for the above presented site GeoB 2908, a disagreement between these two parameters is obvious above the glacial/interglacial boundaries whereas a striking positive correlation exists in the sediment interval below. Kasten et al. (in prep) suggest that the TOC signal in these parts of the sediment has suffered from post-depositional degradation due to the action of downward-progressing oxidation fronts during deglacial nonsteady-state depositional conditions. The fact that the discrepancy between TOC and Ba is even more pronounced at site GeoB 4216 - with TOC contents exhibiting a sharp drop - suggests that the contrast in sedimentation rate and/or bottom-water oxygen contents between glacials and interglacials was stronger than at site GeoB 2908. The shape of the Ba profile (Fig. 5.5) indicates that rather than increased productivity during glacial periods – maximum productivity seems to have occurred during the most pronounced climatic transitions – thus during deglacial periods. This hypothesis is supported by similar Ba peaks found at glacial terminations in sediments of the northwest African margin (Matthewson et al. 1995), the Ontong Java Plateau in the Pacific (Schwarz et al. 1996), the Portuguese margin (Thomson et al. 2000), the Sierra Leone Rise and Ceará Rise in the Atlantic (Kasten et al. 2001) and the upwelling and filament influenced area off Morocco (Moreno et al. 2002; Freudenthal et al. 2002, subm.).

In the high sedimentation regime of the Portuguese margin (Thomson et al. 2000), coincident maxima of Ba, TOC, and diatom abundance are found at glacial terminations implying that the Ba peaks indeed formed in association with productivity events. In contrast, no correlation between Ba and organic carbon is found in the deglacial sediments of the northwest African margin (Matthewson et al. 1995), the Ontong Java Plateau (Schwarz et al. 1996), as well as the Sierra Leone Rise and Ceará Rise (Kasten et al. 2001). These locations are all characterized by considerably lower sedimentation rates compared to the Portuguese margin. Sites GeoB 2908 and GeoB 4216 presented here as well as the study sites of Moreno et al. (2002) and Freudenthal et al. (2002) represent intermediate situations where only the upper part of the TOC-enriched intervals has been oxidized post-depositionally whereas a good correlation between Ba and TOC still exists in the lower un-

oxidized section (cf. Figs. 5.4 and 5.5). The shape and arrangement of the TOC and Ba peaks along the glacial/interglacial boundaries at site GeoB 4216 (Fig. 5.5) show striking similarities to the depth distribution of these two components along active oxidation fronts at the most recent sapropel, S1, in eastern Mediterranean sediments (van Santvoort et al. 1996; Zonneveld et al. 2001) as well as in older partly oxidized sapropel intervals (e.g. van Os et al. 1991). This analogy is strong evidence for oxidation fronts to have been active along the 2/1 and the 6/5 stage boundaries in core GeoB 4216 as well (Fig. 5.5).

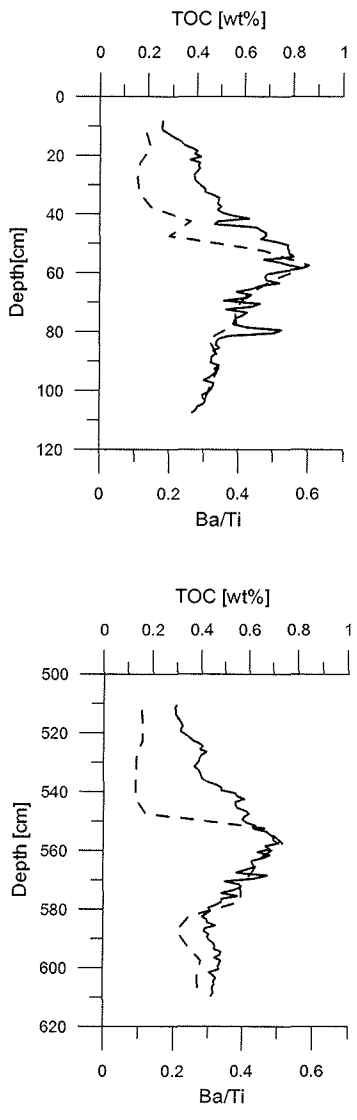

Fig. 5.5: *Organic carbon contents (dashed lines) and solid-phase Ba/Ti ratios (solid lines) versus depth across the 2/1 and the 6/5 OIS boundaries in gravity core GeoB 4216-1 from the upwelling area off Morocco, NW Africa (Kasten et al. in prep).*

As has already been pointed out by Kasten et al. (2001), the degree or depth of "burn-down" – i.e. the post-depositional oxidation of TOC - along glacial/interglacial boundaries is controlled by the overall rate of sedimentation as well as by the magnitude of change in environmental and depositional conditions that occurred during these full climatic transitions. Using a modelling approach, Jung et al. (1997) demonstrated that sedimentation rate is the dominant factor which controls whether a sapropel is oxidized completely or only partly. They showed that preservation of elevated concentrations of non-refractory organic carbon is generally improbable when the sedimentation rate is lower than 1-2 cm/kyr. This value corresponds well to the value of about 2 to 2.5 cm/kyr on average for the sites on the Ceará and Sierra Leone Rise where no corrrelation between Ba and TOC at glacial/interglacial transitions has been found. At stations GeoB 2908 and GeoB 4216 which are characterized by slightly higher sedimentation rates only the upper part of the TOC-enriched interval has been affected by post-depositional oxidation.

These studies illustrate the strong variability in diagenetic overprint and thus in degradation/preservation of organic carbon along glacial/interglacial transitions in dependence on (changes in) depositional and bottom water oxygen conditions. Besides the general constraints of TOC as a productivity proxy, they clearly demonstrate that using organic carbon as a productivity indicator within these transitional sediment intervals bears a particularly high risk of misleading interpretation. These investigations further suggest that other sediment components sensible to oxygen might also be affected by burn-down phenomena – as has been shown by Zonneveld et al. (2001) for organic-walled dinoflagellate cysts in oxidized sapropel intervals. Moreover, as an important secondary effect of aerobic degradation, the extent and species-selectivity of carbonate dissolution driven by the metabolic production of CO_2 during aerobic mineralization of organic matter (e.g. Pfeifer et al. in press; Volbers and Henrich in press; Hensen et al. subm.-a) has to be considered too within these transitional sediment intervals.

Further detailed investigations concerning the various organic/biogenic sediment components are needed to unravel the extent and the controlling factors of post-depositional overprint along glacial/interglacial transitions. Considering the different degrees in preservation of biogenic components within a sedimentary sequence will help to separate preservation from productivity (to improve environmental reconstructions from sedimentary components) and to solve discrepancies between existing productivity reconstructions. A promising approach to tackle with the difficulties in discriminating between productivity and preservation has recently been presented by Versteegh and Zonneveld (2002) based on the differences in degradation rates of various organic sediment components.

5.5. Redistribution of elements and formation of element enrichments within the sulphate/methane transition zone

While numerous studies have shown the effects of reaction fronts acting around the oxic/post-oxic redox boundary only few investigations focus on the sulfate/methane transition zone. Nevertheless, the formation of a number of significant authigenic minerals, namely iron sulfides, barite and carbonates as well as the sulfurization of organic matter at and around this important biogeochemical boundary is well-known (cf, Fig. 5.2). The following examples from the equatorial and South Atlantic will illustrate the strong modification of the primary sediment composition by the biogeochemical processes acting within the zone of anaerobic methane oxidation. They will demonstrate that overprint of the sedimentary record by diagenetic processes can occur several thousands to millions of years after initial deposition of the particulate material. Furthermore, they highlight the potential of these secondary signals to reconstruct variations in geochemical conditions and in the position of redox boundaries and reaction fronts over time. The nature and extent of diagenetic overprint is strongly influenced by the oceanographic, depositional and

geochemical conditions at each particular site. In terrigenous-dominated settings Fe is usually available in high amounts and any hydrogen sulfide produced by anaerobic methane oxidation is immediately converted into Fe sulfides. In depositional environments characterized by high input of biogenic material, hydrogen sulfide is produced in excess of Fe and sulphurization of organic matter becomes the dominating process. As a consequence striking differences in the secondary signals formed as well as in the distribution patterns of trace elements within the sedimentary record evolve as we will show in the following.

Amazon deep-sea fan – iron-dominated setting

The studies by Kasten et al. (1998) and Adler et al. (2000) in sediments of the Amazon Fan can serve as valuable examples for the formation of massive authigenic iron sulfides within the zone of anaerobic methane oxidation under nonsteady-state conditions (Fig. 5.6). The sedimentary environment on the Amazon deep-sea fan is characterized by strong differences in depositional conditions between glacial and interglacial times. While during glacial sealevel lowstands Amazon river load is directly transported to the deep-sea fan via channels, sedimentation during interglacials is dominated by pelagic carbonaceous material because most of the Amazon-discharged terrigenous material is transported to the Northeast parallel to the coast. These differences in the sedimentary regimes also result in extreme contrasts in sediment accumulation rates. While glacial sedimentation rates can be as high as several meters per thousand years, interglacial rates average around only 3 to 4 cm per thousand years. Therefore, the Amazon Fan represents a typical nonsteady-state setting with respect to depositional as well as diagenetic conditions. Furthermore, the sedimentary system of the fan is iron-dominated resulting from the high amounts of lateritic weathering products supplied by the Amazon River. As a consequence, although sulfate reduction is occurring at high rates within the zone of anaerobic methane oxidation, hydrogen sulfide is only detectable at micromolar concentrations in the pore water of these sediments.

The 7.1 m long gravity core GeoB 1514 (5°08.4'N, 46°34.6'W) which was recovered from a water depth of 3509 m on the Amazon Fan is characterized by a distinct enrichment of iron sulfides between 6.0 and 6.5 m sediment depth as can be seen from the solid phase concentrations of sulfur and iron (Fig. 5.6). This iron sulfide peak is located slightly below the current depth of the sulfate/methane transition around 5.3 m. As only minor amounts of free hydrogen sulfide were detectable in the pore water at this site, Kasten et al. (1998) assumed that all HS^- produced by anaerobic methane oxidation is immediately fixed in the sediment as iron sulfides. The solid phase sulfur contents within this pronounced peak therefore represent the integrated amount of deep sulfate reduction that occurred within this depth interval. Kasten et al. (1998) further concluded that the condition that caused the magnitude of this Fe sulfide enrichment was the pronounced decrease in sedimentation and organic carbon accumulation rates during the transition from the Pleistocene to the

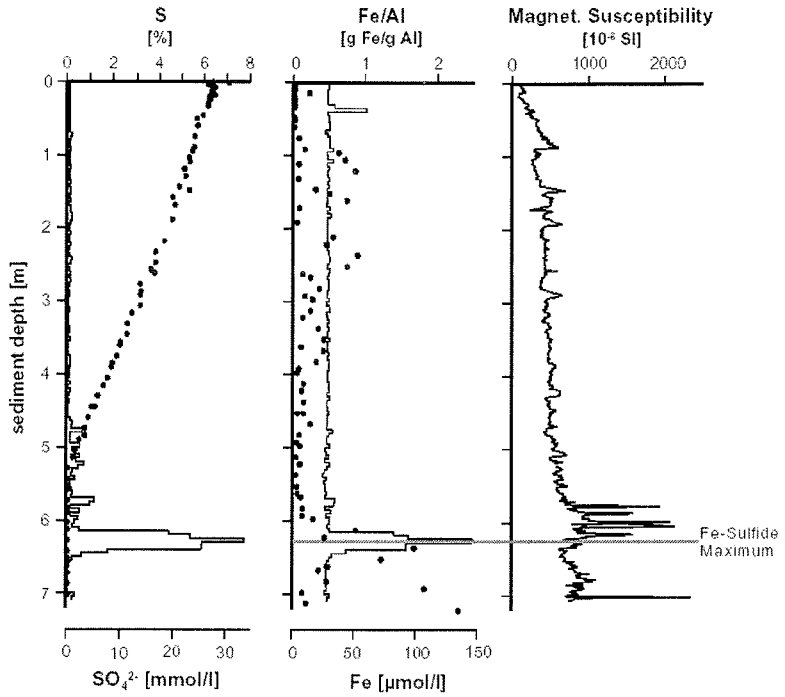

Fig. 5.6: *Solid-phase profiles of total S and Al-normalized concentrations of Fe from total digestion (solid lines), magnetic susceptibiliy (J. Funk, unpubl. data) as well as pore water concentration profiles of SO_4^{2-} and Fe^{2+} (solid circles) for core GeoB 1514-6 from the Amazon deep-sea fan. The SMT is currently located at a depth of 5.3 m. A strong enrichment of Fe sulfides is found between 6 and 6.5 m sediment depth. The horizontal line demonstrates that the iron sulfide maximum does not directly coincide with the peak in magnetic susceptibility. Modified from Kasten et al. (1998) and Kasten and Jørgensen (2000), pore water data taken from Schulz et al. (1994).*

Holocene. While methane fluxes from below remained more or less constant, this strong decrease in sedimentation rate caused a fixation of the zone of anaerobic methane oxidation for a prolonged period of time, thus producing the high amount of authigenic Fe sulfides at this depth.

Besides the strong modification of the bulk sediment composition, nonsteady-state diagenesis within the zone of deep sulfate reduction has also generated a distinct secondary magnetic signal within the sedimentary record. A pronounced maximum in magnetic susceptibility is found slightly above the distinct Fe sulfide peak (Fig. 5.6). As the concentration profile of Fe sulfides does not display a local maximum at the depth of the susceptibility peak, Kasten et al. (1998) suggested the presence of an iron sulfide mineral with a high magnetic potential. X-ray diffraction analyses performed on samples from the depth of the susceptibility maximum indeed revealed the presence of the magnetic iron sulfide mineral, greigite (Fe_3S_4).

Upwelling area off Namibia – sulfide-dominated system

Site GeoB 3718 is located south of Walvis Bay at the continental slope off Namibia (24°53.6'S, 13°09.8'E, water depth: 1312 m). Due to the lack of large rivers terrigenous input is of minor importance at this site. Consequently, solid phase contents of Al and Fe are low contributing 3-10 wt% in terms of Al_2O_3 and 1-5 wt% in terms of Fe_2O_3 (Heuer et al. subm.-a). In contrast, primary productivity within the surface waters and organic matter export to the sediment are high since trade winds cause the upwelling of nutrient-rich water masses. As a result, intense remineralization of C_{org} takes place in the sediment and methanogenesis becomes a significant process even at shallow sediment depths. At station GeoB 3718 organic carbon (C_{org}) makes up 4-11 wt% of the solid phase (Heuer et al. subm.-a) and the pore water study of Niewöhner et al. (1998) has shown a distinct sulfate/methane transition at 6 meters below the sediment/water interface (Fig. 5.7).

The complete consumption of sulfate at this sulfate/methane transition has initiated a redistribution of barite ($BaSO_4$) that can be observed in both the solid phase and the pore water of the 13.7 m long gravity core GeoB 3718-9 (Heuer et al. subm.-a). In the solid phase a distinct enrichment of Ba occurs in the vicinity of the sulfate/methane transition at 6.0 mbsf (Fig. 5.7). Total solid phase contents of barium (Ba_{tot}) invariably exceed 750 ppm in the sediment section between 5.0 and 6.8 mbsf and peak Ba_{tot} concentrations amount up to 6020 ppm at 6.4 mbsf. In contrast, above and below the Ba enrichment Ba_{tot} contents average around 750 ppm and 470 ppm, respectively. Pore water data confirm the precipitation of Ba at the sulfate/methane transition (Fig. 5.7). While dissolved Ba^{2+} is negligible in the sulfate containing pore water throughout the upper 6.0 m of the sediment, the dissolution of barite has produced up to 170 µmol/l dissolved Ba^{2+} in the sulfate-depleted pore water of the underlying sediment section. The sulfate concentration profile indicates upward diffusion of dissolved Ba^{2+} from sulfate-depleted to sulfate rich pore water where the pore water concentration of Ba^{2+} becomes zero due to the precipitation of barite. The contact of Ba^{2+} and sulfate containing pore water coincides with the distinct enrichment of Ba_{tot} in the solid phase of the sediment.

The linear shape of the sulfate pore water profile indicates that at present consumption of sulfate by anaerobic methane oxidation at this site is at a steady state. Sulfate concentrations decrease (linearly) with depth and the diffusive fluxes of sulfate and methane (30.2 $mmol \cdot m^{-2} \cdot a^{-1}$) are balanced (Niewöhner et al. 1998). Moreover, the solid-phase Ba enrichment (Fig. 5.7) suggests that upward Ba^{2+} diffusion has already been exceeding downward barite burial for a considerable period of time. According to Dickens (2001) the precipitation of a diagenetic barite front forms a time-integrated signal of sulfate depletion and can be used to assess changes in the upward methane flux. This approach offers one particular advantage. Barite fronts record a time-integrated signal of sulfate depletion whereas the current pore water profiles of sulfate could have had a complex history.

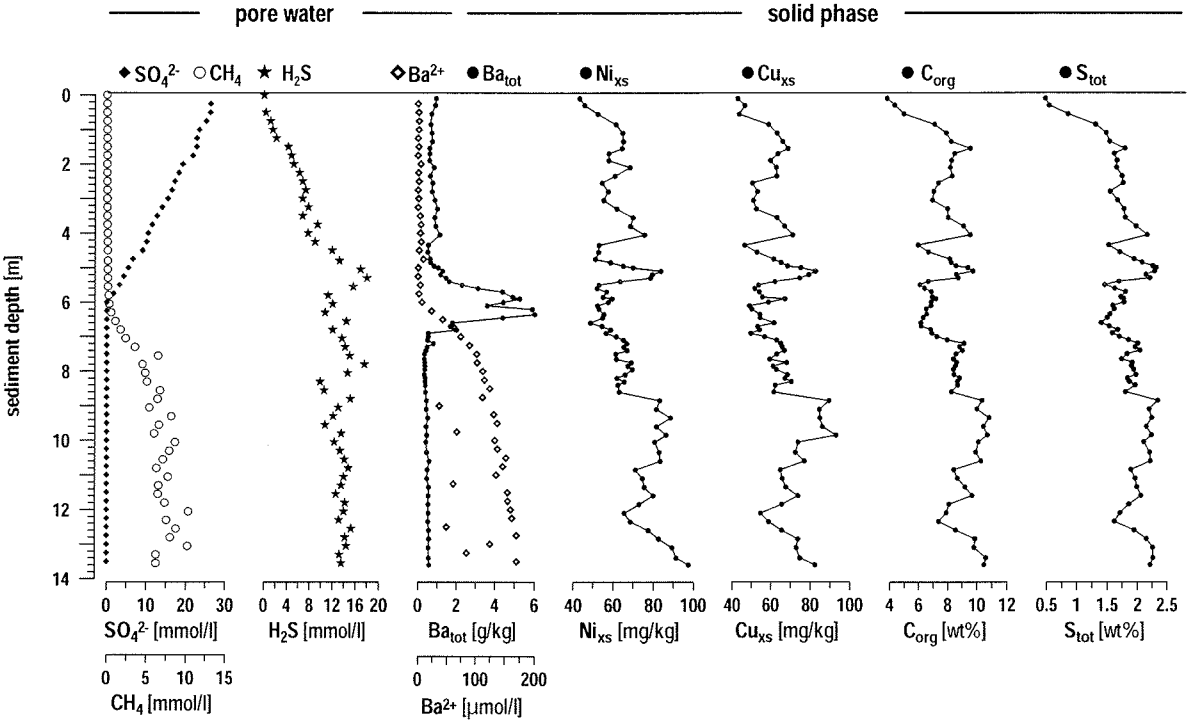

Fig 5.7: *Pore water (symbols) and solid phase (solid lines) data for gravity core GeoB 3718 from the continental slope off Namibia. The sulfate/methane transition is located at a sediment depth of 6 m. SO_4^{2-}, CH_4 and H_2S data according to Niewöhner et al. (1998). All other data taken from Heuer et al. (subm.-a).*

At site GeoB 3718, the amount of Ba that has been enriched in the barite front totals up to 0.220 $g \cdot cm^{-2}$, or $1.61 \cdot 10^{-3}$ moles of Ba for a 1 cm^2 vertical column of sediment (Heuer et al. subm.-a). Assuming steady state conditions, the diffusive flux of Ba^{2+} across the sulfate/methane transition can be calculated from the concentration gradient of dissolved Ba^{2+} and Fick's first law of diffusion. With an observed concentration gradient of $75.4 \cdot 10^{-10}$ $mmol \cdot m^{-3} \cdot m^{-1}$, the Ba^{2+} flux comes up to $2.14 \cdot 10^{-8}$ $mmol \cdot m^{-2} \cdot s^{-1}$ or $6.74 \cdot 10^{-8}$ $mol \cdot cm^{-2} \cdot a^{-1}$. A Ba^{2+} flux of this magnitude would allow to build up the observed Ba enrichment within 23,900 years - provided diagenesis has always been in a steady state. Consequently, the Ba enrichment at site GeoB 3718 suggests that the present methane flux and thus the depth of complete sulfate depletion have been similar for at least 23,900 years (Heuer et al. subm.-a).

At the presented sulfate/methane transition, anaerobic oxidation of methane does not only consume all sulfate but also produces high concentrations of pore water sulfide (Fig. 5.7) (Niewöhner et al. 1998). Thereby methane oxidation provides the means for the sulfurization of organic matter (cf. Sinninghe Damsté and de Leeuw 1990). The reaction of organic matter with dissolved sulfide and polysulfides is of particular importance in sediments with high C_{org} contents and a small supply of reactive Fe that prevents the complete trapping of sulfide as iron sulfides (e.g. Mossmann et al. 1991; Werne et al. 2000).

These conditions are also met at site GeoB 3718 where high amounts of preserved C_{org} go along with low Fe_{tot} contents. In fact, a close correspondence between the total solid phase contents of sulfur (S_{tot}) and the distribution of C_{org} indicates that organic sulfur represents the dominant sulfur species in the sediment (Fig. 5.7) (Heuer et al. subm.-a).

Furthermore, the sulfurization of organic matter seems to control the distribution of trace elements in the solid phase of gravity core GeoB 3718-9 as well (Heuer et al. subm.-a). Based on a normative calculation which devides the total solid phase contents of an element into a lithogenic and an excess fraction, Ni and Cu turned out to have large excess fractions (Ni_{xs}, Cu_{xs}) that match both the solid phase contents of C_{org} and the total sulfur contents (S_{tot}) (Fig. 5.7). Heuer et al. (subm.-a) propose that the correspondence between these trace metals and both C_{org} and S_{tot} results from an early diagenetic reaction of Cu and Ni with secondary organo-sulfur compounds. In this context, the incorporation of Ni and Cu into organic sulfur compounds might proceed either via the trace metals' complexation with sulfur containing functional groups of low-molecular-weight organic sulfur compounds or via the incorporation of metal ions into polysulfide bridges of vulcanized organic macromolecules. Additional evidence for a secondary binding of Ni and Cu as well as Zn and Mo to organic sulfur compounds comes from further investigations at the continental slope off Namibia (Heuer et al. subm.-b).

Niger deep-sea fan

At the Niger deep-sea fan the current position of the sulfate/methane transition was not reached by the 20.3 m long gravity core GeoB 4901 (02°40.7'N, 06°43.2'E, water depth: 2184 m). Dissolved Mn indicates post-oxic conditions in the upper half of the core (0.1 - 12.5 m) while free hydrogen sulfide is present in pore water below 12.5 m sediment depth (Fig. 5.8). Nevertheless, a distinct enrichment of Ba occurs in the solid phase of the sediment at 12.7 m sediment depth and this enrichment might be a fossil diagenetic barite front that formed in the past during a period of increased upward methane flux (Heuer et al. subm.-c).

Support for this hypothesis comes from the distribution of trace elements in the solid phase of gravity core GeoB 4901 (Fig. 5.8) (Heuer et al. subm.-c). Within the oxic and post-oxic zone (0-12.5 m), a good correlation is observed between biogenic Ba and the excess fractions of Ni, Cu, and Zn. The latter elements are known for their nutrient-type relation to productivity in the water column. Thus, their correlation with Ba in the solid phase of the sediment supports the reliability of biogenic Ba as a proxy for paleoproductivity. However, the solid phase contents of Ni, Cu, and Zn do neither match the Ba maximum at 12.5 m sediment depth nor the distribution of Ba in the underlying sulfidic sediment section. This discrepancy can be explained by a redistribution of barite at a fossil sulfate/methane transi-

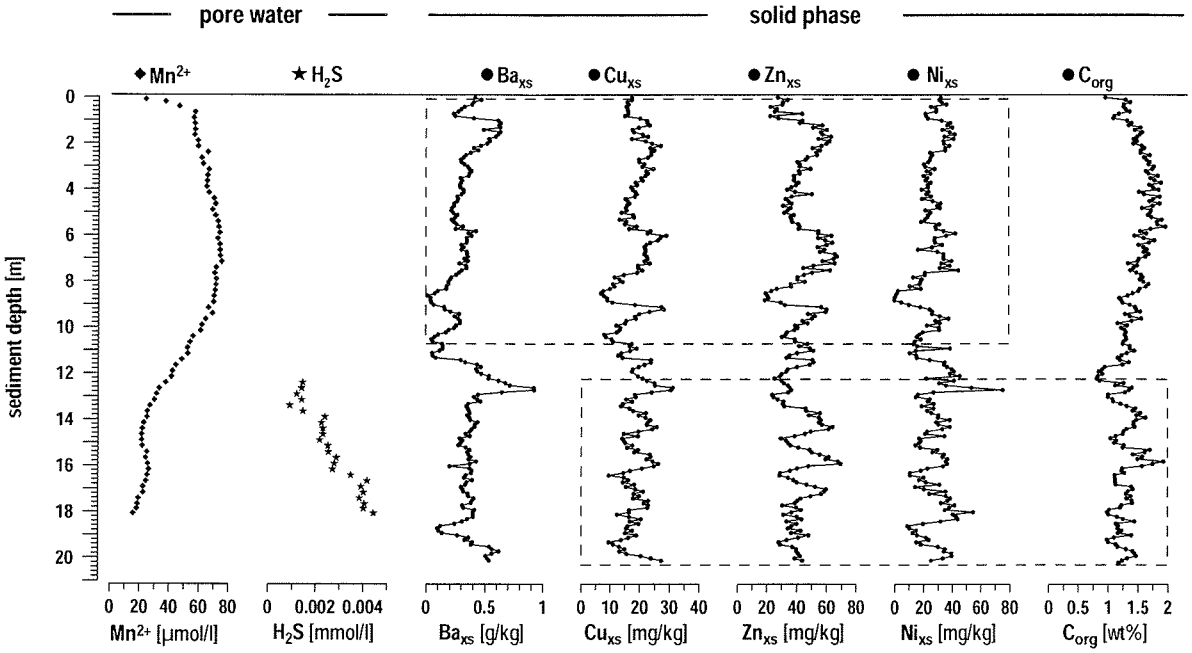

Fig. 5.8: *Pore water (symbols) and solid phase (solid lines) data for gravity core GeoB 4901 from the Niger deep-sea fan. The current depth of the sulfate/methane transition was not penetrated by this core. Heuer et al. (subm.-c) propose that the SMT was located at a much shallower depth, namely around 12.5 m, in the past. Organic carbon data according to Kolonic et al. (in prep). All other data taken from Heuer et al. (subm.-c).*

tion that used to be located at shallower sediment depth than today as proposed by Dickens (2001).

Vice versa, the changing relation between biogenic Ba and the excess fractions of Ni, Cu, and Zn might also result from a redistribution of the latter elements. In the upper 12.5 m of gravity core GeoB 4901, solid phase contents of Ni_{xs}, Cu_{xs}, and Zn_{xs} do not match the distribution of C_{org} since the degradation of organic matter has destroyed the primary signal. However, a close correspondence between Ni, Cu, Zn and C_{org} was identified under sulfidic conditions at greater sediment depth and supports the hypothesis of a secondary binding between trace metals and organic matter in the presence of sulfide (Heuer et al. subm.-c).

On the whole, the upward flux of methane has considerable impact on the composition of the solid phase as it is the crucial factor controlling the depth position of the sulfate/methane transition. Within the SMT, diagenesis can cause a dramatic modification of the primary sediment composition several thousands of years after initial deposition of the sediment. In this way, processes within the SMT lead to a sort of delayed chemical log-in of various elements and minerals and ultimately determine which signals are preserved on longer time scales. Up to now, mostly changes in conditions at the sediment/water interface (C_{org} input, bottom water O_2 content, sedimentation rate) have been identified to initiate nonsteady-state

diagenetic episodes. The studies presented above, however, clearly demonstrate that not only variations in these "influences from above" but also in the "influences from below" in the form of changing upward methane fluxes can trigger non-constant diagenetic situations. These variations in methane flux are driven by processes in the underlying sediment – namely by the proportion of methanogenesis and/or release from gas hydrates.

The extent and nature of diagenetic overprint within the SMT is dependent on the time the SMT is fixed at a particular sediment layer and the overall geochemical characteristics of the sedimentary setting. In Fe-dominated environments, Fe sulfide rich layers are strong indicators for the prolonged fixation of the zone of anaerobic methane oxidation and thus formation during nonsteady-state diagenetic intervals. Sulfurization of organic matter in sulfide-dominated settings enhances preservation of organic matter and produces a close association with a number of trace metals. Although these diagenetic processes also take place under steady-state conditions, changes in the association/correlation of trace elements with either Ba or organic carbon over depth may help to reconstruct the migration of reaction fronts – namely of the SMT – during nonsteady-state periods. Both Fe sulfide enrichments as well as sulfurized organic matter and associated trace metals have a high potential of being preserved in the sedimentary record during further burial below the depth of the SMT. Enrichments of authigenic barite formed within the SMT can be used as valuable tracers for higher methane fluxes in the past and a decrease in methane fluxes over time and thus a subsequent downward migration of the SMT (Dickens 2001; Heuer et al. subm.-c). However, these secondary barites are only stable as long as they are not subject to sulfate-depleted pore water conditions – i.e. as long as they remain above the depth of the SMT.

5.6. Impact of nonsteady-state diagenetic intervals on the shape of sulfate pore water profiles

Periods of nonsteady-state diagenesis do not only produce distinct signals in the sedimentary solid phase but can also have a significant influence on the shape of pore water profiles. In the following we will use interstitial sulfate to demonstrate that the consideration of possible nonsteady-state situations is of utmost importance for the interpretation of pore water profiles.

Biogeochemical transfer reactions have an effect on pore water concentrations of involved reactants. Therefore, changes in pore water concentration gradients – i.e. deviations from the linear shape - are commonly used to identify specific reactions and where they take place (e.g. Schulz 2000). However, it has to be noted that reaction rates deduced from or modeled based on pore water concentration profiles always represent net rates because pore water profiles are the result of all primary and secondary reactions taking place. Gross

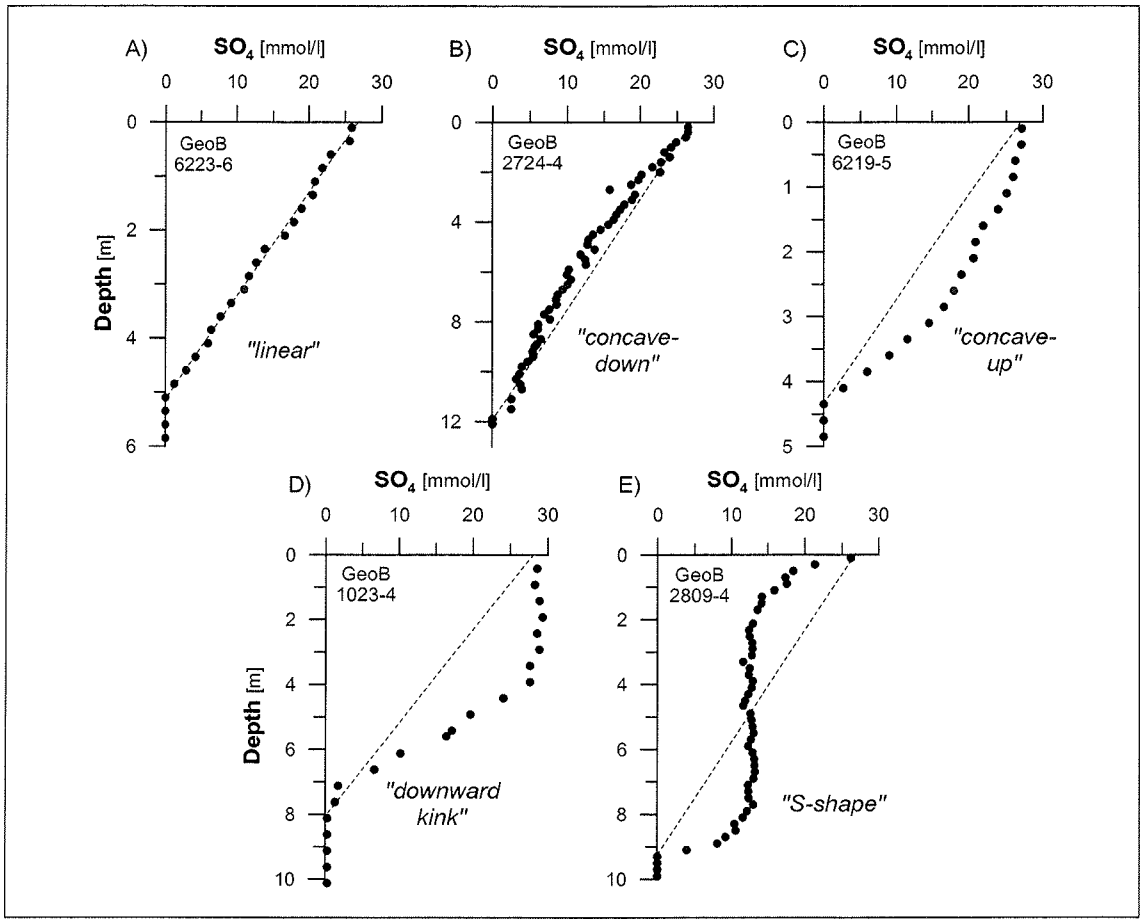

Fig. 5.9: *Examples of the different shapes/types of sulfate pore water profiles as observed in South Atlantic sediments (GeoB 1023-4, Angola Basin; GeoB 2724-4, GeoB 2809-4, GeoB 6223-6, GeoB 6223-6, all Argentine Basin).*

reaction rates can be obtained using radiotracer techniques - e.g., ^{35}S for the determination of sulfate reduction rates (SRR) (e.g. Fossing and Jørgensen 1989). Comparisons of radiotracer-derived SRR with those calculated from pore water profiles often reveal that modeled rates underestimate the values obtained from direct rate measurements. The largest discrepancies between modeled and measured SRR occur close to the sediment surface where highest rates are determined by the $^{35}SO_4$ technique without any detectable gradient change in the sulfate profile (e.g. Fossing et al. 2000; Kasten and Jørgensen 2000). These discrepancies are attributed to the re-oxidation of reduced sulfur species formed during sulfate reduction (Kasten and Jørgensen 2000).

In contrast, also the opposite can be the case – i.e. that obvious changes in pore water gradients do not necessarily have to indicate a reaction but can be the result of a nonsteady-state situation. Borowski et al. (1999) have described the different shapes of sulfate pore water profiles in gas hydrate bearing sediments of the Carolina Rise and the Blake Ridge.

They argued that steep, linear sulfate gradients and shallow depths of the sulfate/methane transition (SMT) are indicators of sites prone to gas hydrate occurrences below. Non-linear sulfate profiles with concave-down curvature were interpreted as background cases for low upward methane flux where a significant amount of sulfate is consumed by dissimilatory sulfate reduction – i.e. for the degradation of organic matter. Figure 5.9 shows examples of the five different types of sulfate profiles which have been examined in about 88 gravity cores recovered during 1989 and 2000 in the South Atlantic. In general, the sulfate penetration depth is controlled by the upward flux of methane which is produced fermentatively or thermogenically in deeper parts of the sediment or supplied from decomposing gas hydrates. Within the sulfate/methane transition (SMT) methane is consumed by anaerobic methane oxidation (AMO) with sulfate according to Eq. 1.

As the SO_4^{2-} concentration in bottom waters can be considered constant over time, the position of the SMT is controlled by the amount of dissolved methane and the depth of its release (Borowski et al. 1999). Therefore, both the accumulation and burial rates of reactive organic compounds are important factors controlling the depth of the SMT. Shallow SO_4^{2-} gradients are generally found in sediments of oligotrophic areas characterized by low organic carbon contents while steep gradients dominate in organic-rich sediments. Apart from variations in the depth position of the SMT, many SO_4^{2-} profiles are characterized by distinct changes in concentration gradients – i.e. they deviate from the linear type of profile (Fig. 5.9). Various attempts to explain these profiles on the basis of steady-state conditions have failed so far, because either sulfate reduction rates did not occur at sufficiently high rates or the necessary electron acceptor (such as reactive ferric iron) was not available in adequate amounts (Haese et al. 1997; Fossing et al. 2000). However, all of these shapes can be explained by the assumption of nonsteady-state conditions in the pore water system.

To illustrate the effects of changing CH_4 fluxes on SO_4^{2-} pore water profiles we have modeled two simplified scenarios within a 15 m long sediment column by applying Fick's second law of diffusion. Besides diffusive transport (with coefficients D_s of 105 and 164 $cm^2\ yr^{-1}$ for SO_4^{2-} and CH_4, respectively) only the cooperative process of anaerobic methane oxidation at the SMT (Eq. 1) is taken into account. Porosity was assumed to decrease exponentially from 90% at the sediment surface to a constant value of 50% below 4 m. The concentration of SO_4^{2-} within the bottom water was kept constant at 27 mmol l^{-1}. The only variable parameter is thus the CH_4 concentration at the bottom of the model area. The initial situation for scenario A represents the steady-state when the CH_4 concentration at a depth of 15 m is 3 mmol l^{-1} (Fig. 5.10-A1). The slight gradient change of the SO_4^{2-} profile close to the sediment surface is caused by the given decrease in porosity (cf. Dickens 2001). Figures 5.10-A2 and 5.10-A3 show the development of the sulfate pore water profile when the CH_4 concentration at the lower boundary is set to 50 mmol l^{-1}. The SMT moves upward and reaches a new steady-state after about 7000 years. Even if such a long period of constant CH_4 flux seems to be unrealistic, the model run definitely demonstrates the effect of an increasing CH_4 release on the corresponding SO_4^{2-} pore water profile. As a result,

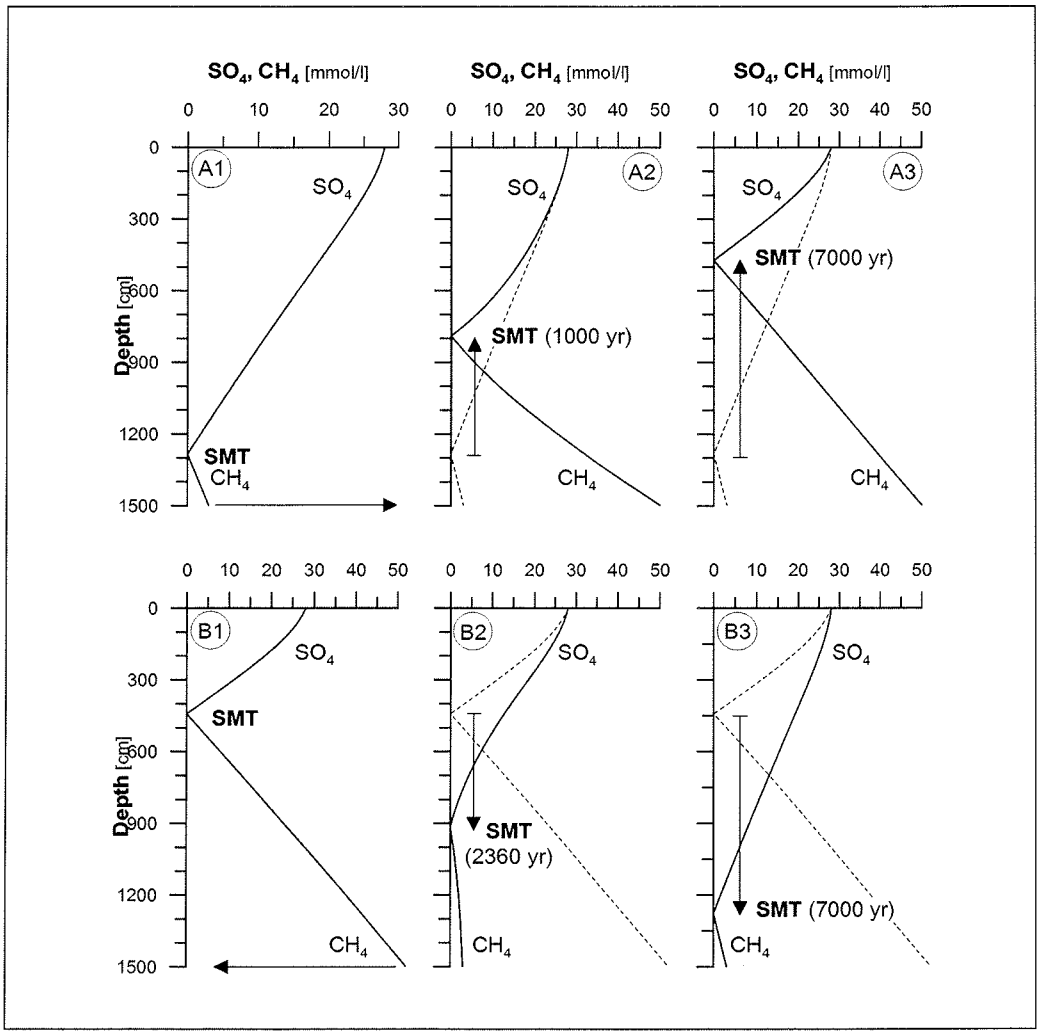

Fig. 5.10: *Modelling of the effects of differing fluxes of methane from below on the shape of sulfate pore water profiles. A) Results of a model run showing the development of the sulfate profile when the CH_4 concentration at the lower boundary is increased from 3 to 50 mmol l^{-1}. Transiently, SO_4^{2-} profiles are of concave-up type. B) Results of a model run where the CH_4 concentration was decreased from 50 to 3 mmol l^{-1}. This scenario temporarily produces SO_4^{2-} profiles of concave-down shape.*

transient shapes are of "concave-up"-type as depicted in Figure 5.9-C. Scenario B (Fig. 5.10-B1 to B3) describes the opposite case when the CH_4 flux decreases over time. Starting with the steady-state situation (A3) this value was reduced to 3 mmol l^{-1} (Fig. 5.10-B1 to B3). During the subsequent downward movement of the SMT, the SO_4^{2-} profile transiently shows a "concave-down"-shape (cf. Fig. 5.9-B). Sulfate reduction rates (SRR) derived from the flux rates within the SMT during the model runs (Fig. 5.11) are in the same range as those determined within the zone of deep sulfate reduction by means of the radiotracer technique (e.g. Fossing et al. 2000). These values are about one order of magnitude lower than those measured close to the sediment surface (Ferdelman et al. 1999).

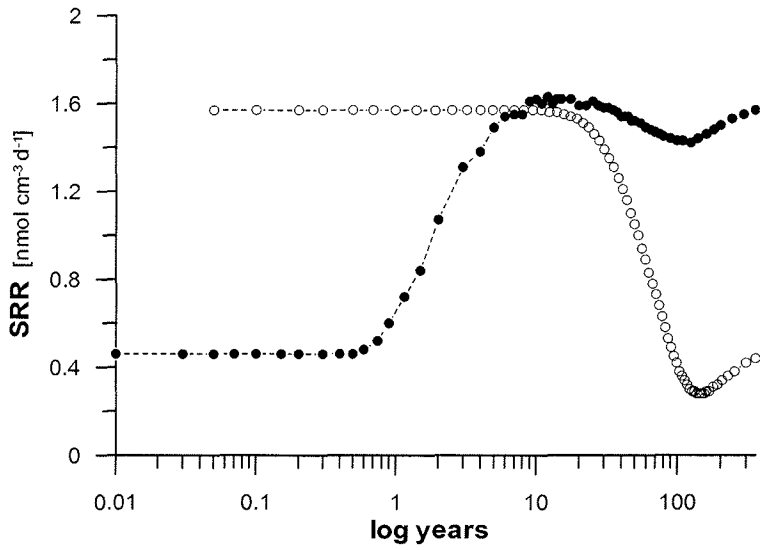

Fig. 5.11: *Development of sulfate reduction rates (SRR) within the sulfate/methane transition (SMT) over time during the model runs A and B shown in Fig. 10. Closed and open symbols represent scenarios A (Figs. 10-A1 to A3) and B (Figs. 10-B1 to B3), respectively. SRR were calculated from the sulfate flux rates at the SMT.*

As there is strong evidence that the release of methane in deep-sea sediments is not a continuous process and constant in space and time (e.g. Norris and Röhl 1999; Dickens 2001) we suggest that nonsteady-state situations in the sulfate/methane system are common and have to be considered when interpreting sulfate profiles. Our modeling approach demonstrates that the usual explanation for concave-down sulfate profiles – i.e. degradation of organic matter by dissimilatory sulfate reduction (e.g. Borowski et al. 1999) – does not always hold true. Nonsteady-state conditions seem to be the only conclusive explanation which is consistent with all available data, and underlines the assumption that SO_4^{2-} pore water profiles, showing significant kinds of the described shapes, do not necessarily have to result from specific (bio)geochemical reactions or non-local pore water transport (cf. Dickens 2001).

Pore water profiles which are characterized by prominent changes (kinks) in the sulfate gradient/profile (cf. Fig. 5.9 D) can hardly be simulated by this approach. After Zabel and Schulz (2001) such profiles originate from the displacement of submarine landslides. When water-saturated deposits are rapidly overthrusted by a package of sediment, the pore water systems in both sections start to adapt to each other. Such drastic sedimentation processes must not set off (bio)geochemical reactions inevitably. This depends on several parameters like the difference in sediment compositions and/or of the geochemical environmental condition in both (lithological) units. In the case presented by Zabel and Schulz (2001), the authors give conclusive evidence for the sliding of a large 10 m thick coherent block of pelagic sediments down the continental slope, overthrusting on a turbidite sequence.

Applying a simple transient model containing an explicit numerical solution for Fick's second law of diffusion, they could demonstrate that effects of submarine landslides on pore water systems are able to explain the observed shapes in SO_4^{2-} profiles (Fig. 5.12). Accordingly, such pore water profiles represent a transitional stage between two or more steady-state stages which are formerly established in the single sediment units. The period until the measured and modeled profiles correspond to each other may give an indication of the adaptation between sediment systems. For the example shown in Figure 5.12, Zabel and Schulz (2001) have estimated a period of 300 ± 25 yr.

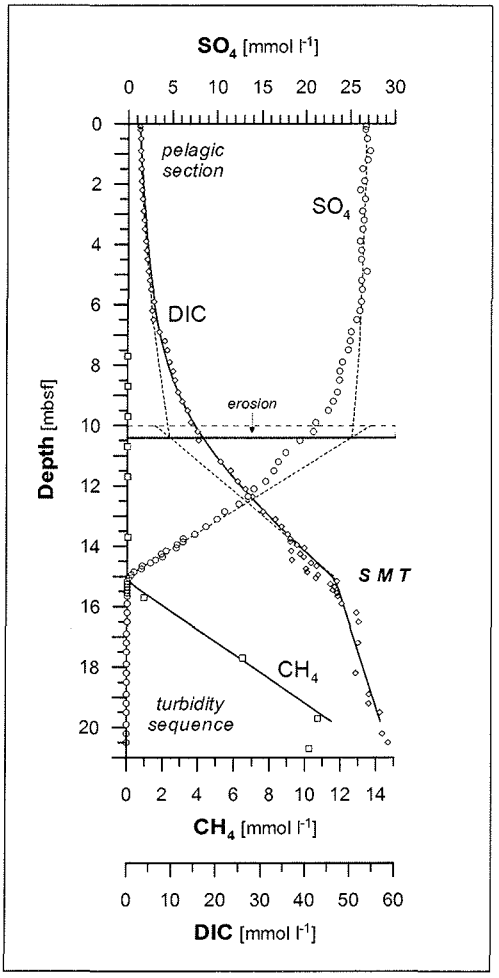

Fig. 5.12: *Submarine landslide in sediments of the Southern Congo Fan. Results of a transient model as compared to measured data. Dashed lines: presumed starting situation representing steady-state conditions in both sediment segments; solid lines: model result after a period of 300 years; shaded depth interval: erosion caused by the overthrusting of the turbidity deposits by the pelagic sequence (after Zabel and Schulz 2001).*

Slightly different, but nevertheless similar may be the explanation for the rare "S-shape" pore water profiles (Fig. 5.9-E). Hydroacoustic and physical property data (magnetic susceptibility and density), solid phase analyses of iron speciation, and also AMS ^{14}C dating of an ikaite crystal from 9.4 m depth (26.770 yr) indicate that at site GeoB 2809 at least two slides or sedimentary events must have occurred to establish the present-day situation (Hensen et al. subm.-b). As a prerequisite for the intermediate and constant pore water SO_4^{2-} concentrations over depth immediately after deposition, complete mixing of the two sediment packages has to be assumed. Hensen et al. (subm.-b) also applied a simple

transport/reaction model to reproduce the S-shape of the sulfate profile at this location. Using this modelling approach an optimal fit for the measured data was obtained after 25 years. After about 500 years – and with a constant CH_4 flux from below - an almost linear profile would result.

As also shown for the kink-type, "re-moved" sediment packages may carry their geochemical signature from their origin, thus the accumulation of different packages with originally different pore water signatures should be able to produce any type of sulfate pore water profile, only forced by the position of the SMT and diffusion. However, it is evident that diffusion is very effective in smoothing the concentration differences and that both, kink- and S-type, are obviously very short-lived phenomena.

5.7. Conclusions and future perspectives

Periods of nonsteady-state diagenesis are common features in sediments of the equatorial and South Atlantic Ocean – even in slowly accumulating pelagic deposits and/or in sediments with overall low organic carbon contents. Sediment intervals affected by pronounced diagenetic overprint under nonsteady-state conditions often occur cyclically within the sedimentary record and are mostly associated with full glacial/interglacial transitions. At numerous sites these diagenetic processes were shown to be still active.

The fact that strongest diagenetic alterations of the primary sediment composition are found across glacial/interglacial boundaries is consistent with glacial terminations being the times of the most profound changes in oceanographic, depositional and geochemical conditions. The resulting imbalance in the sediment/pore water system initiates a number of diagenetic phenomena - like fixation or downward progression of redox boundaries and reaction fronts - which have a high potential for modifying the primary sediment composition and producing distinct secondary signals in the solid-phase. The mechanisms that are likely to have triggered these very "effective" diagenetic processes are decreases in sedimentation rate and organic carbon input as well as increase in bottom water O_2 content due to enhanced NADW production at the onset of interglacial periods.

The strongest diagenetic modifications within a sedimentary redox succession take place in the interval across the oxic/post-oxic and the Fe(II)/Fe(III) redox boundary as well as within the zone of anaerobic methane oxidation. Across the oxic/post-oxic and Fe redox boundary the most important diagenetic processes are the post-depositional aerobic degradation of organic matter, dissolution of carbonate and ferric iron minerals as well as formation of distinct secondary enrichments of redox-sensitive elements. Of the latter authigenic enrichments, those elements which form their solid-phase peaks under post-oxic conditions – e.g. V, Cd, and U - can serve as valuable indicators for decreases in C_{org} burial over time and thus for periods of nonsteady-state diagenesis. The extent of post-depositional oxidation

of organic matter in these transitional sediment intervals was shown to depend on the overall sedimentation rate and the magnitude of change encountered in the various depositional and geochemical factors. A sedimentation rate of about 2 cm/kyr is assumed to be the critical value below which no significant amounts of non-refractory organic carbon are preserved. For this reason deglacial productivity pulses and elevated glacial TOC inputs which have been widespread in the equatorial Atlantic have been oxidized to various degrees by oxidation fronts across glacial terminations. In sediments of the Ceará Rise and the Sierra Leone Rise which are characterized by low sedimentation rates around 2 cm/kyr the initially present deglacial pulses of organic carbon have been completely burned-down - leaving only peaks of biogenic barium as relicts.

The influence of climatically induced changes in sedimentation rate and/or organic carbon burial is not restricted to the oxic/post-oxic and the Fe redox boundary, but well extends to deeper sediment sections. This effect has been illustrated for deposits of the Amazon deep-sea fan, where the strong decrease in sedimentation rate and organic carbon accumulation encountered during the Pleistocene/Holocene transition has caused a fixation of the zone of deep sulfate reduction for a considerable period of time. In this way nonsteady-state diagenesis has a high potential for significantly overprinting the sediment composition several thousands to millions of years after initial deposition. The most relevant diagenetic/ geochemical processes within the zone of anaerobic methane oxidation comprise the formation of authigenic barites, carbonates and iron sulfides (most important in iron-dominated systems) as well as the sulfurization of organic matter (most important in oranic matter rich, sulfide-dominated systems). Enrichments of authigenic barite formed slightly above the SMT can be used to indicate higher methane fluxes in the past and a decrease in methane fluxes over time and thus a subsequent downward migration of the SMT. However, these barites are only stable under sulfate-containing pore water conditions.

Recent investigations in sediments of the Niger deep-sea fan and the upwelling area off Namibia have revealed that sulfurization of organic matter in sulfidic parts of the sediment also strongly affects the solid-phase distribution/association of trace metals. While a significant correlation between Ni, Cu, Zn and Ba exists in non-sulfidic sediments, the presence of free sulfide in pore water is likely to cause the incorporation of these trace elements into organic sulfur compounds producing a close correspondence with the amount of organic matter preserved. The association of these trace elements with either Ba or TOC might therefore be a valuable indicator for sulfidic and non-sulfic conditions and to trace the temporal migration of the sulfate/methane transition during nonsteady-state periods.

The long-term usability of all primary and secondary signals – also of those formed and preserved across the oxic/post-oxic and the Fe redox boundary – is ultimately controlled by the geochemical processes within and below the sulfate/methane transition. While dissolution of authigenic barite as well as productivity-related barite takes place during burial into sulfate-depleted sediment sections, iron sulfides as well as sulfurized organic matter and associated trace elements have a high potential to survive burial below the SMT.

Our studies further demonstrate that nonsteady-state situations cannot only be induced by changes in conditions at the sediment/water interface like productivity, C_{org} burial or sedimentation rate but also by processes in the underlying sediment – namely the formation and/or liberation of CH_4. Besides the above described modifications of the solid phase, variations in the upward flux of methane also have a considerable impact on the shape of sulfate pore water profiles. Modelling the effects of such variations in methane flux on sulfate profiles has demonstrated that considering possible nonsteady-state situations in the sediment/pore water system is of utmost importance for the interpretation of pore water data.

To conclude we intend to emphasize that glacial terminations and sediment sections subject to anaerobic methane oxidation are those intervals which are and have been most severely altered by post-depositional diagenetic processes in an otherwise undisturbed sediment sequence. As this distinct overprint often also goes along with a particularly bad preservation of a number of proxies (e.g. TOC, carbonate, Ba) special care has to be taken when interpreting the records of these components within such sediment sections.

Further detailed and high-resolution studies on the fate of a variety of sediment constituents – e.g. calcareous and organic components - during nonsteady-state diagenesis are required to improve environmental reconstructions from the various sedimentary components and to solve discrepancies between existing productivity reconstructions. Furthermore, the suite and controlling factors of authigenic mineral formation within the sulfate/methane transition – like e.g. iron sulfides – in natural systems is still a matter of debate. Similarly, the geochemical processes involved in the sulfurization of organic matter and the coupling of trace metals to the biogeochemical cycles of sulfur and carbon are not known in detail yet and await further investigation.

Acknowledgements - We would like to thank the captains and crews of the RV Meteor for their support during the numerous cruises. For technical assistance on board and in the home laboratory we are indebted to Sigrid Hinrichs, Karsten Enneking, Susanne Siemer and Silvana Hessler. This research was funded by the Deutsche Forschungsgemeinschaft (contribution no. of Special Research Project SFB 261 at the University of Bremen).

Chapter 6: Summary and Conclusions

This study deals with the impact of early diagenesis on the distribution of trace elements in the solid phase of marine sediments. Investigations comprise detailed geochemical analyses of three 10-20 m long and undisturbed gravity cores from the equatorial and Southeast Atlantic (GeoB 1711-4, GeoB 3718-9, GeoB 4901-8). These cores were particularly suitable for the exploration of element patterns in the solid phase since pore water analyses had revealed a variety of early diagenetic environments and a large vertical extension of redox zones. Solid phase samples were taken every 5-10 cm and analysed for up to 28 elements (cf. periodic table of investigated elements, p. 116). Subsequently, a normative calculation was applied in order to split the measured total element contents up into lithogenic and excess fractions. Based on this approach, three groups of elements could be distinguished in the solid phase of each gravity core:

Group A contains elements whose distribution is governed by the lithogenic sediment fraction. Total solid phase contents of these elements are closely correlated to Al contents, element-aluminium ratios are fairly constant throughout the total length of the cores and calculated lithogenic element fractions account for the major part of the total solid phase contents. The composition of group A varies slightly at the investigated sites and is presented on p. 116-117.

Group B consists of elements whose total solid phase contents are hardly related to the distribution of Al. Moreover, total solid phase contents contain large non-lithogenic excess fractions. These excess fractions have distinct distribution patterns that correspond either to the paleoproductivity pattern given by biogenic Ba or to the preserved amounts of C_{org}. The occurrence of either of both relations depends on the prevalent redox conditions. The composition of group B is presented on p. 116-117.

Group C represents elements whose distribution in the solid phase is governed by the carbonaceous sediment fraction. In the investigated cores only Sr showed a close correlation to Ca.

In the investigated sediments, group A confirmed a constant input of trace elements with terrigenous aluminosilicates and justified the chosen approach for a normative calculation of lithogenic element fractions. In contrast, group B showed most obviously the potential impact of early diagenesis on the solid phase of sediments. The distribution of these trace elements in the solid phase and their correspondence to either Ba or C_{org} turned out to reflect the different early diagenetic milieus of pore waters. Within the **oxic** and **post-oxic** sections of gravity core GeoB 4901 (Niger deep sea fan), excess fractions of Cu, Ni, and Zn (Cu_{xs}, ...) were distributed in close accordance to the paleoproductivity pattern given by biogenic Ba. This correspondence confirms a primary input of Ni, Cu, and Zn with biogenic carrier phases and supports the reliability of biogenic Ba as a proxy for paleoproductivity. At the

same time, neither Cu_{xs}, Ni_{xs}, and Zn_{xs} nor biogenic Ba were directly related to the amount of preserved C_{org}. The different distribution of C_{org} can be attributed to the post-depositional degradation of organic matter.

In the **sulphidic** part of gravity core GeoB 4901, distribution patterns changed distinctly. Excess fractions of Ni, Cu, and Zn were closely related to the contents of preserved C_{org} but they did not show any affinity to the concentration profile of Ba. A close correspondence of Ni_{xs}, Cu_{xs}, Zn_{xs} and moreover Mo_{xs} and As_{xs} to the distribution of preserved C_{org} was also observed in the completely sulphidic sediments on the continental slope off Namibia (GeoB 1711, GeoB 3718). In the latter region, distribution patterns of trace metals and C_{org} resembled additionally also the concentration profile of total sulphur (S_{tot}) in the solid phase of the sediment. All in all, these findings suggest that the similar distribution of group B elements and preserved C_{org} does not result from a primary input of trace metals with organic matter but from an early diagenetic redistribution in the presence of sulphide. Organic molecules are known to incorporate reduced inorganic sulphur species (H_2S and/or polysulphides). This natural sulphurization forms sulphur containing structural units and (poly)sulphide linkages which result in low- and high-molecular weight organic sulphur compounds, respectively (Sinninghe Damsté and de Leeuw, 1990). This study suggests that Ni, Cu, Zn, and Mo, in turn, might be tied to organic sulphur compounds by a complexation with sulphur containing functional groups or by an incorporation into the polysulphide bridges of vulcanised organic macromolecules. If the proposed early diagenetic reactions can be verified by further process studies, a secondary binding between trace metals and sulphurised organic matter might be used in order to reconstruct sulphidic pore water milieus from the solid phase of sediments.

At the **sulphate/methane transition** anaerobic oxidation of methane causes a complete consumption of dissolved sulphate. Thereby it initiates a redistribution of barite ($BaSO_4$). The dissolution of barite limits the use of biogenic Ba as a proxy for paleoproductivity but the precipitation of a diagenetic barite front forms a new signal in the solid phase that is related to the position of the sulphate/methane transition and thus to the upward methane flux. In the solid phase of gravity core GeoB 3718 a distinct Ba front was detected at the active sulphate/methane transition. The concentration profile of Ba^{2+} in pore water confirms the actual dissolution and reprecipitation of barite. Considering the observed upward flux of dissolved Ba^{2+} and the amount of Ba that has been enriched in the solid phase one can estimate how long it has taken to form the present Ba front at the sulphate/methane transition. This approach reveals that the upward methane flux must have been fairly constant at site GeoB 3718 for at least 23,900 years.

Anaerobic oxidation of methane has a two-fold effect with respect to the distribution of trace elements. On the one hand, complete consumption of sulphate initiates a redistribution of Ba. Consequently, solid phase contents of Ba stop to resemble paleoproductivity patterns and any primary relation between Ba and elements of group B is destroyed as well. On the

other hand, sulphide is produced by the reduction of sulphate. The release of inorganic sulphides into pore water supports the sulphurization of organic matter and might also control the suggested complexation of group B elements with organic sulphur compounds in the solid phase of the sediment.

At site GeoB 3718, sulphate depletion, sulphide production and their consequences for the composition of the solid phase could be related to the occurrence of methane at the present sulphate/methane transition. In contrast, no methane was observed in the pore waters of gravity core GeoB 4901. Nevertheless, distribution patterns of Ba and group B elements in the solid phase suggest that a methane driven redistribution of trace elements might have occurred in the upper meters of this sediment during a period of enhanced upward methane flux in the past.

In summary, this study confirms the important role of organic matter for the distribution of trace elements in marine sediments. Under oxic and post-oxic conditions, solid phase contents of Ni, Cu, and Zn were still related to productivity though the degradation of organic matter had destroyed any link to preserved C_{org} contents. Under sulphidic conditions, elements of group B showed a close relation to preserved amounts of C_{org}. This relation indicates that organic matter might also be involved in a fixation of trace metals to the solid phase if a surplus of sulphide supports the sulphurization of organic compounds. Moreover, degradation of organic matter has long been known to fuel a variety of early diagenetic redox processes in sediments. The impact of these reactions on the distribution of trace elements has become particularly obvious in sediments where a change in productivity had caused a period of non-steady state diagenesis. Under these circumstances redox zones remain at a particular sediment depth for a prolonged period of time and distinct enrichments of trace elements can evolve in the solid phase of the sediment. This study draws attention to a further aspect of organic matter degradation namely the fermentation of organic matter. This process might affect the solid phase of the sediment as well since the subsequent anaerobic oxidation of methane initiates several early diagenetic processes at the sulphate/methane transition. However, this reaction front differs distinctly from reaction fronts that are related to productivity and burial of C_{org} since the upward methane flux is ultimately controlled by processes in the underlying sediment.

Finally, three major conclusions can be drawn about the potential use of trace metals for the reconstruction of palaeoenvironments, namely:

(a) The distribution of Ni, Cu, and Zn in the solid phase of sediments can confirm Ba as a proxy for either paleoproductivity or methane flux.

(b) Aside from distinct enrichments of trace elements in the solid phase that document periods of non-steady state diagenesis, continuous solid phase patterns of group B elements and their relation to Ba, C_{org}, and S_{tot} have a strong potential for a reconstruction of redox milieus in pore waters.

(c) The distribution of trace metals in the solid phase of sediments is particularly useful for the reconstruction of paleoenvironments since solid phase records document the impact of early diagenetic processes for a longer period of time than pore water does.

Deutsche Zusammenfassung

In der vorliegenden Studie wurde die Verteilung von Spurenelementen in der Festphase mariner Sedimente untersucht. Dabei galt es vor allem weiter aufzuklären, wie sich frühdiagenetische Prozesse auf die Zusammensetzung der Festphase auswirken. Die frühdiagenetische Mobilisierung und Umverteilung redox-sensitiver Elemente ist ein bereits gut untersuchtes Phänomen. Allerdings konzentrieren sich die bisherigen Arbeiten zumeist auf das aktuelle Geschehen an der Sediment/Wasser-Grenze oder auf Sedimentabschnitte, in denen Turbidite, Sapropele oder Glazial/Interglazial Wechsel die frühdiagenetischen Abläufe so einschneidend verändert haben, dass es in einer anschließenden Anpassungsphase mit nicht-stationären Bedingungen zu besonderen Elementanreicherungen kommen konnte. Wie sich Eintrag und Abbau organischer Substanz und die daraus resultierenden geochemischen Milieus auf die Verteilung von Spurenelementen in den oberen Metern des Sedimentes auswirken, ist dagegen bisher kaum untersucht worden.

Um dieser Frage nachzugehen, wurden aus bereits gut untersuchten Bereichen des Südatlantiks drei 10 - 20 m lange Schwerelotkerne ausgewählt, deren Porenwässer verschiedene charakteristische geochemischen Milieus aufweisen. Die Sedimentkerne stammen zum einen aus dem durch terrigenen Eintrag geprägten Tiefseefächer des Nigers (GeoB 4901, 2184 m Wassertiefe) und zum anderen aus dem hochproduktiven Auftriebsgebiet vor Namibia (GeoB 1711, 1967 m Wassertiefe und GeoB 3718, 1312 m Wassertiefe). Während sich im Tiefseefächer des Nigers einzelne Redoxzonen über mehrere Meter ausdehnen und eine klare Abfolge von oxischen, post-oxischen und sulfidischen Bedingungen ergeben, ist das Sediment am Kontinentalhang vor Namibia bereits kurz unterhalb der Sediment/Wasser-Grenzschicht sulfidisch. An der Station GeoB 3718 wurde darüber hinaus auch der methanogene bzw. methanhaltige Bereich des Sedimentes erreicht.

Zur systematischen Untersuchung der Festphase wurden die Sedimentkerne durchgehend in engen Abständen von 5 - 10 cm beprobt. Die Proben wurden gefriergetrocknet, gemörsert und nach saurem Mikrowellen-Vollaufschluß einer Multielement-Analyse mittels ICP-AES unterzogen. Eine Übersicht über die 28 analysierten Elemente befindet sich auf Seite 116.

Nachdem der Gesamtgehalt eines Elementes in der Festphase rechnerisch in einen lithogenen Anteil und einen daneben existierenden Überschuß unterteilt worden war, konnten in den verschiedenen Kernen jeweils drei Gruppen von Spurenelementen unterschieden werden. Während in Gruppe A der Gesamtgehalt der Elemente durch den lithogenen Anteil in der terrigenen Sedimentfraktion bestimmt wird, weist jedes Element in Gruppe B neben der lithogenen Fraktion einen erheblichen Überschuß auf. Die Überschußfraktionen der Gruppe B zeigen außerdem eigenständige Verteilungsmuster, die mit Eintrag und Erhaltung von organischer Substanz zusammenhängen und dabei in einer deutlichen Beziehung zum geochemischen Milieu des Porenwassers stehen. Gruppe C beinhaltet Calcium und Strontium, deren Verteilung allein durch den Carbonatgehalt der Festphase bestimmt werden. Daneben

wurden Barium als bekanntem Proxy für Primärproduktion und Mangan als frühdiagenetisch leicht mobilisierbarem Element eine Sonderstellung eingeräumt. Die Zusammensetzung der einzelnen Gruppen an den verschiedenen Stationen kann der Darstellung auf Seite 116 f. entnommen werden.

Hinsichtlich der Frage, ob die Verteilung von Spurenelementen in der Festphase des Sedimentes das geochemische Milieu des Porenwassers widerspiegelt, lieferten die Elemente der Gruppe B und ihre Beziehung zum Produktivitätsproxy Barium (Ba_{xs}) und zur organischen Substanz die wichtigsten Ergebnisse. Die Überschußfraktionen von Nickel, Kupfer und Zink (Ni_{xs}, Cu_{xs}, Zn_{xs}) zeigten im Tiefseefächer des Nigers unter oxischen und post-oxischen Bedingungen eine ähnliches Konzentrationsprofil wie Ba_{xs} aber keine Beziehung zur erhaltenen Menge organischen Kohlenstoffs (C_{org}). Ni, Cu und Zn sind in der Wassersäule nährstoffartig verteilt. Ihr mit Ba_{xs} übereinstimmendes Verteilungsmuster in der Festphase des Sedimentes deutet darauf hin, dass sie entsprechend ihrem primären biogenen Eintrag festgelegt und erhalten wurden. Auf diese Weise stützen Ni_{xs}, Cu_{xs} und Zn_{xs} die Interpretation von Ba_{xs} als Produktivitätsproxy. Demgegenüber ist die ursprüngliche Beziehung dieser Elemente zu C_{org} durch den Abbau der organischen Substanz im Sediment verloren gegangen. Da die enge Beziehung zwischen Ni_{xs}, Cu_{xs}, Zn_{xs} und Ba_{xs} in der Festphase mit dem Wechsel im geochemischen Milieu des Porenwassers endet und im sulfidischen Sedimentbereich nicht festgestellt wurde, kann ihr Vorliegen zugleich als ein Anzeiger für oxische oder post-oxische Bedingungen verstanden werden. Bemerkenswert ist hierbei, dass die sich ähnelnde Verteilung von Ni_{xs}, Cu_{xs}, Zn_{xs} und Ba_{xs} nicht durch die Reduktion von Mn-Oxiden beeinflußt wird und in der gewählten Tiefenauflösung keine Beziehung zu fossilen Mn-Anreicherungen zeigt.

Obwohl im Tiefseefächer des Nigers in den oberen Metern des Sedimentes keine Beziehung zwischen Ni_{xs}, Cu_{xs}, Zn_{xs} und der erhaltenen organischen Substanz bestand, war in größeren Sedimenttiefen unter den dort vorliegenden sulfidischen Bedingungen eine deutliche Korrelation zwischen den genannten Spurenelementen und C_{org} zu erkennen. Eine eindeutige Beziehung zwischen den Überschußfraktionen von Ni, Cu und Zn und der erhaltenen organischen Substanz wurde auch in den durchweg sulfidischen Sedimenten vor Namibia beobachtet. Dort zeigte außerdem Mo_{xs} eine ähnliche Verteilung wie C_{org}. Dies ist bemerkenswert, da Molybdän in der Wassersäule keine nährstoffartige Verteilung hat. Zugleich wurde in der Festphase dieses Sedimentes eine enge Korrelation zwischen den Gehalten an C_{org} und Schwefel (S_{tot}) festgestellt.

Da die beschriebene Beziehung zwischen den Spurenelementen und C_{org} erst im tiefen bzw. sulfidischen Sediment auftritt, liegt der Schluß nahe, dass sie einen frühdiagenetischen Ursprung hat und durch Sulfid vermittelt wird. Für diese Interpretation sprechen auch die teilweise enge Korrelation von C_{org} und S_{tot} in der Festphase und die Tatsache, dass es sich bei Ni, Cu, Zn und Mo um Sulfidbildner handelt. Der entscheidende frühdiagenetische Prozeß ist dabei möglicherweise die Sulfurisierung organischer Substanz, da sie schwefelhaltige

funktionelle Gruppen und Polysulfidbrücken bildet, die wiederum Potenzial für die Komplexierung und Festlegung von Ni, Cu, Zn und Mo bieten. Falls die frühdiagenetische Festlegung von Spurenelementen bei der Sulfurisierung organischer Substanz durch weitere Untersuchungen bestätigt werden kann, könnte die hier beschriebene Beziehung zwischen den Überschußfraktionen von Ni, Cu, Zn und Mo und der organischen Substanz als ein in der Festphase gespeicherter Anzeiger für das sulfidische Milieu des Porenwassers genutzt werden.

Der Übergang zum methanhaltigen Bereich des Sedimentes zeichnet sich nicht nur durch das Vorkommen sondern auch durch die anaerobe Oxidation von Methan aus, die eine vollständige Aufzehrung von gelöstem Sulfat mit sich bringt. Da unter diesen Bedingungen die Lösung von Baryt ($BaSO_4$) einsetzt, kommt es zu einer Umverteilung von Ba in der Festphase des Sedimentes. In der vorliegenden Studie konnte die Verlagerung von Ba im Bereich des Sulfat/Methan-Übergangs sowohl im Porenwasser als auch in der Festphase des Sedimentkerns GeoB 3718 beobachtet werden. Dabei wurde deutlich, dass Ba_{xs} mit der Lösung von Baryt zwar einerseits seine Funktion als Proxy für Primärproduktion verliert, andererseits aber die anschließende Ausfällung und Anreicherung von Ba im Bereich der Sulfat/Methan-Übergangszone ein neues Signal bildet, das zur Rekonstruktion des Methan-Flusses genutzt werden kann. So deutet die frühdiagenetische Anreicherung von Ba an der Station GeoB 3718 vor Namibia darauf hin, dass der aktuelle Methan-Fluß bereits seit 23.900 Jahren aktiv ist.

Die Reduktion von Sulfat im Zuge der anaeroben Methanoxidation bewirkt einerseits die vollständige Aufzehrung von gelöstem Sulfat andererseits aber ebenso eine erhebliche Produktion von Sulfid. Sie trägt dadurch maßgeblich zu dem durchweg sulfidische Milieu im Porenwasser der beiden Sedimentkerne bei, die am Kontinentalhang vor Namibia entnommen wurden. Auf diese Weise werden durch den aufwärts gerichteten Methanfluß, der seinen Ursprung im tiefen Sediment hat, die Ausfällung von Sulfiden, die Sulfurisierung organischer Substanz und möglicherweise die sekundäre Festlegung von Spurenelementen durch organische Schwefelverbindungen angetrieben.

Dass der aufwärts gerichtete Methanfluß über die tiefe Sulfatreduktion auch auf die Festphase einwirkt und einerseits zur Ausbildung einer Ba Front führt, andererseits eine enge Korrelation zwischen C_{org}, S_{tot} und Spurenelementen begünstigt, kann am Kontinentalhang vor Namibia als aktueller Vorgang beobachtet werden. Im Tiefseefächer des Nigers liegt der methanhaltige Bereich zur Zeit unterhalb der durchteuften oberen 20 m des Sedimentes. Es ist jedoch vorstellbar, dass zu einem früheren Zeitpunkt ein stärkerer Methanfluß aufgetreten ist. Ein solcher würde sowohl die Ba Anreicherung in 12,5 m Sedimenttiefe als auch die Korrelation zwischen C_{org} und Spurenelementen im darunter liegenden sulfidischen Milieu erklären.

Abschließend läßt sich festhalten, dass in der Festphase der untersuchten Sedimente insbesondere die Verteilung von Ba und die Beziehung von Ni, Cu, Zn und Mo zu Ba, C_{org} und S_{tot} wichtige Aussagen über das geochemische Milieu des Porenwassers erlauben. Diese Elemente bilden in den oberen Metern des Sedimentes Signale, die Rückschlüsse auf den Stoffhaushalt des Sedimentes ermöglichen. Darüber hinaus zeigte sich, dass neben der Primärproduktion und Einbettung von organischer Substanz auch der Aufstieg von Methan einen großen Einfluß auf die Verteilung von Spurenelementen in der Festphase des Sedimentes haben kann. Für die Rekonstruktion von Veränderungen in der Primärproduktion oder im Methanfluß bietet die Festphase den großen Vorteil, frühdiagenetische Signale über einen längeren Zeitraum hinweg zu speichern und so auch fossile Situationen zu dokumentieren. Demgegenüber kann die Zusammensetzung des Porenwassers nur die aktuellen Prozesse widerspiegeln.

Periodic table of investigated elements

H																	He
Li	Be											B	C	N	O	F	Ne
Na	Mg											Al	Si	P	S	Cl	Ar
K	Ca	Sc	Ti	V	Cr	Mn	Fe	Co	Ni	Cu	Zn	Ga	Ge	As	Se	Br	Kr
Rb	Sr	Y	Zr	Nb	Mo	Tc	Ru	Rh	Pd	Ag	Cd	In	Sn	Sb	Te	I	Xe
Cs	Ba	La-Lu	Hf	Ta	W	Re	Os	Ir	Pt	Au	Hg	Tl	Pb	Bi	Po	At	Rn
Fr	Ra	Ac-Lr	Rf/Ku	Ha/Ns													

La	Ce	Pr	Nd	Pm	Sm	Eu	Gd	Tb	Dy	Ho	Er	Tm	Yb	Lu
Ac	Th	Pa	U	Np	Pu	Am	Cm	Bk	Cf	Es	Fm	Md	No	Lr

analysed by ICP-AES after acid microwave digestion of freeze dried solid phase samples

data sets are stored at the geological and environmental data network Pangaea (http://www.pangaea.de)

Groups of elements in the solid phase of gravity core GeoB 1711-4, upwelling region off Namibia

H																	He
Li	Be											B	C	N	O	F	Ne
Na	Mg											Al	Si	P	S	Cl	Ar
K	Ca	Sc	Ti	V	Cr	Mn	Fe	Co	Ni	Cu	Zn	Ga	Ge	As	Se	Br	Kr
Rb	Sr	Y	Zr	Nb	Mo	Tc	Ru	Rh	Pd	Ag	Cd	In	Sn	Sb	Te	I	Xe
Cs	Ba	La-Lu	Hf	Ta	W	Re	Os	Ir	Pt	Au	Hg	Tl	Pb	Bi	Po	At	Rn
Fr	Ra	Ac-Lr	Rf/Ku	Ha/Ns													

La	Ce	Pr	Nd	Pm	Sm	Eu	Gd	Tb	Dy	Ho	Er	Tm	Yb	Lu
Ac	Th	Pa	U	Np	Pu	Am	Cm	Bk	Cf	Es	Fm	Md	No	Lr

group A | group B | group C

data sets are stored at the geological and environmental data network Pangaea (http://www.pangaea.de)

Groups of elements in the solid phase of gravity core GeoB 4901-8, Niger deep sea fan

H																	He
Li	Be											B	C	N	O	F	Ne
Na	Mg											Al	Si	P	S	Cl	Ar
K	Ca	Sc	Ti	V	Cr	Mn	Fe	Co	Ni	Cu	Zn	Ga	Ge	As	Se	Br	Kr
Rb	Sr	Y	Zr	Nb	Mo	Tc	Ru	Rh	Pd	Ag	Cd	In	Sn	Sb	Te	I	Xe
Cs	Ba	La-Lu	Hf	Ta	W	Re	Os	Ir	Pt	Au	Hg	Tl	Pb	Bi	Po	At	Rn
Fr	Ra	Ac-Lr	Rf/Ku	Ha/Ns													

La	Ce	Pr	Nd	Pm	Sm	Eu	Gd	Tb	Dy	Ho	Er	Tm	Yb	Lu
Ac	Th	Pa	U	Np	Pu	Am	Cm	Bk	Cf	Es	Fm	Md	No	Lr

group A | group B | group C

data sets are stored at the geological and environmental data network Pangaea (http://www.pangaea.de)

Groups of elements in the solid phase of gravity core GeoB 3718-9, upwelling region off Namibia

H																	He
Li	Be											B	C	N	O	F	Ne
Na	Mg											Al	Si	P	S	Cl	Ar
K	Ca	Sc	Ti	V	Cr	Mn	Fe	Co	Ni	Cu	Zn	Ga	Ge	As	Se	Br	Kr
Rb	Sr	Y	Zr	Nb	Mo	Tc	Ru	Rh	Pd	Ag	Cd	In	Sn	Sb	Te	I	Xe
Cs	Ba	La-Lu	Hf	Ta	W	Re	Os	Ir	Pt	Au	Hg	Tl	Pb	Bi	Po	At	Rn
Fr	Ra	Ac-Lr	Rf/Ku	Ha/Ns													

La	Ce	Pr	Nd	Pm	Sm	Eu	Gd	Tb	Dy	Ho	Er	Tm	Yb	Lu
Ac	Th	Pa	U	Np	Pu	Am	Cm	Bk	Cf	Es	Fm	Md	No	Lr

group A | group B | group C

data sets are stored at the geological and environmental data network Pangaea (http://www.pangaea.de)

References

Adam P., Schmid J. C., Mycke B., Strazielle C., Connan J., Huc A., Riva A., and Albrecht P. (1993) Structural investigation of nonpolar sulphur cross-linked macromolecules in petroleum. *Geochim. Cosmochim. Acta* **57**, 3395 - 3419.

Adam P., Schneckenburger P., Schaeffer P., and Albrecht P. (2000) Clues to early diagenetic sulfurization processes from mild chemical cleavage of labile sulfur-rich geomacromolecules. *Geochim. Cosmochim. Acta* **64**(20), 3485 - 3503.

Adegbie A. T., Schneider R. R., Moos C., Zabel M., Röhl U., and Wefer G. (subm.) Late Quaternary paleoenvironmental conditions over western central Africa: evidence from Niger fan sediments. *Mar. Geol.*

Adler M., Hensen C., Kasten S., and Schulz H. D. (2000) Computer simulation of deep sulfate reduction in sediments of the Amazon Fan. *Int J Earth Sci (Geologische Rundschau)* **88**, 641 - 654.

Adler M., Hensen C., Wenzhöfer F., Pfeifer K., and Schulz H. D. (2001) Modeling of subsurface calcite dissolution by oxic respiration in supralysoclinal deep-sea sediments. *Mar. Geol.* **177**, 167 - 189.

Bender M. L. and Heggie D. T. (1984) Fate of organic carbon reaching the deep-sea floor: a status report. *Geochim. Cosmochim. Acta* **48**, 977 - 986.

Berelson W. M., Hammond D. E., and Johnson K. S. (1987) Benthic fluxes and the cycling of biogenic silica and carbon in two southern California borderland basins. *Geochim. Cosmochim. Acta* **51**, 1345 - 1363.

Berger W. H., Smetacek V. S., and Wefer G. (1989) Ocean productivity and paleoproductivity - An overview. In *Productivity of the Ocean: Present and Past* (ed. W. H. Berger, V. S. Smetacek, and G. Wefer). Springer, Berlin, Heidelberg, New York, pp. 1 - 34.

Berner R. A. (1969) Migration of iron and sulfur within anaerobic sediments during early diagenesis. *Amer. J. Sci.* **267**, 19 - 42.

Berner R. A. (1980) *Early diagenesis: A theoretical approach.* Princeton University Press, Princeton, N.J., 241 pp.

Berner R. A. (1981) A new geochemical classification of sedimentary environment. *J. Sediment. Petrol.* **51**, 359 - 365.

Berner R. A. (1984) Sedimentary pyrite formation: An update. *Geochim. Cosmochim. Acta* **48**, 605 - 615.

Bishop J. K. B. (1988) The barite-opal-organic carbon association in oceanic particulate matter. *Nature* **332**, 341 - 343.

Boetius A., Ravenschlag K., Schubert C. J., Rickert D., Widdel F., Gieseke A., Amann R., Jørgensen B. B., Witte U., and Pfannkuche O. (2000) A marine microbial consortium apparently mediating anaerobic oxidation of methane. *Nature* **407**, 623 - 626.

Bohrmann G., Greinert J., Suess E., and Torres M. (1998) Authigenic carbonates from the Cascadia subduction zone and their relation to gas hydrate stability. *Geology* **26**, 647 - 650.

Bonatti E., Fisher D. E., Joensuu O., and Rydell H. S. (1971) Postdepositional mobility of some transition elements, phosphorus, uranium and thorium in deep sea sediments. *Geochim. Cosmochim. Acta* **35**, 189 - 201.

Borowski W. S., Paull C. K., and Ussler I. W. (1999) Global and local variations of interstitial sulfate gradients in deep-water, continental margin sediments: Sensitivity to underlying methane and gas hydrate. *Mar. Geol.* **159**, 131 - 154.

Boudreau, B. P. (1997) Diagenetic models and their implementation: modelling transport and reactions in aquatic sediments. Springer, Berlin, Heidelberg, New York, 414 pp.

Brewer P. G. (1975) Minor Elements in Sea Water. In *Chemical Oceanography*, Vol. 1 (ed. J. P. Riley and G. Skirrow). Academic Press, London, pp. 415-496.

Brüchert V., Pérez M. E., and Lange C. B. (2000) Coupled primary production, benthic foraminiferal assemblage, and sufur diagenesis in organic-rich sediments of the Benguela upwelling system. *Mar. Geol.* **163**, 27 - 40.

Bruland K. W. (1983) Trace Elements in Sea-water. In *Chemical Oceanography*, Vol. 8 (ed. J. P. Riley and G. Skirrow). Academic Press, London, pp. 157-220.

Brumsack H. J. (1986) The inorganic geochemistry of Cretaceous black shales (DSDP Leg 41) in comparison to modern upwelling sediments from the Gulf of California. In *North Atlantic Palaeoceanography*, Vol. 21 (ed. C. P. Summerhayes and N. J. Shackleton). Blackwell Scientific Publications, Oxford, pp. 447 - 462.

Calvert S. E. and Pedersen T. F. (1993) Geochemistry of recent oxic and anoxic marine sediments: Implications for the geological record. *Mar. Geol.* **113**, 67 - 88.

Calvert S. E. and Price N. B. (1972) Diffusion and reaction profiles of dissolved manganese in the porewaters of marine sediments. *Earth Planet. Sci. Lett.* **16**, 245 - 249.

Canfield D. E. (1989) Reactive iron in marine sediments. *Geochim. Cosmochim. Acta* **53**, 619 - 632.

Chester R. (1999) *Marine Geochemistry*. 2nd Ed., Blackwell Science, Oxford, 506 p.

Colley S., Thomson J., Wilson T. R. S., and Higgs N. C. (1984) Post-depositional migration of elements during diagenesis in brown clay and turbidite sequences in the North East Atlantic. *Geochim. Cosmochim. Acta* **48**, 1223 - 1235.

Collier R. and Edmond J. (1984) The trace element geochemistry of marine biogenic particulate matter. *Prog. Oceanog.* **13**, 113 - 199.

Collier R. W. and Edmond J. M. (1983) Plankton composition and trace element fluxes from the surface ocean. In *Trace metals in sea water* (ed. C. S. Wong, B. Boyle, K. W. Bruland, J. D. Burton, and E. D. Goldberg). Plenum, New York, pp. 789 - 809.

Daesslé L. W., Cronan D. S., Marchig V., and Wiedicke M. (2000) Hydrothermal sedimentation adjacent to the propagating Valu Fa Ridge, Lau Basin, SW Pacific. *Mar. Geol.* **162**, 479 - 500.

De Graaf W., Sinninghe Damsté J. S., and de Leeuw J. W. (1992) Laboratory simulation of natural sulphurisation I. Formation of monomeric and oligomeric isoprenoid

polysulphides by low-temperature reactions of inorganic polysulphides with phythol and phytadiens. *Geochim. Cosmochim. Acta* **56**, 4321 - 4328.

De Lange G. J., van Os B., Pruysers A., Middelburg J. J., Castradori D., van Santvoort P., Müller P. J., Eggenkamp H., and Prahl F. G. (1994) Possible early diagenetic alterations of paleo proxies. In *Carbon cycling in the glacial ocean: Constraints on the ocean's role in global change* (ed. R. Zahn, F. F. Pedersen, M. A. Kaminski, and L. Labeyrie). NATO ASI Series, Vol. I 17, Springer, Berlin, Heidelberg, New York, pp. 225 - 258.

Dehairs F., Chesselet R., and Jedwab J. (1980) Discrete suspended particles of barite and the barium cycle in the open ocean. *Earth Planet. Sci. Lett.* **49**, 528 - 550.

Dickens G. R. (2001) Sulfate profiles and barium fronts in sediment on the Blake Ridge: Present and past methane fluxes through a large gas hydrate reservoir. *Geochim. Cosmochim. Acta* **65**(4), 529 - 543.

Donner B. and Giese M. (1992) Stratigraphie und Smear-Slide-Analysen. In *Bericht und erste Ergebnisse über die Fahrt M20/2*, Vol. No. 25 (ed. H. D. Schulz and cruise participants), pp. 51 - 80. Fachbereich Geowissenschaften, Universität Bremen.

Dymond J. and Collier R. (1996) Particulate barium fluxes and their relationships to biological productivity. *Deep-Sea Research II* **43**(4 - 6), 1283 - 1308.

Dymond J., Suess E., and Lyle M. (1992) Barium in deep-sea sediment: A geochemical proxy for paleoproductivity. *Paleoceanogr.* **12**(2), 163-181.

Eglinton T. I., Irvine J. E., Vairavamurthy A., Zhou W., and Manowitz B. (1994) Formation and diagenesis of macromolecular organic sulfur in Peru margin sediments. *Org. Geochem.* **22**(781 - 799).

Elderfield H., McCaffrey R. J., Luedtke N., Bender M., and Truesdale V. W. (1981) Chemical diagenesis in Narragansett Bay sediments. *Amer. J. Sci.* **281**, 1021 - 1055.

Embley R. W. and Morley J. J. (1980) Quaternary sedimentation and paleoenvironmental studies off Namibia (South-West Africa). *Mar. Geol.* **36**, 183 - 204.

Ferdelmann T. G., Fossing H., and Neumann K. (1999) Sulfate reduction in surface sediments of the southeast Atlantic continental margin between 15°38'S (Angola and Namibia). *Limnol. Oceanogr.* **44**, 650 - 661.

Finney B. P. and Lyle M. W. (1988) Sedimentation at MANOP site H (eastern equatorial Pacific) over the past 400.000 Years: Climatically induced redox variations and their effects on transition metal cycling. *Paleoceanogr.* **3**(2), 169 - 189.

Flood R. D., Piper D. J. W., Klaus A. and cruise participants (1995) Proc. ODP, Init. Repts. 155, College Station, TX (Ocean Drilling Program).

Fossing H., Jørgensen B. B. (1989) Measurement of bacterial sulfate reduction in sediments: Evaluation of a single-step chromium reduction method. *Biogeochem.* **8**, 205 - 222.

Fossing H., Ferdelman, T. F., and Berg P. (2000) Sulfate reduction and methane oxidation in continental margin sediments influenced by irrigation (South-East Atlantic off Namibia). *Geochim. Cosmochim. Acta* **64**(5), 897 - 910.

Francois R. (1988) A study on the regulation of the concentrations of some trace metals (Rb, Sr, Zn, Pb, Cu, V, Cr, Ni, Mn and Mo) in Saanich Inlet sediments, British Columbia, Canada. *Mar. Geol.* **83**, 285 - 308.

Francois R., Honjo S., Manganini S. J., and Ravizza G. E. (1995) Biogenic barium fluxes to the deep sea: Implications for paleoproductivity reconstruction. *Global Biogeochemical Cycles* **9**(2), 289 - 303.

Freudenthal T., Kasten S., and Meggers H. (subm.) Glacial trade wind intensity controlled by latitudinal sea surface temperature gradients. *Geology*.

Freudenthal T., Meggers H., Henderiks J., Kuhlmann H., Moreno A., and Wefer G. (in press) Upwelling intensity and filament activity off Morocco during the last 250,000 years. *Deep-Sea Research II* .

Froelich P. N., Klinkhammer G. P., Bender M. L., Luedtke N. A., Heath G. R., Cullen D., Dauphin P., Hammond D., Hartman B., and Maynard V. (1979) Early oxidation of organic matter in pelagic sediments of the eastern equatorial Atlantic: Suboxic diagenesis. *Geochim. Cosmochim. Acta* **43**, 1075 - 1090.

Funk J. A., von Dobeneck T., Wagner T., and Kasten S. (subm.) Late Quaternary sedimentation and early diagenesis in the equatorial Atlantic Ocean: Patterns, trends and processes deduced from rock magnetic and geochemical records. In *The South Atlantic in the Late Quaternary: Reconstruction of Mass Budget and Current Systems* (eds. G. Wefer, S. Mulitza, and V. Ratmeyer). Springer, Berlin, Heidelberg, New York.

Fütterer D. K. (2000) The solid phase of marine sediments. In *Marine Geochemistry* (eds. H. D. Schulz and M. Zabel), pp. 1 - 25. Springer.

Gerringa L. J. A. (1990) Aerobic degradation of organic matter and the mobility of Cu, Cd, Ni, Pb, Zn, Fe, and Mn in marine sediment slurries. *Mar. Chem.* **29**, 355 - 374.

Gingele F. (1992) *Zur klimaabhängigen Bildung biogener und terrigener Sedimente und ihrer Veränderungen durch die Frühdiagenese im zentralen und östlichen Südatlantik.* Berichte aus dem Fachbereich Geowissenschaften der Universität Bremen, No. 26

Gingele F. X. and Dahmke A. (1994) Discrete barite particles and barium as tracers of paleoproductivity in South Atlantic sediments. *Paleoceanogr.* **9**(1), 151 - 168.

Gingele F. X., Zabel M., Kasten S., Bonn W. J., and Nürnberg C. C. (1999) Biogenic barium as a proxy for paleoproductivity: methods and limitations of application. In *Use of proxies in Paleoceanography: Examples from the South Atlantic* (eds. G. Fischer and G. Wefer). Springer, Berlin, Heidelberg, New York, pp. 345 - 364.

Gladney E. S. and Roelandts I. (1988) 1987 compilation of elemental concentration data for USGS BHVO-1, MAG-1, QLO-1, RGM-1, Scc-1, SDC-1, SGR-1 and STM-1. *Geostand. Newsl.* **12**, 253 - 362.

Glasby G. P. (2000) Manganese: predominant role of nodules and crusts. In *Marine Geochemistry* (ed. H. D. Schulz and M. Zabel), Springer, Berlin, Heidelberg, New York, pp. 335 - 372.

Gobeil C., Silverberg N., Sundby B., and Cossa D. (1987) Cadmium diagenesis in Laurentian Trough sediments. *Geochim. Cosmochim. Acta* **51**, 589 - 596.

Goldberg E. D. (1954) Marine geochemistry I - Chemical scavengers of the sea. *Jouranl of Geology* **62**, 249 - 265.

Goldberg E. D. and Arrhenius G. O. S. (1958) Chemistry of Pacific pelagic sediments. *Geochim. Cosmochim. Acta* **13**, 153 - 212.

Graybeal A. L. and Heath G. R. (1984) Remobilization of transition metals in surficial pelagic sediments from the eastern Pacific. *Geochim. Cosmochim. Acta* **48**, 965 - 975.

Haese R. R., Wallmann K., Dahmke A., Kretzmann U., Müller P. J., and Schulz H. D. (1997) Iron species determination to investigate early diagenetic reactivity in marine sediments. *Geochim. Cosmochim. Acta* **61**(1), 63 - 72.

Hartgers W. A., Lopez J. F., Sinninghe Damsté J. S., Reiss C., Maxwell J. R., and Grimalt J. O. (1997) Sulfur-binding in recent environments: II. Speciation of sulfur and iron and implications for the occurrence of organo-sulfur compounds. *Geochim. Cosmochim. Acta* **61**, 4769 - 4788.

Heggie D., Kahn D., and Fischer K. (1986) Trace metals in metalliferous sediments, MANOP site M: interfacial pore water profiles. *Earth Planet. Sci. Lett.* **80**, 106 - 116.

Hensen C., Pfeifer K., Wenzhöfer F., Volbers A., Schulz S., Romero O., and Seiter K. (subm.-a) Fluxes at the benthic boundary layer - A global view from the South Atlantic. In *The South Atlantic in the Late Quaternary: Reconstruction of Mass Budget and Current Systems* (ed. G. Wefer, S. Mulitza, and V. Ratmeyer). Springer, Berlin, Heidelberg, New York.

Hensen C., Zabel M., Pfeifer K., Schwenk T., Kasten S., and Schulz H. D. (subm.-b) Control of anaerobic methane oxidation by sedimentary events - reconstruction of time scales and quantitative importance. *Geochim. Cosmochim. Acta.*

Hensen C., Zabel M., and Schulz H. D. (2000) A comparison of benthic nutrient fluxes from deep-sea sediments off Namibia and Argentina. *Deep-Sea Research II* **47**, 2029 - 2050.

Herzig P. M. and Hannington M. D. (2000) Input from the Deep: Hot Vents and Cold Seeps. In *Marine Geochemistry* (ed. H. D. Schulz and M. Zabel), pp. 397 - 416. Springer, Berlin, Heidelberg, New York.

Heuer V., Kasten S., Hensen C., and Schulz H. D. (subm.-a) Early diagenesis at the sulphate/methane transition: (re)distribution of barium and other trace elements in sediments on the continental slope off Namibia, Southeast Atlantic. *Marine Geology*

Heuer V., Kasten S., and Schulz H. D. (subm.-b) Does sulphurization create an early diagenetic link between trace elements and organic matter? - Evidence from the upwelling region off Namibia, Southeast Atlantic. *Geochim. Cosmochim. Acta.*

Heuer V., Kasten S., and Schulz H. D. (subm.-c) Trace elements reflecting primary production, degradation and preservation of organic matter in sediments from the Niger deep sea fan, equatorial Atlantic. *Earth Planet. Sci. Lett.*.

Higgs N. C., Thomson J., Wilson T. R. S., and Croudace I. W. (1994) Modification and complete removal of eastern Mediterranean sapropels by postdepositional oxidation. *Geology* **22**, 423 - 426.

Huerta-Diaz M. and Morse J. W. (1990) A quantitative method for determination of trace metal concentrations in sedimentary pyrite. *Mar. Chem.* **29**, 119 - 144.

Huerta-Diaz M. A. and Morse J. W. (1992) Pyritization of trace metals in anoxic marine sediments. *Geochim. Cosmochim. Acta* **56**, 2681-2702.

Iversen N. and Jørgensen B. B. (1985) Anaerobic methane oxidation rates at the sulfate-methane transition in marine sediments from Kattegat and Skagerrak (Denmark). *Limnol. Oceanogr.* **30**, 944 - 955.

Jørgensen B. B. (1982) Mineralization of organic matter in the sea bed - The role of sulphate reduction. *Nature* **296**, 643 - 645.

Jørgensen B. B. (2000) Bacteria and Marine Biogeochemistry. In *Marine Geochemistry* (ed. H. D. Schulz and M. Zabel). Springer, Berlin, Heidelberg, New York, pp. 173 - 207.

Jørgensen B. B., Weber A., and Zopfi J. (2001) Sulfate reduction and anaerobic methane oxidation in Black Sea sediments. *Deep-Sea Research I* **48**, 2097 - 2120.

Jung M., Ilmberger J., Mangini A., and Emeis K.-C. (1997) Why some Mediterranean sapropels survived burn-down (and others did not). *Mar. Geol.* **141**, 51 - 60.

Kasten S., Freudenthal T., Gingele F. X., von Dobeneck T., and Schulz H. D. (1998) Simultaneous formation of iron-rich layers at different redox boundaries in sediments of the Amazon Deep-Sea Fan. *Geochim. Cosmochim. Acta* **62**(13), 2253 - 2264.

Kasten S., Haese R. R., Zabel M., Rühlemann C., and Schulz H. D. (2001) Barium peaks at glacial terminations in sediments of the equatorial Atlantic Ocean - relicts of deglacial productivity pulses? *Chem. Geol.* **175**, 635 - 651.

Kasten S. and Jørgensen B. B. (2000) Sulfate reduction in marine sediments. In *Marine Geochemistry* (ed. H. D. Schulz and M. Zabel). Springer-Verlag. Berlin, Heidelberg, New York, pp. 263 - 282.

Kasten S., Zabel M., Heuer V., and Hensen C. (subm.) Nonsteady-state diagenesis and its documentation and preservation in marine sediment/pore water systems. In *The South Atlantic in the Late Quaternary: Reconstruction of Mass Budget and Current Systems* (ed. G. Wefer, S. Mulitza, and V. Ratmeyer). Springer, Berlin, Heidelberg, New York.

Kirst G. J., Schneider R. R., Müller P. J., von Storch I., and Wefer G. (1999) Late Quaternary temperature variability in the Benguela current system derived from alkenones. *Quaternary Research* **52**, 92 - 103.

Klinkhammer G., Heggie D. T., and Graham D. W. (1982) Metal diagenesis in oxic marine sediments. *Earth Planet. Sci. Lett.* **61**, 211 - 219.

Klinkhammer G. P. (1980) Early diagenesis in sediments from the eastern equatorial Pacific, II. Pore water metal results. *Earth Planet. Sci. Lett.* **49**, 81 - 101.

Kohnen M. E. T., Sinninghe Damsté J. S., Kock-van Dalen A. C., and de Leeuw J. W. (1991) Di- or polysulphide-bound biomarkers in sulphur-rich geomacromolecules as revealed by selective chemolysis. *Geochim. Cosmochim. Acta* **55**, 1375 - 1394.

Kumar N., Anderson R. F., and Biscaye P. E. (1996) Remineralization of particulate authigenic trace metals in the Middle Atlantic Bight: Implications for proxies of export production. *Geochim. Cosmochim. Acta* **60**(18), 3383 - 3397.

Li A.-H. (1981) Ultimate removal mechanism of elements from the ocean. *Geochim. Cosmochim. Acta* **45**, 1659 - 1664.

Li Y.-H. and Gregory S. (1974) Diffusion of ions in sea water and in deep-sea sediments. *Geochim. Cosmochim. Acta* **38**, 703 - 714.

Lisitzin A. P. (1996) *Oceanic sedimentation: lithology and geochemistry*. American Geophysical Union, Washington, D.C., 400 p.

Little M. G., Schneider R. R., Kroon D., Price B., Bickert T., and Wefer G. (1997) Rapid palaeoceanographic changes in the Benguela Upwelling System for the last 160,000 years as indicated by abundances of planktonic foraminifera. *Palaeogeography, Palaeoclimatology, Palaeoecology* **130**, 135 - 161.

Lückge A., Ercegovac M., Strauss H., and Littke R. (1999) Early diagenetic alteration of organic matter by sulfate reduction in Quaternary sediments from the northeastern Arabian Sea. *Mar. Geol.* **158**, 1 - 13.

Lynn D. C. and Bonatti E. (1965) Mobility of manganese in diagenesis of deep-sea sediments. *Mar. Geol.* **3**, 457 - 474.

Mangini A., Jung M., and Laukenmann S. (2001) What do we learn from peaks of uranium and of manganese in deep sea sediments? *Mar. Geol.*(177), 63 - 78.

Martin J. and Knauer G. A. (1973) The elemental composition of plankton. *Geochim. Cosmochim. Acta* **37**, 1639 - 1653.

Matthewson A. P., Shimmield G. B., Kroon D., and Fallik A. E. (1995) A 300 kyr high-resolution aridity record of the north African continent. *Paleoceanogr.* **10**, 677 - 692.

McGeary D. F. R. and Damuth J. E. (1973) Postglacial iron-rich crusts in hemipelagic deep-sea sediments. *Geol. Soc. Amer. Bull.* **84**, 1201 - 1212.

Mero J. L. (1965) *The Mineral Resources of the Sea*. Elsevier, Amsterdam, 312 p.

Mienert J, Posewang J, Baumann M (1998) Gas hydrates along the northeastern Atlantic margin: possible hydrate-bound margin instabilities and possible release of methane. In: Henriet, J.P. & J. Mienert (eds.) Gas Hydrates: Relevance to World Margin Stability and Climate Change. Geol. Soc., London, Spec. Publ., 137, pp. 275-291.

Moreno A., Nave S., Kuhlmann H., Canals M., Targarona J., Freudenthal T., and Abrantes F. (2002) Productivity response in the North Canary Basin to climate changes during the last 250,000 yr: a multi-proxy approach. *Earth Planet. Sci. Lett.* **196**, 147 - 159.

Morford J. L. and Emerson S. (1999) The geochemistry of redox sensitive trace metals in sediments. *Geochim. Cosmochim. Acta* **63**(11/12), 1735 - 1750.

Morse J. W. (1994) Interactions of trace metals with authigenic sulfide minerals: implications for their bioavailability. *Mar. Chem.* **46**, 1-6.

Morse J. W. and Arakaki T. (1993) Adsorption and coprecipitation of divalent metals with mackinawite (FeS). *Geochim. Cosmochim. Acta* **57**, 3635 - 3640.

Mossmann J. R., Aplin A. C., Curtis C. D., and Coleman M. L. (1991) Geochemistry of inorganic and organic sulphur in organic-rich sediments from the Peru Margin. *Geochim. Cosmochim. Acta* **55**, 3581 - 3595.

Müller P. J., Erlenkeuser H., and von Grafenstein R. (1983) Glacial-interglacial cycles in ocean productivity inferred from organic carbon contents in eastern North Atlantic sediment cores. In *Coastal upwelling: It s sedimentary record* (ed. J. Thiede and E. Suess). Plenum Press, New York, pp. 365 - 398.

Müller P. J. and Suess E. (1979) Productivity, sedimentation rate, and sedimentary organic matter in the oceans: I. Organic carbon preservation. *Deep-Sea Res.* **26A**, 1347 - 1362.

Niewöhner C., Hensen C., Kasten S., Zabel M., and Schulz H. D. (1998) Deep sulfate reduction completely mediated by anaerobic methane oxidation in sediments of the upwelling area off Namibia. *Geochim. Cosmochim. Acta* **62**(3), 455-464.

Norris R. D. and Röhl U. (1999) Carbon cycling and chronology of climate warming during Palaeocene/Eocene transition. *Nature* **401**, 775 - 778.

Passier H. F., Dekkers M. J., and de Lange G. J. (1998) Sediment chemistry and magnetic properties in an anormalously reducing core from the eastern Mediterranean Sea. *Chem. Geol.* **152**, 287 - 306.

Passier H. F., Middelburg J. J., de Lange G. J., and Böttcher M. E. (1999) Modes of sapropel formation in the eastern Mediterranean: some constraints based on pyrite properties. *Mar. Geol.* **153**, 199 - 219.

Passier H. F., Middelburg J. J., van Os B. J. H., and de Lange G. J. (1996) Diagenetic pyritisation under eastern Mediterranean sapropels caused by downward sulphide diffusion. *Geochim. Cosmochim. Acta* **60**(5), 751 - 763.

Pedersen T. F. and Calvert S. E. (1990) Anoxia versus productivity: What controls the formation of organic-carbon-rich sediments and sedimentary rocks? *The American Association of Petroleum Geologists Bulletin* **74**, 454 - 466.

Pfeifer K., Hensen C., M. A., Wenzhöfer F., Weber B., and Schulz H. D. (in press) Modeling of subsurface calcite dissolution - including the respiration and re-oxidation processes of marine sediments in the region of equatorial upwelling off Gabon. *Geochim. Cosmochim. Acta.*

Pfeifer K., Kasten S., Hensen C., and Schulz H. D. (2001) Reconstruction of primary productivity from the barium contents in surface sediments of the South Atlantic Ocean. *Mar. Geol.* **177**, 13 - 24.

Postma D. and Jakobsen R. (1996) Redox zonation: Equilibrium constraints on the Fe(III)/SO4-reduction interface. *Geochim. Cosmochim. Acta* **60**, 3169 - 3175.

Pruysers P. A., de Lange G. J., and Middelburg J. J. (1991) Geochemistry of eastern Mediterranean sediments: Primary sediment composition and diagenetic alterations. *Mar. Geol.* **100**, 137 - 154.

Pruysers P. A., de Lange G. J., Middelburg J. J., and Hydes D. J. (1993) The diagenetic formation of metal-rich layers in sapropel-containing sediments in the eastern Mediterranean. *Geochim. Cosmochim. Acta* **57**, 527 - 536.

Reimers C. E. and Smith K. L. (1986) Reconciling measured and predicted fluxes of oxygen across the deep sea sediment-water interface. *Limnol. Oceanogr.* **31**, 305 - 318.

Rothwell R. G., Thomson J., and Kähler G. (1998) Low-sea-level emplacement of a very large Late Pleistocene 'megaturbidite' in the western Mediterranean Sea. *Nature* **392**, 377-380.

Rühlemann C., Müller P. J., and Schneider R. R. (1999) Organic carbon and carbonate as paleoproductivity proxies: Examples from high and low productivity areas of the tropical Atlantic. In *Use of proxies in Paleoceanography: Examples from the South Atlantic* (ed. G. Fischer and G. Wefer). Springer, Berlin, Heidelberg, New York, pp. 315 - 344.

Rullkötter J. (2000) Organic Matter: The Driving Force for Early Diagenesis. In *Marine Geochemistry* (ed. H. D. Schulz and M. Zabel). Springer, Berlin, Heidelberg, New York, pp. 129 - 172.

Sawlan J. J. and Murray J. W. (1983) Trace metal remobilization in the interstitial waters of red clay and hemipelagic marine sediments. *Earth and Planatery Science Letters* **64**, 213 - 230.

Schinzel U., Dahmke A., and Schulz H. D. (1993) Reaktionen von Eisen(III)-Oxidhydraten während der Frühdiagenese in marinen Sedimenten: Experimentelle Untersuchungen. *Zeitschrift der deutschen geologischen Gesellschaft* **144**, 224 - 247.

Schippers A. and Jørgensen B. B. (2002) Biogeochemsitry of pyrite and iron sulfide oxidation in marine sediments. *Geochim. Cosmochim. Acta* **66**(1), 58 - 92.

Schouten S., de Graaf W., Sinninghe Damsté J. S., van Driel G. B., and de Leeuw J. W. (1994a) Laboratory simulation of natural sulphurization. II. Reaction of multifunctionalized lipids with inorganic polysulphides at low temperatures. *Advances in Geochemistry 1993 (eds. G. Telnæs, G. van Graas, K. Øygard) Organic Geochemistry* **22**, 825 - 834.

Schouten S., van Driel G. B., Sinninghe Damsté J. S., and de Leeuw J. W. (1994b) Natural sulphurization of ketones and aldehydes: a key reaction in the formation of organic sulphur compounds. *Geochim. Cosmochim. Acta* **58**, 511 - 5116.

Schubert C. J., Nürnberg D., Scheele N., Pauer F., and Kriews M. (1997) 13C isotope depletion in ikaite crystals: evidence for methane release from the Siberian shelves? *Geo-Mar Lett* **17**, 169 - 174.

Schulz H. D. (2000) Quantification of early diagenesis: dissolved constituents in marine pore water. In *Marine Geochemistry* (ed. H. D. Schulz and M. Zabel). Springer, Berlin, Heidelberg, New York, pp. 85 - 128.

Schulz H. D. and cruise participants. (1992) *Bericht und erste Ergebnisse über die METEOR-Fahrt M20/2, Abidjan-Dakar, 27.12.1991 - 3.2.1992.* Fachbereich Geowissenschaften, Universität Bremen.

Schulz HD, and cruise participants (1995) *Geo Bremen South Atlantic 1994, Cruise No.29, 17 June – 5 September 1994.* Meteor-Berichte, Universität Hamburg, 95-2, 323 pp

Schulz H. D. and cruise participants. (1996) *Report and Preliminary Results of Meteor Cruise M 34/2 Walvis Bay - Walvis Bay, 29.01.1996 - 18.02.1996.* Fachbereich Geowissenschaften, Universität Bremen.

Schulz H. D. and cruise participants. (1998) *Report and Preliminary Results of Meteor Cruise M 41/1 Malaga - Libreville, 13.2.-15.3. 1998.* Fachbereich Geowissenschaften, Universität Bremen.

Schulz H. D., Dahmke A., Schinzel U., Wallmann K., and Zabel M. (1994) Early diagenetic processes, fluxes, and reaction rates in sediments of the South Atlantic. *Geochim. Cosmochim. Acta* **58**(9), 2041 - 2060.

Schwarz B., Mangini A., and Segl M. (1996) Geochemistry of a piston core from Ontong Java Plateau (western equatorial Pacific): evidence for sediment redistribution and changes in paleoproductivity. *Geologische Rundschau* **85**, 536 - 545.

Shaw T. J., Gieskes J. M., and Jahnke R. A. (1990) Early diagenesis in differing depositional environments: The response of transition metals in pore water. *Geochim. Cosmochim. Acta* **54**, 1233 - 1246.

Sinninghe Damsté J. S. and de Leeuw J. W. (1990) Analysis, structure and geochemical significance of organically-bound sulphur in the geosphere: State of the art and future research. *Advances in Organic Geochemistry 1989 (eds. B. Durand, F. Behar) Organic Geochemistry* **16**, 1077 - 1101.

Sinninghe Damsté J. S., Kok M. D., Köster J., and Schouten S. (1998) Sulfurized carbohydrates: an important sedimentary sink for organic carbon? *Earth Planet. Sci. Lett.* **164**, 7 - 13.

Sinninghe Damsté J. S., Rijpstra W. I., de Leeuw J. W., and Schenck P. A. (1988) Origin of organic sulphur compounds and sulphur-containing high molecular weight substances in sediments and immature crude oils. *Advances in Organic Geochemistry 1987 (eds. L. Mattavelli and L. Novelli) Organic Geochemistry* **13**, 593 - 606.

Sinninghe Damsté J. S., Rijystra W. I. C., de Leeuw J. W., and Schenck P. A. (1989) Quenching of labile functionalized lipids by inorganic sulphur species: evidence for the formation of sedimentary organic sulphur compounds at the early stages of diagenesis. *Geochim. Cosmochim. Acta* **53**, 1443 - 1455.

Sternbeck J., Sohlenius G., and Hallberg R. O. (2000) Sedimentary trace elements as proxies to depositional changes induced by a holocene fresh-brackish water transition. *Aquatic Geochemistry* **6**, 325 - 345.

Stumm W. and Morgan J. J. (1996) *Aquatic Chemistry*. Wiley & Sons, New York, 1022 p.

Tarduno J. A. (1994) Temporal trends of magnetic dissolution in the pelagic realm: Gauging paleoproductivity? *Earth Planet. Sci. Lett.* **123**, 39-48.

Tarduno J. A. and Wilkison S. L. (1996) Non-steady state magnetic mineral reduction, chemical lock-in, and delayed remanence acquisition in pelagic sediments. *Earth Planet. Sci. Lett.* **144**, 315 - 326.

Thamdrup B., Fossing H., and Jørgensen B. B. (1994) Manganese, iron, and sulfur cycling in a coastal marine sediment, Aarhus Bay, Denmark. *Geochim. Cosmochim. Acta* **58**(23), 5115 - 5129.

Thomson J., Carpenter M. S. N., Colley S., Wilson T. R. S., Elderfield H., and Kennedy H. (1984a) Metal accumulation rates in northwest Atlantic pelagic sediments. *Geochim. Cosmochim. Acta* **48**, 1935 - 1948.

Thomson J., Higgs N. C., and Colley S. (1996) Diagenetic redistributions of redox-sensitive elements in northeast Atlantic glacial/interglacial transition sediments. *Earth Planet. Sci. Lett.* **139**, 365 - 377.

Thomson J., Higgs N. C., Croudace I. W., Colley S., and Hydes D. J. (1993) Redox zonation of elements at an oxic / post-oxic boundary in deep-sea sediments. *Geochim. Cosmochim. Acta* **57**, 579 - 595.

Thomson J., Higgs N. C., Wilson T. R. S., Croudace I. W., de Lange G. J., and van Santvoort P. J. M. (1995) Redistribution and geochemical behaviour of redox-sensitive elements around S1, the most recent eastern Mediterranean sapropel. *Geochim. Cosmochim. Acta* **59**(17), 3487 - 3501.

Thomson J., Jarvis I., Green D. R. H., and Green D. (1998a) 32. Oxidation fronts in Madeira abyssal plain turbidites: persistence of early diagenetic trace-element enrichments during burial, site 950. In *Proceedings of the Ocean Drilling Program, Scientific Results*, Vol. 157 (ed. P. P. E. Weaver, H.-U. Schmincke, J. V. Firth, and W. Duffield), pp. 559 - 571.

Thomson J., Jarvis I., Green D. R. H., Green D. A., and Clayton T. (1998b) Mobility and immobility of redox-sensitive elements in deep-sea turbidites during shallow burial. *Geochim. Cosmochim. Acta* **62**(4), 543 - 656.

Thomson J., Nixon S., Summerhayes C. P., Rohling E. J., Schönfeld J., Zahn R., Grootes P., Abrantes F., Gaspar L., and Vaqueiro S. (2000) Enhanced productivity on the Iberian margin during glacial/interglacial transitions revealed by barium and diatoms. *Journal of the Geological Society, London* **157**, 667 - 677.

Thomson J., Wallace H. E., Colley S., and Toole J. (1990) Authigenic uranium in Atlantic sediments of the last glacial stage - a diagenetic phenomenon. *Earth Planet. Sci. Lett.* **98**, 222 - 232.

Thomson J., Wilson T. R. S., Culkin F., and Hydes D. J. (1984b) Non-steady state diagenetic record in eastern equatorial Atlantic sediments. *Earth Planet. Sci. Lett.* **71**, 23 - 30.

Torres M. E., Brumsack H. J., Bohrmann G., and Emeis K. C. (1996) Barite fronts in continental margin sediments: A new look at barium remobilization in the zone of sulfate reduction and formation of heavy barites in diagenetic fronts. *Chem. Geol.* **127**, 125 - 139.

Trefry J. H. and Presley B. J. (1982) Manganese fluxes from Mississippi Delta sediments. *Geochim. Cosmochim. Acta* **46**, 1715 - 1726.

Turekian K. K. (1977) The fate of metals in the ocean. *Geochim. Cosmochim. Acta* **41**, 1131 - 1144.

Vairavamurthy M. A., Goldenberg W. S., Ouyang S., and Khalid S. (2000) The interaction of hydrophilic thiols with cadmium: investigation with a simple model, 3-mercaptopropionic acid. *Mar. Chem.* **70**, 181 - 189.

Van Os B. J. H., Middelburg J. J., and de Lange G. J. (1991) Possible diagenetic mobilization of barium in sapropelic sediment from the eastern Mediterranean. *Mar. Geol.* **100**, 125 - 136.

Van Santvoort P. J. M., de Lange G. J., Langereis C. G., Dekkers M. J., and Paterne M. (1997) Geochemical and paleomagnetic evidence for the occurrence of "missing" sapropels in eastern Mediterranean sediments. *Paleoceanogr.* **12**(6), 773 - 786.

Van Santvoort P. J. M., de Lange G. J., Thomson J., Cussen H., Wilson T. R. S., Krom M. D., and Ströhle K. (1996) Active post-depositional oxidation of the most recent sapropel (S1) in sediments of the eastern Mediterranean Sea. *Geochim. Cosmochim. Acta* **60**(21), 4007-4024.

Versteegh G. J. M. and Zonneveld K. A. F. (2002) Use of selective degradation to separate preservation from productivity. *Geology* **30**(7), 615-618.

Volbers A. N. A. and Henrich R. (in press) Present water mass calcium carbonate corrosiveness in the eastern South Atlantic inferred from ultrastructural breakdown of Globigerina bulloides in surface sediments. *Mar. Geol.*

Von Breymann M. T. K., Emeis K. C., and Suess E. (1992) Water depth and diagenetic constraints on the use of barium as a paleoproductivity indicator. In *Upwelling Systems: Evolution since the Early Miocene*, Vol. 64 (ed. C. P. Summerhayes). Geol Soc Spec Publ., London, pp. 273 - 284.

Wakeham S. G. and Lee C. (1993) Production, transport, and alteration of particulate organic matter in the marine water column. In *Organic Geochemistry* (ed. M. H. Engel and S. A. Macko). Plenum Press, New York, pp. 145 - 169.

Wakeham S. G., Sinninghe Damsté J. S., Kohnen M. E. L., and de Leeuw J. W. (1995) Organic sulfur compounds formed during early diagenesis in Black Sea sediments. *Geochim. Cosmochim. Acta* **59**, 521 - 533.

Wallace H. E., Thomson J., Wilson T. R. S., Weaver P. P. E., Higgs N. C., and Hydes D. J. (1988) Active diagenetic formation of metal-rich layers in N. E. Atlantic sediments. *Geochim. Cosmochim. Acta* **52**, 1557 -1 569.

Wedepohl K. H. (1995) The composition of the continental crust. *Geochim. Cosmochim. Acta* **59**(7), 1217 - 1232.

Wefer G., Berger W. H., Bijma J., and Fischer G. (1999) Clues to ocean history: a brief overview of proxies. In *Use of proxies in Paleoceanography: Examples from the South Atlantic* (ed. G. Fischer and G. Wefer). Springer, Berlin, Heidelberg, New York, pp. 1 - 68.

Wefer G. and cruise participants (1997) *Report and preliminary results of Meteor cruise M 37/1, Lisbon – Las Palmas, 04.12.1996 – 23.12.1996.* Berichte, Fachbereich Geowissenschaften, Universität Bremen, **90**, 79 pp.

Wefer G. and Fischer G. (1993) Seasonal patterns of vertical particle flux in equatorial and coastal upwelling areas of the eastern Atlantic. *Deep-Sea Research I* **40**(8), 1613 - 1645.

Werne J. P., Hollander D. J., Behrens A., Schaeffer P., Albrecht P., and Sinninghe Damsté J. S. (2000) Timing of early diagenetic sulfurization of organic matter: A precursor-product relationship in Holocene sediments of the anoxic Cariaco Basin, Venezuela. *Geochim. Cosmochim. Acta* **64**(10), 1741 - 1751.

Westerlund S. F. G., Anderson L. G., Hall P. O. J., Iverfeldt A., van der Loeff M. M. R., and Sundby B. (1986) Benthic fluxes of cadmium, copper, nickel, zinc and lead in the coastal environment. *Geochim. Cosmochim. Acta* **50**, 1289 - 1296.

Wilson T. R. S., Thomson J., Colley S., Hydes D. J., Higgs N. C., and Sörensen J. (1985) Early organic diagenesis: the significance of progressive subsurface oxidation fronts in pelagic sediments. *Geochim. Cosmochim. Acta* **49**, 811 - 822.

Wilson T. R. S., Thomson J., Hydes D. J., Colley S., Culkin F., and Sorensen J. (1986a) Metal-rich layers in pelagic sediments. *Science* **234**, 1129.

Wilson T. R. S., Thomson J., Hydes D. J., Colley S., Culkin F., and Sörensen J. (1986b) Oxidation fronts in pelagic sediments: diagenetic formation of metal-rich layers. *Science* **232**, 972 - 975.

Zabel M., Hensen C., and Schülter M. (2000) Back to the Ocean Cycles: Benthic Fluxes and Their Distribution Patterns. In *Marine Geochemistry* (ed. H. D. Schulz and M. Zabel). Springer, Berlin, Heidelberg, New York, pp. 373 - 395.

Zabel M. and Schulz H. D. (2001) Importance of submarine landslides for non-steady state conditions in pore water systems - lower Zaire (Congo) deep-sea fan. *Mar. Geol.* **176**, 87 - 99.

Zabel M., Wagner T., Schneider R. R., Adegbie A., and Kolonic S. (2001) Late Quaternary climate change in Central Africa as inferred from terrigenous input to the Niger Fan. *Quaternary Research* **56**, 207 - 217.

Zhang H., Davison W., Miller S., and Tych W. (1995) In situ high resolution measurements of fluxes of Ni, Cu, Fe, and Mn and concentrations of Zn and Cd in porewaters by DGT. *Geochim. Cosmochim. Acta* **59**(20), 4181 - 4192.

Zonneveld K. A. F., Versteegh G. J. M., and de Lange G. J. (2001) Palaeoproductivity and post-depositional aerobic organic matter decay reflected by dinoflagellate cyst assemblages of the Eastern Mediterranean S1 sapropel. *Mar. Geol.*(172), 181 - 195.

List of Figures

List of Tables

Danksagung

Mein besonderer Dank gilt Professor Dr. Horst D. Schulz für die Vergabe und Betreuung dieser Arbeit. Die zahlreichen richtungsweisenden Diskussionen und sein stetes Interesse am Fortgang der Arbeit waren mir eine große Unterstützung. Ausdrücklich bedanken möchte ich mich auch für die ausgezeichneten Arbeitsbedingungen und für die Hilfsbereitschaft bei allen Fragen und Sorgen.

Professor Dr. Bo B. Jørgensen danke ich für die freundliche Übernahme des Zweitgutachtens.

Herzlich bedanken möchte ich mich ebenfalls bei den Kolleginnen und Kollegen des Fachbereichs Geowissenschaften der Universität Bremen und besonders bei allen Mitgliedern der Arbeitsgruppe Geochemie und Hydrogeologie, die zum Gelingen dieser Arbeit beigetragen haben. Mein besonderer Dank gilt Dr. Sabine Kasten für die kritische Durchsicht der Manuskripte, für viele intensive Diskussionen und für ihre Geduld und motivierende Begeisterungsfähigkeit. - Dr. Christian Hensen und Dr. Matthias Zabel danke ich für ihre fachlichen Anregungen und für das freundschaftliche und aufmunternde Interesse an meiner Arbeit. - Dr. Martin Kölling verdanke ich, dass mein Leben auch bei technischen Problemen im Labor oder am PC immer völlig sorgenfrei blieb. - Im Labor standen mir Sigrid Hinrichs, Silvana Hessler, Karsten Enneking und Susanne Siemer hilfreich, zuverlässig und mit viel guter Laune zur Seite. Kerstin Dierks, Dr. Joseph Hell und Markus Schmidt haben durch ihren unermüdlichen Einsatz bei der Probenaufbereitung geholfen, den Grundstein für diese Arbeit zu legen. Ihnen allen möchte ich hiermit herzlich danken. - Sadat Kolonic, Dr. Thomas Wagner und Inka Ebert danke ich für die großzügige Bereitstellung und Messung von C_{org} Daten. Anja Reitz und Lars Jacque haben mit ihren Laborarbeiten viele gute Diskussionen ausgelöst und Daten gewonnen, die zum Teil in das Kapitel 5 eingegangen sind, wofür Ihnen auch an dieser Stelle gedankt sei. Melanie Dillon danke ich für die Einblicke in die Welt der sedimentmagnetischen Parameter. - Ein besonderer Dank geht schließlich an Dr. Kay Hamer für die vielen gemeinsamen Pausen, in denen er mich mit frischem Kaffee und neuen Denkanstößen versorgt hat.

Für wertvolle Diskussionen und Anregungen - insbesondere zum Thema Schwefel und organische Geochemie - danke ich darüber hinaus Dr. Thomas Wagner (Universität Bremen), Dr. Jaap Sinnighe Damsté (NIOZ, Texel), Dr. Volker Brüchert (MPI für marine Mikrobiologie, Bremen) und Dr. Gert de Lange (Universiteit Utrecht).

Mein Dank gilt weiterhin allen Besatzungsmitgliedern der Forschungsschiffe FS Meteor und RV Aegaio für die gute Versorgung während der Fahrten M46/2, M46/3 und der Trans-Mediterranean Cruise (MTP-II, MATER). Der Deutschen Forschungsgemeinschaft danke ich ausdrücklich für die Finanzierung dieser Arbeit. Daneben geht mein Dank an die EU für die Finanzierung meiner Teilnahme am Marine Science and Technology (MAST) Advanced Study Course "The Mediterranean Marine System", der diese Arbeit abrundete.

Dankend möchte ich auch an die erinnern, die mein Studium mit besonderer Aufmerksamkeit begleitet haben, insbesondere Professor Dr. Reimer Herrmann und Dr. Stefan Peiffer an der Universität Bayreuth sowie Dr. Don House an der University of Canterbury, Neuseeland. Ebenfalls danken möchte ich meinen Freundinnen und Freunden aus Bayreuther und Cottbuser Tagen, die mir über alle Ortswechsel hinweg treu geblieben sind. Mein besonderer Dank gilt an dieser Stelle jedoch meinen Eltern, die mich in allen Lebenslagen liebevoll und großzügig unterstützt haben.

Bei Kerstin Pfeifer, meiner engsten Bremer Kollegin, möchte ich mich bedanken für viele (nicht nur) wissenschaftliche Gespräche und mehr noch für ihre Toleranz und ihren Humor, durch die die drei Jahre in unserem Büro und die zehn gemeinsamen Wochen auf See zu einer guten Zeit wurden, die ich immer gern in Erinnerung behalten werde.

Abschließend danke ich von ganzem Herzen meinem Freund, Dr. Thomas Heinkele, für die unerschöpfliche Energie und liebevolle Fürsorge, mir der er diese Arbeit unterstützt hat, für viele spannende Gespräche über marine und terrestrische Böden - und dafür, dass in der Endphase dieser Arbeit die anderen Seiten des Lebens nicht ganz in Vergessenheit geraten sind.